

PROCESSING AND CHARACTERISATION OF SIC PLATELET REINFORCED BOROSILICATE COMPOSITES

by

AVINASH R. B. VERMA

3 T-1
ME/1993/4
VSP



DEPARTMENT OF METALLURGICAL ENGINEERING
INDIAN INSTITUTE OF TECHNOLOGY KANPUR
JULY, 1993

PROCESSING AND CHARACTERISATION OF SiC PLATELET REINFORCED
BOROSILICATE COMPOSITES

*A Thesis Submitted
in Partial Fulfilment of the Requirements
for the Degree of
MASTER OF TECHNOLOGY*

by

AVINASH R. B. VERMA

to the

DEPARTMENT OF METALLURGICAL ENGINEERING
INDIAN INSTITUTE OF TECHNOLOGY KANPUR
July, 1993

ME-1993-M-VER-PRO

18 AUG 1993 /MET

CENTRAL LIBRARY
I.I.T. KANPUR

ISS. No. A.I.16271

15.7.93
D.P.

CERTIFICATE

This is to certify that the present work, entitl "Processing and Characterization of SiC Platelet Reinforced Borosilicate Composites", by Avinash R.B. Verma has been carried out under our supervision and it has not been submitted elsewhere for a degree.

Dr. G. S. Murty
Professor
Department of Metallurgical Engg
Indian Institute of Technology
Kanpur

Dr. V.S. R. Murthy
Assistant Professor
Department of Metallurgical Engg
Indian Institute of Technology
Kanpur

July, 1993

ABSTRACT

Silicate matrix composites have been emerging as leading contenders for different high temperature structural applications due to their ease of fabrication, ability to crystallise into various phases having varied thermal expansion and good toughness with the incorporation of reinforcements.

In this study, SiC platelets reinforced borosilicate glass matrix composites have been selected for investigation because of their thermal expansion match. Borosilicate - SiC (platelet) composites were processed by hot pressing with varying volume fraction of reinforcement in the range of 10-50 vol%. Initially the borosilicate matrix pellets were cold compacted and sintered. However, borosilicate, during sintering crystallised to cristobalite (polymorph of silica) which has a higher thermal expansion coefficient compared to the base matrix and resulted in matrix microcracking. To suppress the crystallisation of cristobalite, hot pressing conditions have been identified. The microstructures of the composites were characterized by optical microscopy as well as SEM. Their mechanical behaviour was studied in compression at room temperature as well as elevated temperatures upto 700° C.

Composites fabricated with various volume fraction of SiC(p) exhibited good strength values in compression and a maximum value of 510 MPa (4 times of base matrix strength) has been obtained with 40% dispersion. Beyond this, poor infiltration of glass resulted in decrement of properties. Strength values are also compared with theoretically calculated values based on the

existing models in the literature and are found to be in good agreement. The dominant mechanism for strength increment is load transfer while crack deflection is mainly responsible for increase in toughness. Finally , the superplastic flow behaviour of SiC(P) borosilicate composites has ben examined in the vicinity of glass transition temperature (T_g). While all the composites exhibited Newtonian viscous flow characteristics that are conducive to superplastic behaviour, their flow stress has increased considerably with increasing volume fraction of SiC platelets.

ACKNOWLEDGEMENT

I wish to express my deep sense of indebtedness and gratitude to Dr. G. S. Murty and Dr. V. S. R. Murthy, Department of Metallurgical Engineering, IIT Kanpur, who proposed, guided and helped this work to completion through their uncountable suggestions and encouragement. Further I would like to thank my friends Mr. Manoj Kumar and Mr. J. S. Dubey for their constant encouragement and help through out my work.

July, 1993
Kanpur

AVINASH R. B. VERMA

CONTENTS

PAGE N

ABSTRACT

LIST OF FIGURES

LIST OF TABLES

CHAPTER 1 INTRODUCTION

1.1 General Introduction	1
1.2 Historical Developments in Ceramic Composites	4
1.3 Applications and Future Potential	7

CHAPTER 2 LITERATURE REVIEW

2.1 Fiber Reinforced Composites	12
2.1.1 Introduction	12
2.1.2 Composite Components	15
2.1.2.1 Fibre Reinforcements	15
2.1.2.2 Matrix	17
2.1.3 Processing Techniques	19
2.1.3.1 Slurry Infiltration and Mixing Techniques	20
2.1.3.2 Sol gel and Polymer Hydrolysis Techniques	21
2.1.3.3 Melt Infiltration	22
2.1.3.4 Chemical Vapour Infiltration and In situ Chemical Reaction Techniques	22
2.1.4 Role of Interface	24
2.1.5 Mechanical Behaviour	25
2.1.5.1 Matrix Cracking Stress	26
2.1.5.2 Crack Opening	29
2.1.5.3 Pull out Length	29

2.1.5.4 Ultimate Strength	30
2.1.5.5 Toughness	30
2.1.6 Fiber Reinforced Glass and Glass-ceramic Composites	31
2.2 Whisker Reinforced Ceramic Composites	35
2.2.1 Whiskers	36
2.2.2 Mixing and Compact Formation	38
2.2.3 Densification Techniques	39
2.2.3.1 Hot Pressing	39
2.2.3.2 Pressureless Sintering/Hot Isostatic Pressing	41
2.2.4 Mechanical Behaviour	42
2.2.4.1 Strength	42
2.2.4.2 Toughening Mechanisms	44
i. Crack Deflection	
ii. Microcracking	
iii. Crack Bridging	
iv. Whisker Pullout	
2.2.5 Strength and Toughness Increase in Whisker Reinforced Composites	48
2.3 Platelet Composites	50
2.3.1 Fabrication of Platelet Composites	52
2.3.2 Mechanical Behaviour	52
2.4 Superplasticity in Glass Ceramic Composites	55
2.5 Objectives of This Study	60
CHAPTER 3 EXPERIMENTAL DETAILS	
3.1 Matrix and Platelets	69

3.2 Matrix Preparation	69
3.3 Fabrication of Composites	70
3.3.1 Dry Mixing	70
3.3.2 Hot Pressing of Composites	70
3.4 Characterisation of Composites	72
3.4.1 Optical Microscopy	72
3.4.2 X-ray Diffraction	72
3.4.3 Scanning Electron Microscopy	73
3.5 Density Measurements	73
3.6 Strength Measurements	73
3.7 Superplastic Testing of the Composites	74
 CHAPTER 4 RESULTS AND DISCUSSION	
4.1 Borosilicate (Pyrex)-SiC Composites	76
4.1.1 Borosilicate (Pyrex) Glass	76
4.1.2 SiC Platelets	76
4.2 Sintering of Pyrex Glass	80
4.3 Hot Pressing of Pyrex Glass	85
4.4 Hot Pressed Pyrex-SiC Platelet Composites	87
4.5 Density Measurements for Pyrex-SiC Composites	89
4.6 Mechanical Behaviour of Pyrex-SiC Composites	89
4.6.1 Compressive Strength	89
4.6.2 Fracture Behaviour	100
4.6.3 Temperature Dependence of Strength	103
4.6.4 Effect of Vol % Loading of Strength	105
4.6.5 Elevated Temperature Testing of Pyrex - SiC Composites	106
CHAPTER 5 CONCLUSIONS	118

REFERENCES	9
Chapter 1	62
Chapter 2	
Chapter 4	117

LIST OF FIGURES

PAGE

Fig. 2.1 Schematic of the Forced Flow Thermal Gradient CVI Process	23
Fig. 2.2 Stress Strain Curve for Fibre Composites	26
Fig. 2.3 A Schematic Indicating the Various Contributions to the Steady State Toughness in Fibre Composites	32
Fig. 2.4 Comparison of the MOR and K_{IC} Values for various Composite Systems and their Temperature Dependence	34
Fig. 2.5 Flow Chart for the Fabrication of Whisker Reinforced Ceramics	40
Fig. 2.6[a] Shape Effect on the Strengthening of Composite Systems	46
Fig. 2.6[b] Effect of L/D ratio on the Toughness of Composite Systems	46
Fig. 2.7 Fracture Toughness and Bending Strength of SiC-Platelet Reinforced Silicon Nitride	54
Fig. 3.1 Schematic of the Hot Pressing Setup	71
Fig. 4.1 DTA Plot for Determining Glass Transition Temperataure of Pyrex Glass	77
Fig. 4.2 Phase Diagram for Borosilicate Glass System	78
Fig. 4.3 XRD of SiC Platelets Showing Various Poly Types	82
Fig. 4.4 Comparison of the XRD Patterns of Pyrex (Sintered) with H.P. Samples Containing Various Vol. % SiC Platelets for α -Cristoblite Formation	8
Fig. 4.5 Density Measurements for Pyrex-SiC Composites (HP)	94
Fig. 4.6 Compressive Strength of Pyrex-SiC Composites	9

Fig. 4.7 Variation in the Compressive Strength of Pyrex-SiC Composite With Increasing Vol. % of SiC Platelets	97
Fig. 4.8 Temperature Dependence of Strength of Pyrex-SiC Composites	104
Fig. 4.9 Strength of Pyrex-SiC Composites with Varying Vol. % at Different Temperatures	108
Fig. 4.10 Confirmation of Newtonian Behaviour of Pyrex-glass	109
Fig. 4.11 Comparison of Flow Stress at 675°C (Pyrex-SiC)	110
Fig. 4.12 Comparison of Flow Stress at 700°C (Pyrex-SiC)	111
Fig. 4.13 Changing Strain Rate Test in Compression at 675°C for Pyrex	112
Fig. 4.14 Changing Strain Rate Test in Compression at 700°C for Pyrex-SiC 10 Vol.%	113
Fig. 4.15 Increase in the level of Flow Stress of Pyrex Glass (675°C) by incorporating various Vol. % SiC Platelets.	114
Fig. 4.16 Increase in the level of Flow Stress of Pyrex Glass (700°C) by incorporating various Vol. % SiC Platelets	115
Fig. 4.17 Arrhenius Plot for Pyrex Glass	116

LIST OF PHOTOGRAPHS**PAGE N^O**

Fig. 4 Ph-1	SiC Platelets	81
Fig. 4 Ph-2	Sintered Pyrex (T 900°C) (HF etched)	86
Fig. 4 Ph-3	Hot Pressed Pyrex (T 900°C) (HF etched)	86
Fig. 4 Ph-4	Pyrex-SiC Composite Microstructures (10 Vol.% to 50 Vol.%)	88
Fig. 4 Ph-5	Hot Pressed Pyrex-SiC (10 Vol. %) (BE)	90
Fig. 4 Ph-6a	Hot Pressed Pyrex-SiC (10 Vol %) (HF etched)	91
Fig. 4 Ph-6b	Hot Pressed Pyrex-SiC (50 Vol.%) (HF etched)	91
Fig. 4 Ph-7a	Fractured Surface (Pyrex-SiC Composite) Showing Crack Deflection Process	101
Fig. 4 Ph-7b	Fractured Surface (Pyrex-SiC Composite) Showing Crack Twisting Process	101
Fig. 4 Ph-7c	Fractured Surface (Pyrex-SiC Composite) Showing Pullout Process	101

LIST OF TABLES**PAGE N^O**

Table 2.1 Fracture Toughness Levels Achieved to date via Different Approaches to the Reinforcement of Ceramic Materials	13
Table 2.2 Strength and Toughness Increase in Fiber Reinforced Composites Compared with other Reinforcements	14
Table 2.3 Major Non-Oxide Fibres Used in Ceramic Matrix	16
Table 2.4 Major Matrix Materials Used in Ceramic Matrix Composites	18
Table 2.5 Mechanical Properties of the Various Whisker Composite Systems	51
Table 4.1 Properties of Composite Components	79
Table 4.2 Compressive Strength of Pyrex-SiC Composites	92
Table 4.3 Theoretical Predictions of the Strength and Effective Modulus of Pyrex-SiC Composites	93
Table 4.4 Strength of Pyrex-SiC Platelet Composites From Literature	102

I INTRODUCTION

1.1) General Introduction

Composite materials are produced when two or more materials or phases are synergistically combined to give a combination of properties that cannot be attained in the original materials. These new class of materials are designed to give beneficial combinations of strength, stiffness, high temperature performance, thermal conductivity and corrosion resistance. The properties of the composite are entirely dependent on the constituents and the physical, chemical and mechanical interactions between the phases. Reinforcement-matrix combinations are chosen to provide the properties and stability defined by the application, however, a variety of factors from processing to chemical and mechanical compatibility must be considered in the design of a composite system.

A large number of material systems are currently under consideration. Matrices can be broadly classified as polymer, metal or ceramic while reinforcements can be classified into continuous or discontinuous reinforcements, which include short fibres, whiskers, platelets and particulates.

Polymers have low stiffness and(in the right range of temperature) are ductile. Polymer matrices can be divided into two distinct groups: thermosets and thermoplastics. At present E-glass, S-glass and graphite are by far the most dominant reinforcements. The major aerospace reinforcements are boron, carbon/graphite, kevlar and aramid(1-5). Thermoset materials range from the low cost commercial polyesters to epoxies(limited to

applications below about 150°C). Other thermosetting resins, including bismaleimide and polyimide, allow increases to about 200°C and 300°C respectively. Typical thermoplastics used are polyether sulfone(PES) polyetherimide(PEI), polyetheretherketone(PEEK), polyetherketone(PEK) and polyphenylene sulphide(PPS). The main polymer of current interest is PEEK which while having still limited temperature capability(140°C) has excellent resistance to impact damage.

Development of Metal Matrix Composites(MMCs) began around two decades back. The first major MMC that was developed in the late 1960's was a boron fibre reinforced aluminium. Its application was in the tubular struts used in the mid fuselage of the space shuttle Orbiter. MMCs started attracting commercial attention in 1980's. Currently MMCs are being developed using relatively ductile high strength matrices of aluminium, magnesium and titanium with continuous or discontinuous carbon, SiC, B or Al₂O₃ fibres and with high modulus reinforcements such as SiC or B₄C(6-10).

However the major limitation of the family of PMCs and MMCs is that their performance is limited to lower temperatures. The typical range for PMCs is from 100°C to 300°C and MMCs from 200°C to 1100°C. They fail to perform at elevated temperatures above 1000°C as structural materials.

During the last decade, tremendous emphasis has been placed on developing high-performance materials for use in elevated-temperature applications because advanced designs for high-velocity aircraft, efficient power-conversion systems and aerospace applications at high

temperatures in a variety of environments. Conventional metals and alloys do not possess the thermal stability or elevated-temperature properties to meet those requirements.

Oxide and non-oxide ceramics exhibit relatively high strength and stability at elevated temperatures. These materials have low densities and are chemically inert. The major contenders for high temperature applications are the silicon based ceramics (SiC, Si_3N_4 and SiAlON derivatives) based on the intrinsic properties of high specific stiffness, low thermal expansion and oxidation resistance(11-13). These microstructures are normally diphasic, resulting from the sintering additions. For instance, boron and carbon are added to SiC as surface active solid state sintering catalysts, which remain in dispersed form. Si_3N_4 and SiAlONs are consolidated by a liquid phase sintering route, and normally the grain boundary silicate phase remains as amorphous. The grain boundary liquid in these systems, influences the growth of major phases with resultant improvement in fracture toughness over most of equiaxed microstructures.

Zirconia based ceramics(14,15) are an important development of the late 1970's aiding in the improvement of low temperature strength and toughness. These materials occupy an important place among engineering materials because of the toughening effect based on a martensitic phase transformation. However, toughness increment achieved due to this transformation is limited to approximately 700°C (16-18). Additionally, the relatively high thermal expansion and low thermal conductivity for ZrO_2 presents a thermal shock problem.

The reliability of monolithics for structural applications is

limited by variability in mechanical strength and low toughness (3-12 MPa $m^{1/2}$). Property variability is normally due to processing or microstructure related flaws e.g. grain growth, voids, inclusions, impurities etc. Ceramic materials exhibiting low strength and toughness can be improved further by a second phase addition, typically 10-30 vol% range. The second phase additions inhibit crack propagation by crack deflection, crack bridging and fibre pullout. The primary criteria for selection of second phase (fibres, particles, platelets, whiskers) are that they should be stable (thermodynamically and chemically) and allow the retention of improved mechanical properties at higher temperatures. Keeping this in view, a wide variety of Ceramic Matrix Composite (CMC's) materials are being developed with dispersion of platelets, whiskers and semi-continuous, high strength and high-modulus fibres(19,20). Dispersion of these reinforcements improve the toughness values by several orders of magnitude (especially with fibres).

1.2) Historical Developments in Ceramic Composites

The concept of ceramic-composites is not new. Throughout history, fibers have been added to brittle materials to improve their properties. Straw and animal hair were mixed with clay and the mixture formed into bricks or pottery. The fiber acted to improve the handleability of the materials prior to drying or firing and to increase the strength and fracture resistance of the finished product. It has been suggested that goat hair was added to pottery in ancient times and upon firing was converted to carbon. These materials may be the first examples of

carbon-fibre-reinforced ceramic composites(21,22).

Although the advantages of ceramic composites have been recognised for many years, most of the developments in this field have occurred in the past twenty years. In some early work, randomly oriented, discontinuous metal fibres were incorporated into a range of ceramic matrices(23,24). The result was improved toughness, and in some cases, increased strength. Unfortunately, these modest improvements were accompanied by significant disadvantages in that the densities were increased relative to the monolithic materials, the ceramic matrices failed to protect the fibres from degradation in damaging environments, and the thermal expansion mismatch between fibres and matrices resulted in premature failure of the composites because of matrix cracking upon temperature cycling. By the late 1960's, the development of these composite materials had been abandoned to pursue more promising ventures.

The development of low-density, high strength carbon fibres led to renewed interest in fiber-reinforced composites. In contrast to the earlier research that attempted to improve the toughness of brittle ceramics by the addition of ductile metal fibres, researchers began to investigate the possibility of reinforcing brittle matrices with the relatively brittle carbon fibres. The majority of the initial efforts, were in the development of carbon-carbon composites for defence applications, however, carbon-carbon composites begin to oxidise in air at temperatures above 700K, thereby limiting their usefulness.

Some of the original research examining the toughening of ceramic matrices by the addition of carbon fibers was initiated in

carbon-fibre-reinforced ceramic composites(21,22).

Although the advantages of ceramic composites have been recognised for many years, most of the developments in this field have occurred in the past twenty years. In some early work, randomly oriented, discontinuous metal fibres were incorporated into a range of ceramic matrices(23,24). The result was improved toughness, and in some cases, increased strength. Unfortunately, these modest improvements were accompanied by significant disadvantages in that the densities were increased relative to the monolithic materials, the ceramic matrices failed to protect the fibres from degradation in damaging environments, and the thermal expansion mismatch between fibres and matrices resulted in premature failure of the composites because of matrix cracking upon temperature cycling. By the late 1960's, the development of these composite materials had been abandoned to pursue more promising ventures.

The development of low-density, high strength carbon fibres led to renewed interest in fiber-reinforced composites. In contrast to the earlier research that attempted to improve the toughness of brittle ceramics by the addition of ductile metal fibres, researchers began to investigate the possibility of reinforcing brittle matrices with the relatively brittle carbon fibres. The majority of the initial efforts, were in the development of carbon-carbon composites for defence applications, however, carbon-carbon composites begin to oxidise in air at temperatures above 700K, thereby limiting their usefulness.

Some of the original research examining the toughening of ceramic matrices by the addition of carbon fibers was initiated in

the late 1960's and early 1970's at Harwell and at the National Physical Laboratory in England(25,26). Large increases in the work of fracture were attained by incorporating carbon fibres into glass and glass-ceramic matrices. The composites demonstrated high strength and toughness and could be fabricated using techniques similar to those already well established in the production of polymeric matrix composites. However, these materials lacked thermal stability because of the relatively large differences in the fiber and matrix thermal expansions and the poor oxidation resistance of the carbon fibers. Interest in the materials waned as efforts to improve the oxidation resistance of the carbon-fiber-glass matrix composites were unsuccessful.

Research continued to develop a low-cost oxidation-resistant fibre with good mechanical properties. Yajima et. al.(27,28) developed a continuous fine-grained SiC fiber having high strength and excellent oxidation resistance which has revolutionised the field of composites. The fibers were synthesised from polycarbosilane, an organometallic precursor, and processing was similar to that used in the production of carbon fibers. The fibers consisted mainly of SiC but also contained silica and free carbon. The introduction of the Nicalon (trade name used by Nippon Carbon Company Ltd., Tokyo, Japan) fibers spawned a new era in the development of ceramic composites.

Another related development was that Al_2O_3 could be toughened by SiC whiskers(29). This lead to a major thrust in the research of whisker-reinforced CMCs. Important increments in strength, fracture toughness and Weibull's modulus have been demonstrated for whisker reinforced oxide and nitride ceramics. For example,

Hot Pressed (HP) Al_2O_3 containing 40% SiC whiskers has a MOR increment of 500 MPa over monolithic Al_2O_3 . K_{Ic} increases from 4.5 to 8.5 MPa $\text{m}^{1/2}$ and there is a remarkable insensitivity to thermal shock up to at least 1000°C(30). HP Si_3N_4 composites with 30% SiC have been fabricated with 700 MPa MOR comparable with monolithic ceramics, but combined with higher Weibull modulus and work-of-fracture (WOF).

However the greatest flexibility may be obtained from the use of silicate glasses and their crystalline derivatives (glass ceramics) which may be tailored to a wide range of chemistry, softening point and thermal expansion mismatch with the reinforcing phases.

1.3) Applications and future potential

Particulate and whisker reinforced ceramics have superior properties compared to their monolithic state and are therefore replacing these in many applications where slightly higher production costs can be offset by improvement in performance. In applications such as cutting and forming tools, wear parts in machinery, nozzles, valve seals and bearings, improvements in toughness and hardness translate into longer life and a reduced frequency of delays caused by catastrophic failure. The most successful single application of whisker and particulate composites is as cutting tool inserts.

An important driving force for the development of whisker/fibre reinforced ceramic composites has been the potential for their use in automotive and aerospace engines and other energy conversion systems. Above all, an increase in the operating

temperatures of such equipment would lead to increased efficiency and reduced exhaust emissions. The feasibility of producing and running such components as combustion chambers, catalyser substrates, engine valves, impeller and turbine blades has been demonstrated.

A second area of potential application still awaiting improved reliability is biological implants. Ceramic materials generally show excellent compatibility with biological tissue and fluids.

Though the ceramic-matrix composites (particularly the long-fibre composites) offer a higher mechanical reliability, they do not possess the necessary microstructural stability at the high temperatures necessary in combustion engines and other high temperature aerospace applications. The main reasons for this appear to be: (a) structural degradation or oxidation of fibers at high service temperatures and (b) incompatibility of the constituent phases in oxidising environments at high service temperatures. Currently, considerable research activity is being devoted to developing fibres with high stability (e.g. continuous, monocrystalline fibers) and to finding compatible ceramic combinations. Another approach that is being pursued is to find a protective coating system for C/C composites to prevent oxidation.

References: Chapter 1

- 1) Broutman L. J., Krock R. J., "Interfaces in Polymer-Matrix Composites", Academic Press, New York and London (1974)
- 2) Broutman L. J., Krock R. H., "Mechanics of Composite Materials" Academic Press, New York and London (1974)
- 3) Richardson M. O. W. editor, "Polymer Engineering Composites" Applied Science Publishers, Elsevier (1976)
- 4) Lubin G. editor, "Handbook of Fiberglass and Advanced Plastic Composites" Van Nostrand Reinhold, New York Chapters 2-5, 13-20
- 5) Billmeyer F. W., "Textbook of Polymer Science" Wiley-Interscience New York (1971)
- 6) Divecha A. P., Fishman S. G., Karmarkar S. D., "Silicon Carbide Reinforced Aluminium - A formable Composite" Journal of Metals, 12-17 (1981)
- 7) Divecha A. P., Fishman S. G., "Progress in the Development of SiC/Al Alloys" SAMPE Quarterly 40-42 (1981)
- 8) Metcalfe A. G., Klein M. J., "Interfaces in Metal Matrix Composites" Vol. 1 Composite Materials edited by Metcalfe A. G., Academic Press, New York, 1974 pp.125
- 9) Hack J. E., Amateau M. F., "Mechanical Behaviour of Metal-Matrix Composites" The Metallurgical Society of AMIE (1981)
- 10) Piggott M. R. "Load Bearing Fibre Composites" Pergamon Press (1980)
- 11) Heuer A. H., Fryburg G. A., Ogbiji L. U., Mitchell T. E., " β - α Transformation in Polycrystalline SiC: 1-5", Journal of the American Ceramic Society, 65 9-10 (1978)
- 12) Jack K. H., "Review: SiAlON's and related Nitrogen Ceramics" J. Mat. Sci., 11 pp1135-1158 (1976)
- 13) Trigg M. B., Tani E., "Effect of Fabrication Routes and Heat Treatments on the Microstructure of Silicon Nitride Based Materials" Materials Science Forum 34-36 539-597 (1988)
- 14) Evans A. G., Drory M. D., et.al. "Martensitic Transformations in Zirconia: Particle Size Effects and Toughening" Acta. Metall., 29 447-56 (1981)
- 15) Lange F. F., "Transformation Toughening in Zirconia Part 1-5" Journal of Material Science, 17 225 (1982)
- 16) Stump D. M., Budiansky B., "Crack Growth Resistance in Transformation-Toughened Ceramics" Int. J. Solids Struct., 25 635-46 (1989)

- 17) Swain M. V., Rose L. R. F., "Strength Limitations of Transformation-Toughened Zirconia Alloy" J. Am. Ceram. Soc., 69[7] 511-18 (1986)
- 18) Amazigo J. C., Budiansky B., "Interaction of Particulate and Transformation Toughening" J. Mech. Phys. Solids, 36 581-95 (1988)
- 19) Buljan S. T., Pasto A. E., Kim H. J., "Ceramic Whisker and Particulate Composites: Properties Reliability and Applications" Bull. Am. Ceram. Soc., 68[2] 387 (1989)
- 20) Ziegler G., "Advanced Ceramic Developments Trends" cfi/Ber. DKG. 9 pp68 (1991)
- 21) Millberg L. S., "The Search for Ductile Ceramics" J. Metals 39[11] 10-13 (1987)
- 22) Holiday L., "Ceramic Systems" pp. 91-127 in Composite Materials, Elsevier Publishing Company, New York, (1966)
- 23) Baskin Y., Arenberg A., Handwerk J. H., "Thoria Reinforced by Metal Fibres" Am. Ceram. Soc. Bull., 38 345-48 (1959)
- 24) Baskin Y., Harado Y., Handwerk J. H., "Some Physical Properties of Thoria Reinforced by Metal Fibres" J. Am. Ceram. Soc., 43 498-92 (1960)
- 25) Phillips D. C., "The Fracture Energy of Carbon-Fibre Reinforced Glass" J. Mat. Sci., 7 1175-91 (1972)
- 26) Phillips D. C., Sambell R. A. J., Brown D. H., "The Mechanical Properties of Carbon Fibre Reinforced Pyrex Glass" J. Mat. Sci., 7 1454-64 (1972)
- 27) Sambell R. A. J., Brown D. H., Phillips D. C., "Carbon Fiber Composites with Ceramic and Glass Matrices, Part 1: Discontinuous Fibers" J. Mat. Sci., 7 663-75 (1972)
- 28) Yajima S. et.al., "Synthesis of Continuous SiC Fibres with High Tensile Strength" J. Am. Ceram. Soc., 59(7-8) 324-27 (1976)
- 29) Yajima S., et.al., "Anomalous Characteristics of the Microcrystalline State of SiC Fibres" Nature 27[21] 706-7 (1979)
- 30) Wei G. C., Becher P. F., "Development of SiC Whisker-Reinforced Composites" Am Ceram. Soc. Bull., 64[2] 298-304 (1985)

II LITERATURE REVIEW

Ceramic composites are classified on the basis on the type of reinforcements used:

- a) continuous reinforcements (i.e. fibres)
- b) discontinuous reinforcements (i.e. particulates, platelets, whiskers and short fibres)

The main objective of using the composites approach in ceramic systems is to increase the toughness of the ceramics. The strength increase is of secondary importance. The strength increase in both continuous and discontinuous reinforcement based composites is based on load transfer. However, the level of strength increase in continuous fibre reinforced composites is more compared to discontinuous reinforcement based composites. This is because there is perfect load transfer in continuous fibre composites. In discontinuous reinforcement based composites the load transfer is dependent on the ratio of critical length to the actual length of the reinforcement. As the l/d ratio of the reinforcement decreases, the load transfer capability decreases, in the extreme case of the l/d ratio being one (particulate composites) the load transfer is minimum.

The main difference in the two categories of composites is in the various mechanisms of toughness. In fiber reinforced composites major contribution for toughness comes from fibre pullout which is of lesser extent in case of discontinuous composites (however, pullout is significant in short fibre composites). There the mechanisms are limited to crack deflection and microcracking and in some cases (whiskers and platelets) crack

bridging. In the absence of pullout, the toughness increments in discontinuous composites is of the order of 2 to 3 times whereas in continuous fibre composites it is of the order of 8 to 10 times.(Table 2.1)

In this chapter, both continuous and discontinuous reinforcement based composites, their base matrix and reinforcements, composite fabrication, mechanical properties(strength and toughness) are briefly discussed and reviewed.

2.1) Fiber Reinforced Composites

2.1.1) Introduction

Fiber-reinforced ceramics matrix composites are a promising class of structural materials for applications where high strength, high stiffness, low thermal expansion, low density and high temperature stability are desirable attributes either singly or in combination. Work in recent years has shown that large gains in fracture strength and toughness are achievable(Table 2.2). Progress has been made towards identifying the failure mechanisms and understanding the intrinsic fiber matrix interface properties necessary to take advantage of strengthening and toughening mechanisms(1,2). Greatly improved reliability(high weibull modulus) at strengths higher than the best of monolithic polycrystalline ceramics has been reported(3).

For a given fiber configuration(e.g. uniaxial or cross-weaved) general microstructure requirements for high strength are that the volume fraction of fibers should be high, distribution uniform and the matrix dense and homogenous.(1) It

Toughening mechanism	Fracture toughness [MNm ^{-3/2}]	Composite system (matrix/reinforcements)
Microcracking	~10	$\text{Al}_2\text{O}_3/\text{ZrO}_2$
Transformation toughening	~20	ZrO_2 (MgO)
Particle reinforcement	~ 8	$\text{Si}_3\text{N}_4/\text{SiC}$
Platelet reinforcement	~ 8 (~14)	HIP-RBSN/SiC $\text{Si}_3\text{N}_4/\text{SiC}^*$
Whisker reinforcement	~ 8.5	$\text{Al}_2\text{O}_3/\text{SiC}$ $\text{Si}_3\text{N}_4/\text{SiC}$
Fiber reinforcement	>30 ≥25 >30 ~16	glass/SiC glass-ceramic/SiC SiC/SiC $\text{Si}_3\text{N}_4/\text{SiC}$
Metallic inclusions	~25	$\text{Al}_2\text{O}_3/\text{Al}$ $\text{Al}_2\text{O}_3/\text{Ni}$

Table 2.1) Fracture toughness levels achieved to date via different approaches to the reinforcement of ceramic materials.

Material	Flexural Strength (MPa)	K_{IC} (MPa·m ^{1/2})
SiC fiber-reinforced borosilicate glass	830	18.9
Monolithic LAS	200	2
SiC fiber-reinforced LAS glass-ceramic	830	17
SiC-coated C fibers		
in SiO ₂ matrix	950	
in Al ₂ O ₃ matrix		10.5
Polycrystalline Al ₂ O ₃	550	4-5
SiC-whisker reinforced Al ₂ O ₃	800	8.7
Al ₂ O ₃ -ZrO ₂	458	5.29
Al ₂ O ₃ -ZrO ₂		13.5
ZrO ₂ (TZP)	954	11.6
Hot-pressed SiC	700	
Sintered SiC	439	
Hot-pressed Si ₃ N ₄	873	
Reaction-bonded Si ₃ N ₄	260	
Hot-pressed Si ₃ N ₄	473	3.7-4.5
SiC whisker-reinforced Si ₃ N ₄	454	
SiC whisker-reinforced Si ₃ N ₄	800	15.6
SiC whisker-reinforced Si ₃ N ₄		56
SiC whisker-reinforced Si ₃ N ₄	900	

Table 2.2) Strength and toughness increase in fibre-reinforced composites compared with other reinforcements

is easy to obtain such homogenous dense matrices using silicate matrices because of their potential for melt processing and viscous flow in densification. Refractory crystalline matrix composites(e.g. SiC-SiC) on the other hand are typically prepared by methods which often result in substantial matrix porosity(5 to 15 vol%)(1,4).

2.1.2) Composite Components

2.1.2.1) Fibre Reinforcements

For continuous fibre reinforced composites, high modulus oxidation resistant fibres with small diameter are ideal. Additionally, reinforcing fibres should be capable of retaining the structure, stiffness and strength under processing and service conditions i.e. $> 1000^{\circ}\text{C}$. Keeping these in view, a wide range of oxide and non-oxide ceramic fibers suitable for ceramic matrix reinforcement have been developed.

Carbon fibres offer a wide range of mechanical properties. However, they exhibit poor oxidation resistance at elevated temperatures. Although oxide fibres(e.g. Al_2O_3) are capable of withstanding higher temperatures, reactivity with silicate matrices and poor creep properties discouraged their use in high temperature ceramic composites. Fibres based on the compounds of SiC and Si_3N_4 have received greater attention due to their improved stability in oxidising conditions and reduced reactivity during processing.

There are primarily two routes for the manufacture of non-oxide fibres.

a) polymer precursor route in which the polymer-to-ceramic

Fibre	Manufacturer	Manufacturing method	Diameter μm	Density g/cm^3	Average tensile strength MPa	Tensile modulus -GPa	Maximum Temperature Use, $^\circ\text{C}$
Nicalon	Nippon Carbon Co. Ltd Japan	organic precursor	10-15	2.50	2750	200	1000
Tyranno	Ube Industries Ltd Japan	organic precursor	8-10	2.50	2760	200	1000
SCS-6 monofilament	AVCO speciality materials/Textron; USA	chemical vapour deposition	~142	3.05	3450	420	1200
Sigma monofilament	Berghof, Tubingen FRG	chemical vapour deposition	~100	3.40	3450	400	1200
SiC *	MERC, USA	pitch precursor	7-10	3.00	3000	415	1400
Si ₃ N ₄	Toa Nenryo Kogyo KK Japan	organic precursor	10	2.50	3300	300	1200
Si ₃ N ₄ HPZ fibre	Dow Corning USA	organic precursor	10	2.35	2300	160	1400

Table 2.3) Major non-oxide fibres used in ceramic-matrix composites.

* Development stage

conversion takes place in various stages with progressive structure adjustments

b) Chemical Vapour Deposition (CVD) route in which the ceramic is deposited on a core to obtain large diameter fibres(called monofilaments)

compared to monofilaments(diameter = $100\text{-}150\mu\text{m}$) , fibres developed from polymer presursor route(called yarns) are finer in diameter(diameter = $8\text{-}15\mu\text{m}$) and are ideally suited for CMC fabrication.

Although many organosilicon polymers have been explored for the development of SiC and Si_3N_4 fibres, only polycarbosilane, polytitanocarbosilane and polysilazane have emerged as potential starting materials for the production of continuous silicon(oxy) carbide i.e.(NICALON), Si-Ti-C-O i.e.(TYRANNO) and silicon(oxycarbo)nitride i.e.(HPZ) fibres respectively. Of these NICALON is the most extensively used fibre in ceramic composites. The mechanical properties of various non-oxide fibres which are used for CMC applications are given in the table(2.3)

2.1.2.2) Matrix

In CMCs both silicate as well as non silicate matrices are used as base matrix materials. The matrix should be refractory, with low thermal expansion and resistance to oxidation. It should also be infiltrated easily. Silicate matrices are used due to the following reasons:

Significant strengthening is achieved for those matrix-fibre combinations where the Young's modulus of the fibre is substantially large compared to that of the matrix. For glass and

Matrix type	Major constituents	Major crystalline phase	density g/cm ³	thermal expansion coefficient ($^{\circ}\text{C}^{-1} \times 10^{-6}$)	ultimate maximum use temp $^{\circ}\text{C}$ (based on melting or softening)
GLASSES					
Borosilicate	Na ₂ O, B ₂ O ₃ , SiO ₂	-	2.23	3.3	600
Aluminosilicate	MgO, CaO, SiO ₂	-	2.64	5.2	700
High Silica	SiO ₂	-	2.53	0.6	1150
GLASS-CERAMICS					
LAS	Li ₂ O Al ₂ O ₃ , SiO ₂	β -spodumene (hexagonal)	2.67	0.9	1000
MAS	MgO, Al ₂ O ₃ , SiO ₂	Cordierite (orthorhombic)	2.53	2.6	1200
BMAS	BaO, MgO, Al ₂ O ₃ , SiO ₂	Barium Osumilitte (hexagonal)	2.77	2.7	1250
CAS	CaO, Al ₂ O ₃ , SiO ₂	Anorthite (monoclinic)	2.75	4.5	1550
BAS	BaO, Al ₂ O ₃ , SiO ₂	Monoclinic celstian Hexacelsian	3.10-3.40	2.8-8.0	1700
Mullite	Al ₂ O ₃ , SiO ₂	Mullite (rhombohedral)	3.00	5.3	1500

Table 2.4) Major matrix materials used in ceramic-matrix composites.

glass-ceramic matrix, elastic moduli are in the range of 60 to 85 GPa while the reinforcing fibres are generally characterised by an elastic modulus in excess of 210 GPa and in some cases as high as 700 GPa(). Another important aspect of these composites is that they can be fabricated in a manner analogous to that used for resin matrix composites. This is due to the fact that the glass matrix can be readily deformed and flowed in its low viscosity state at elevated temperatures. Not only can glasses be used in this process but also glass-ceramics, which provide the greatest potential for high temperature applications. Glass-ceramics provide the unique capability to densify a composite in the glassy state and then subsequently crystallise the matrix to achieve high temperature stability.

Another important factor for the composite behaviour is the thermal expansion mismatch between the fibres(α_f) and matrices(α_m). By slightly varying the chemical composition of the particular glass or glass-ceramic it is possible to vary the co-efficient of thermal expansion(α_m) over a wide range of values thus tailoring the residual stresses at the interface.

The most extensively used silicate matrices are Borosilicate and glass ceramics like L-A-S, M-A-S. The various matrix materials and their mechanical properties are given in Table(2.4)

2.1.3) Processing Techniques

The various processing methods used to produce ceramic matrix composites can be divided into four general categories(5) The first of these includes traditional mixing and slurry infiltration technique, which remains at present the most effective means for

many systems. The second class includes chemical synthesis routes such as sol-gel and polymer precursor processing, which offer greatly reduced processing temperatures, among other advantages, if problems of low yield and excessive matrix shrinkage can be resolved. A third category is melt infiltration, which follows much successful work in polymer-matrix and metal-matrix composites. Melt processing is particularly attractive for the high matrix densities it affords, but is limited to relatively low-melting glasses, crystalline ceramics or glass-ceramic systems. A final group includes techniques based on chemical vapour infiltration(CVI) and in-situ chemical reactions, such as reaction bonding. These techniques along with polymer precursor synthesis, seem especially suited for processing of non oxide ceramic matrices.

2.1.3.1) Slurry Infiltration and Mixing Techniques

The most common technique used to produce ceramic matrix composites(CMC's) is the slurry infiltration process, in which a fiber preform(e.g. a tow) is impregnated by passage through a slurry mixture containing the matrix material and subsequently gathered and dried. The dried tow is then cut, laid into desired configurations(often multilayered) and hot pressed(HP).

The slurry mixture usually contains at least three components, the carrier liquid, the matrix powder and an organic binder. Wetting agents are sometimes employed to facilitate infiltration, depending on the specific system being processed. Following binder burnout, densification of the composite occurs on HP as the matrix particles rearrange, sinter or flow viscously between the fibers, filling void space. This technique has to date

been used most effectively with glass and glass-ceramic matrix composites(6-8). Initially carbon fiber reinforcements were used but more recently attention has been focussed on SiC(NICALON) reinforcements for higher temperature applications, particularly in the work of Prewo, Brennan and co-workers(9-12). A wide variety of glass and glass-ceramic matrices have been used by these authors, including borosilicate(PYREX), high silica, and aluminosilicate glasses and L-A-S, M-A-S, glass-ceramic systems.

2.1.3.2) Sol-gel and Polymer Pyrolysis Techniques

The advantages perceived in employing sol-gel or polymer pyrolysis routes to process matrix materials include:

- 1) greater compositional homogeneity in single-phase matrices
- 2) the potential for forming unique multiphase matrices
- 3) greater ease of infiltration and forming, including possible adaptation to pressure forming and injection moulding techniques.
- 4) Most importantly processing temperatures lower by hundreds of degrees Centigrade compared to conventional processing techniques.

For covalent ceramics in particular, pyrolysis of polymeric precursors offer the potential for greatly reduced processing temperatures(<1400°C) compared to solid-state reactions, with greater yield than CVD processes. Examples include, but are not limited to, polymeric precursors to SiC and Si_3N_4 (13-16). The principal disadvantages of both techniques however are the high shrinkage and low yield compared to slurry techniques, which seem to preclude formation of dense matrices without further processing steps.

2.1.3.3) Melt Infiltration:

There are substantial advantages that may be realised compared to other methods including

- 1) fully-dense and flaw-free matrices formed in a single processing step
- 2) minimal dimensional change from preform to final product.
- 3) suitability for virtually any fiber reinforcement geometry.

However the obstacles most likely to be encountered in applying this method to ceramic matrices are

- 1) fiber damaging chemical reactions at the higher melting temperatures required.
- 2) lower rates of infiltration resulting from the orders-of-magnitude greater fluid viscosity encountered for ceramic systems compared to metals. In addition thermal expansion mismatch and the volume change on solidification can lead to matrix tensile stresses in melt processing, which are more critical for a brittle ceramic system than for ductile matrices.

2.1.3.4) Chemical Vapour Infiltration(CVI) and In-Situ Chemical Reaction Techniques

Recent developments show that it is feasible to form entire matrices through chemical vapour infiltration(CVI). A CVI formed SiC matrix is in fact commercially available(17). By manipulating pressure and temperature gradients during deposition on a fiber preform contained in a die chamber with specially designed gas flow characteristics Caputo and Lackey(18,19) achieved 70 to 90% dense SiC and Si_3N_4 matrices on SiC and Si_3N_4 fiber preforms(fig2.1).

The attractive features of this technique are the use of a

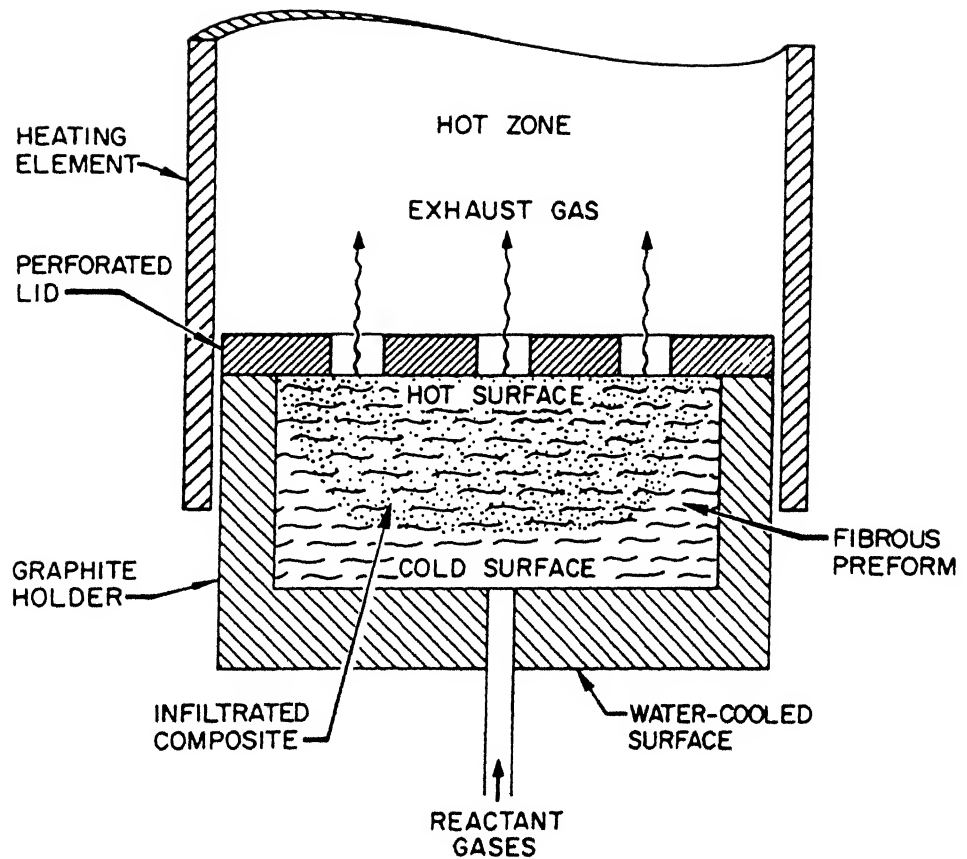


Fig. 2.1) Schematic of the forced-flow thermal-gradient CVI process.

single, continuous deposition step rather than multiple infiltrations, the ability to deposit a wide variety of compositions, and the potential for forming complex shapes by manipulating die design, similar to casting processes.

CMC's can be developed by means of in-situ chemical reactions between two or more elemental powders with or without the addition of gases. One such important in-situ technique is reaction bonding. It can be utilised to prepare Si_3N_4 reinforced with refractory fibers through a simple modification of the process normally used for producing reaction bonded Si_3N_4 (RBSN)(20). That is, the whiskers or fibers can be dispersed into the silicon powder before nitridization.

2.1.4) Role of the Interface

The mechanical properties of fibre composites are influenced strongly by the fiber-matrix interface. The interfacial bond affects matrix-cracking and composite-fracture behaviour. For composites having a very strong interfacial bond, a crack propagating in the matrix will pass undisturbed through the fibres and the composite will fail in a brittle manner, much the same as the unreinforced matrix material does. For composites having poorly bonded interfaces, the fracture process begins progressively with debonding at the fiber-matrix interface, followed by subsequent matrix failure, fibre slip and pullout, and finally fiber failure. These energy-absorbing mechanisms all contribute to improve fracture toughness and are controlled by the strength of the fiber-matrix bond. Marshall and Evans(2) have deduced from measurements of an SiC fiber-reinforced glass-ceramic

which exhibits outstanding properties, that the interface is very weakly bonded. In silicate matrix composites, during the densification, a fortuitous diffusion occurs between the matrix and the SiC fibres and low coherence carbon rich layer forms at the interface. This carbon rich layer is found to be responsible for the enhanced properties of the composite. However, the carbon layer which has formed at the interface is prone to oxidation at higher temperatures and the reaction between the fibers and the matrix leads to deterioration in the composite properties.

Rice et.al.(21) and Bender et.al.(22) have suggested that low cohesive coatings which decrease interface bonding leads to increases in strength and toughness. These coatings are also less prone to oxidation. Understanding and tailoring the interface for the best compromise between strength and toughness at high temperatures is therefore an important area and is expanding rapidly. Additionally the available nonoxide fibres exhibit very poor oxidation resistance and efforts are being made to increase stability of these fibres upto 1600°C.

2.1.5) Mechanical Behaviour

In general, the fibers in a ceramic-ceramic composite have a higher strain-to-failure than that of the matrix, and it is assumed that the ceramic matrix materials are essentially brittle. When a ceramic-ceramic composite is stressed the brittle matrix will fail before the fibres fail. In the event of matrix failure, the load is transferred from the matrix to the fibres. The rule of mixtures will govern the elastic modulus in stage I. As loading continues, the fibers will strain and multiple cracking of the

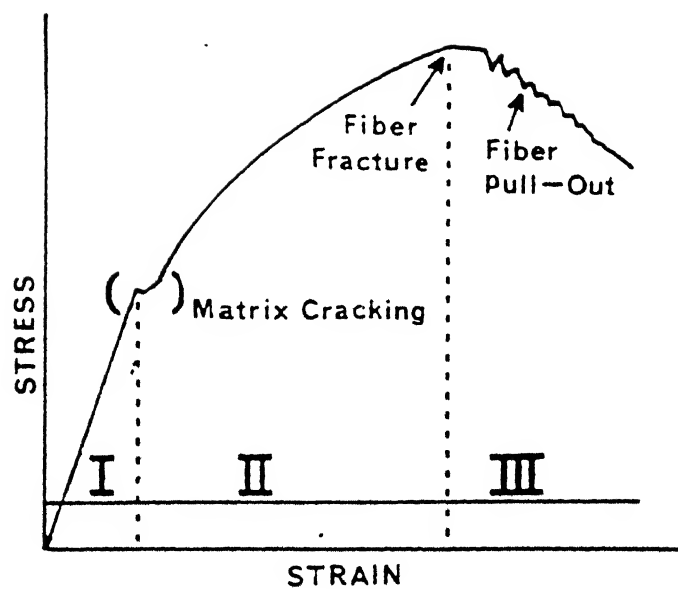


Fig. 2.2) Stress-strain curve for fibre composites

matrix will occur. This will result in a deviation from composite elastic behaviour(stage I) to a reduced modulus associated with elastic extension of fiber(stage II). A maximum stress(UTS) occurs with fibre-bundle failure which may be followed by fibre pull-out(stageIII) which contributes to the total work-of-fracture(WOF)(fig2.2). The important characteristics of this ideal response are:

- 1) A high failure strain and tolerance of overstressing(such as thermal shock or impact loading) which would cause instant failure in a monolithic ceramic.
- 2) An insensitivity to matrix-flaws and hence component size(unlike the weakest link failure of monolithic ceramics) due to a limitation to crack tip stress intensity caused by fibre-bridging of crack surfaces.

This ideal composite behaviour is achieved only for relatively weak fibre-matrix interface bonding and for unidirectional reinforcement.

The specific microstructural parameters that govern Mode I failure(23) are the relative fibre/matrix interface debond toughness, Γ_i/Γ_f , the misfit(thermal expansion) strain between fibre and matrix ϵ_{ui}^T , the friction co-efficient at the debonded interface μ , the statistical parameters that characterise the fibre strength, S_o and m , the matrix toughness Γ_m and the fibre volume fraction v_f . The prerequisite for toughness is that $\Gamma_i/\Gamma_f < 1/4$ to allow crack-front debonding. Subject to this requirements the misfit strains must be small and preferably negative such that the interface is in tension. Furthermore, for a continuous fiber, the friction co-efficient along the debonded interface should be

small. The ideal fiber properties include a high median strength(large S_o) and large variability(small m) as needed to encourage large pull-out lengths. When r_i/r_f and μ are both small, the tensile stress-strain behaviour illustrated in the figure is obtained(fig2.2). Three features of this curve are important, matrix cracking at a stress σ_o , fiber-bundle failure at σ_u , and pullout.

2.1.5.1) The Matrix Cracking Stress(σ_o)

The stress σ_o at which matrix cracking occurs has been the most extensively studied behaviour in ceramic matrix composites. For composites in which the residual stress normal to the interface σ_N , is tensile and the interface properties can be effectively represented by an unique sliding stress τ , the lower bound steady-state matrix cracking stress(24).

$$\sigma_o/E = \sigma^*/E - P/E_m \quad (2.1)$$

$$\text{where } \frac{\sigma^*}{E} = \left[\frac{6v_f^2 E_f \tau r_m}{(1-v)E E R} \right]^{1/2} \quad (2.2)$$

with P being the axial residual stress in the matrix. This result is independent of the matrix crack length because the crack is fully bridged by fibers(2). Measurements performed on many different glass and ceramic matrix composites have verified that this equation provides an adequate representation of matrix cracking provided that $\tau < 20\text{MPa}$ (25). Values of τ in this range have been demonstrated for fibres coated either with carbon or boron nitride.

2.1.5.2) Crack opening

The mechanical properties of uniaxially reinforced CMCs are largely governed by the relationships between the opening of a matrix crack u and the stresses τ , exerted on the crack by the intact bridging fibres and the failed fibres as they pullout. The traction $t(u)$ is well known for composites in which debonding occurs easily (very small r_i/r_f) which also slide easily along the debonded interface (small τ). Easy debonding and sliding provides a crack opening function that depends on the sign of the misfit strain, as well as the toughness of the debond interface, through their effect on the sliding resistance. Sliding can be described by a coulomb friction law

$$\tau = \mu q_N \quad (2.3)$$

In this case, prior to the incidence of fibre failure t and u are related by

$$t = \frac{2v_f E}{E_m(1 - v_f)} \left[\frac{\tau E_f}{R} \right] u^{1/2} \quad (2.4)$$

This equation is used to describe the mechanical behaviour that is obtained while the fibres are largely intact. At another extreme when all of the fibres have failed, the traction on any fibre is

$$t_i = 2v_f \tau (h_i - u)/R \quad (2.5)$$

where h_i is the distance from the matrix crack plane at which that fibre failed.

2.1.5.3) Pull-out Length

The location of fibre failure vis-a-vis the matrix crack plane is of critical importance because this location governs the pullout length h_p . Both theory(26) and experiment(27) suggest

that, for aligned reinforcements h_p is governed by weakest link statistics. For the simplest case, wherein the sliding stress τ remains constant, an expression for the mean pull-out length is

$$(2h_p/R)^{m+1} = [1/2\pi(m+1)^m](A_o/R^2)(S_o/\tau)^m \Gamma [(m+2)/(m+1)] \quad (2.6)$$

where Γ in this expression is the gamma function and A_o is a reference area for the fibres (usually set equal to 1m^2). Consequently for aligned fibres, it is evident that h_p/R is essentially governed by S_o/τ high fibre strength and low sliding resistance encourage large pull-out lengths.

2.1.5.4) Ultimate Strength

When matrix cracking precedes ultimate failure the ultimate strength coincides with fibre bundle failure. A simple estimate of this strength based on weakest link statistics that neglect interaction effects between failed fibres and ignores the stress supported by fractured fibres by means of stress transfer from the matrix through interface friction gives

$$\sigma_u = v_f S \exp - \left[\frac{(1 - (1 - \tau S/RS)^{m+1})}{(m+1)(1 - (1 - \tau S/RS)^m)} \right] \quad (2.7)$$

The effect of the sliding stress on σ_u appears directly, as well as through its effect on the crack spacings, while the effect of residual stress is presented through its effect on τ .

2.1.5.5) Toughness

For fibre reinforced ceramics which fracture by the growth of a single dominant flaw in Mode I, there are four effects which

influence toughness(28) (fig. 2.3). Debonding generates new surfaces and contributes positively to toughness. Frictional dissipation upon pullout results in local heating and again contributes positively. Residual stresses present in the material are particularly relieved by matrix cracking and debonding and thus detract from the toughness. Finally, when the fibres fail, some of the elastic energy stored in the fibre is dissipated through acoustic waves and appears as a positive contribution to toughness. The above effects are indicative of resistance-curve behaviour, because each contribution is only fully realised when the fibres fail and pullout. For the simplest, physically relevant level this toughness is given by

$$\Delta G_a = v_f [S^2/E - E(\epsilon_{ii}^T)^2 + 4\Gamma_i/R(1 - v_f)] + 2\pi v_f h_p^2 / R \quad (2.8)$$

the first term is a bridging contribution that derives from the stored strain energy dissipated as acoustic waves, with S being the reinforcement strength. The second term is the loss of residual strain energy caused by matrix crack extension and debonding. The third term reflects the new surface area caused by debonding, and the fourth term is the pullout contribution, dissipated by frictional sliding of the interfaces.

Experience indicates that the residual strain term is small in systems of practical utility and can often be neglected. The largest potential for toughness resides in the pullout term provided that h_p/R is large.

2.1.6) Fiber Reinforced Glass and Glass-Ceramic Composites

The reinforcements include large diameter($150\mu\text{m}$) filaments of

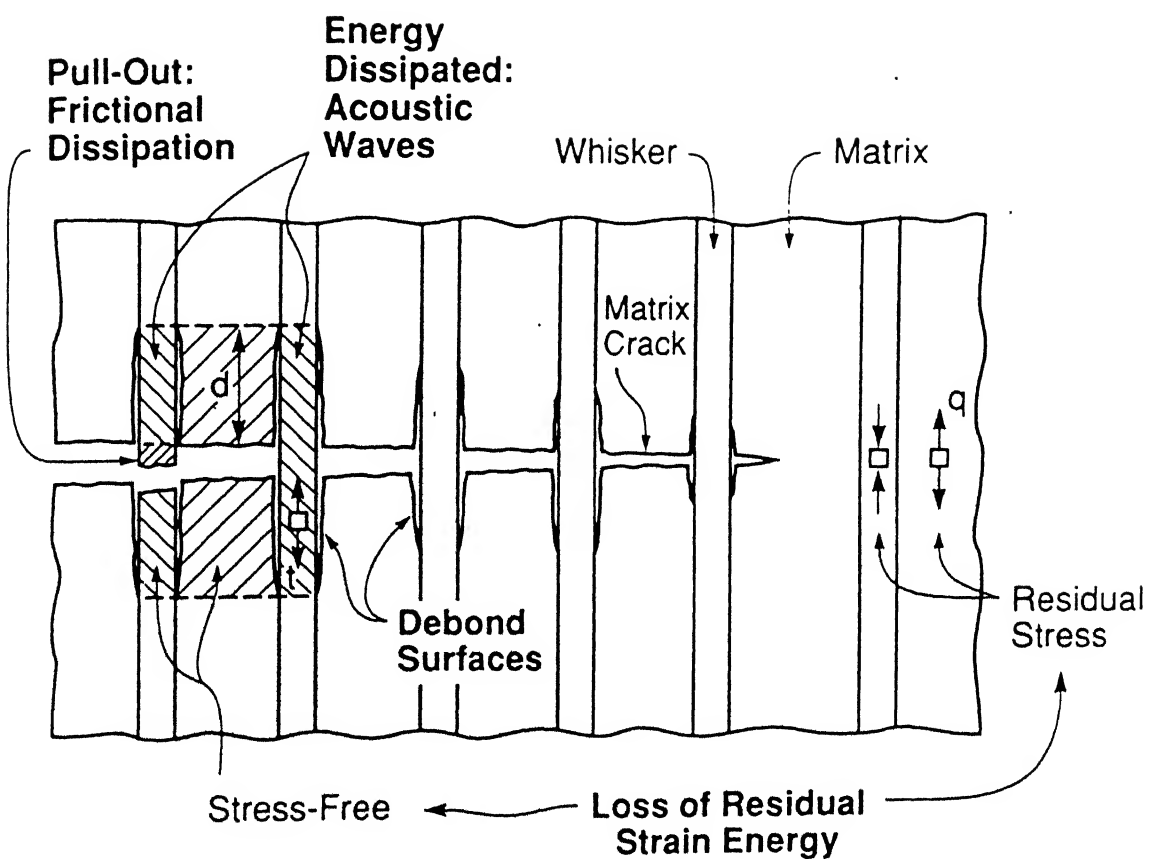


Fig. 2.3) , A schematic indicating the various contributions to the steady-state toughness in fibre composites

boron and silicon carbide, smaller diameter yarns(individual fibre diameter of 7 to 30 μ m) of graphite, alumina, aluminosilicate glasses, boron nitride and silicon carbide and whiskers of silicon carbide and silicon nitride. Till date the greatest effort has been devoted to yarn reinforced composites, particularly those reinforced with graphite fibre yarn and silicon carbide yarn.

Of these fibre reinforcements and their composites, the one that was first developed was based on graphite yarn. Graphite fibre reinforced glass matrix composites(29-31) have demonstrated a wide range of attributes which include high strength, high stiffness, excellent toughness and low density(2gms./cm³). The major disadvantage of this type of composites is that the graphite fibres are readily oxidised at elevated temperatures in air.

This limitation was overcome by replacing carbon fibre with heat-resistant silicon carbide fibre. This family of silicate matrix composites have been found to combine strength, toughness and the potential for high temperature oxidation resistance. Experiments have demonstrated that a SiC-fibre-reinforced borosilicate glass matrix(PYREX) composite system is capable of achieving excellent mechanical properties at temperatures of upto 600°C(10) and a high silica glass matrix system achieved peak strength at 1000°C(11). While these systems resulted in exceptionally high levels of fracture toughness and flexural strength, the full utilisation of the high temperature strength of the fibre reinforcement requires the use of higher temperature matrices. It is towards this goal that glass ceramic matrices like L-A-S and M-A-S have come in use(32).(fig. 2.4)

boron and silicon carbide, smaller diameter yarns(individual fibre diameter of 7 to 30 μm) of graphite, alumina, aluminosilicate glasses, boron nitride and silicon carbide and whiskers of silicon carbide and silicon nitride. Till date the greatest effort has been devoted to yarn reinforced composites, particularly those reinforced with graphite fibre yarn and silicon carbide yarn.

Of these fibre reinforcements and their composites, the one that was first developed was based on graphite yarn. Graphite fibre reinforced glass matrix composites(29-31) have demonstrated a wide range of attributes which include high strength, high stiffness, excellent toughness and low density(2gms./cm³). The major disadvantage of this type of composites is that the graphite fibres are readily oxidised at elevated temperatures in air.

This limitation was overcome by replacing carbon fibre with heat-resistant silicon carbide fibre. This family of silicate matrix composites have been found to combine strength, toughness and the potential for high temperature oxidation resistance. Experiments have demonstrated that a SiC-fibre-reinforced borosilicate glass matrix(PYREX) composite system is capable of achieving excellent mechanical properties at temperatures of upto 600°C(10) and a high silica glass matrix system achieved peak strength at 1000°C(11). While these systems resulted in exceptionally high levels of fracture toughness and flexural strength, the full utilisation of the high temperature strength of the fibre reinforcement requires the use of higher temperature matrices. It is towards this goal that glass ceramic matrices like L-A-S and M-A-S have come in use(32).(fig. 2.4)

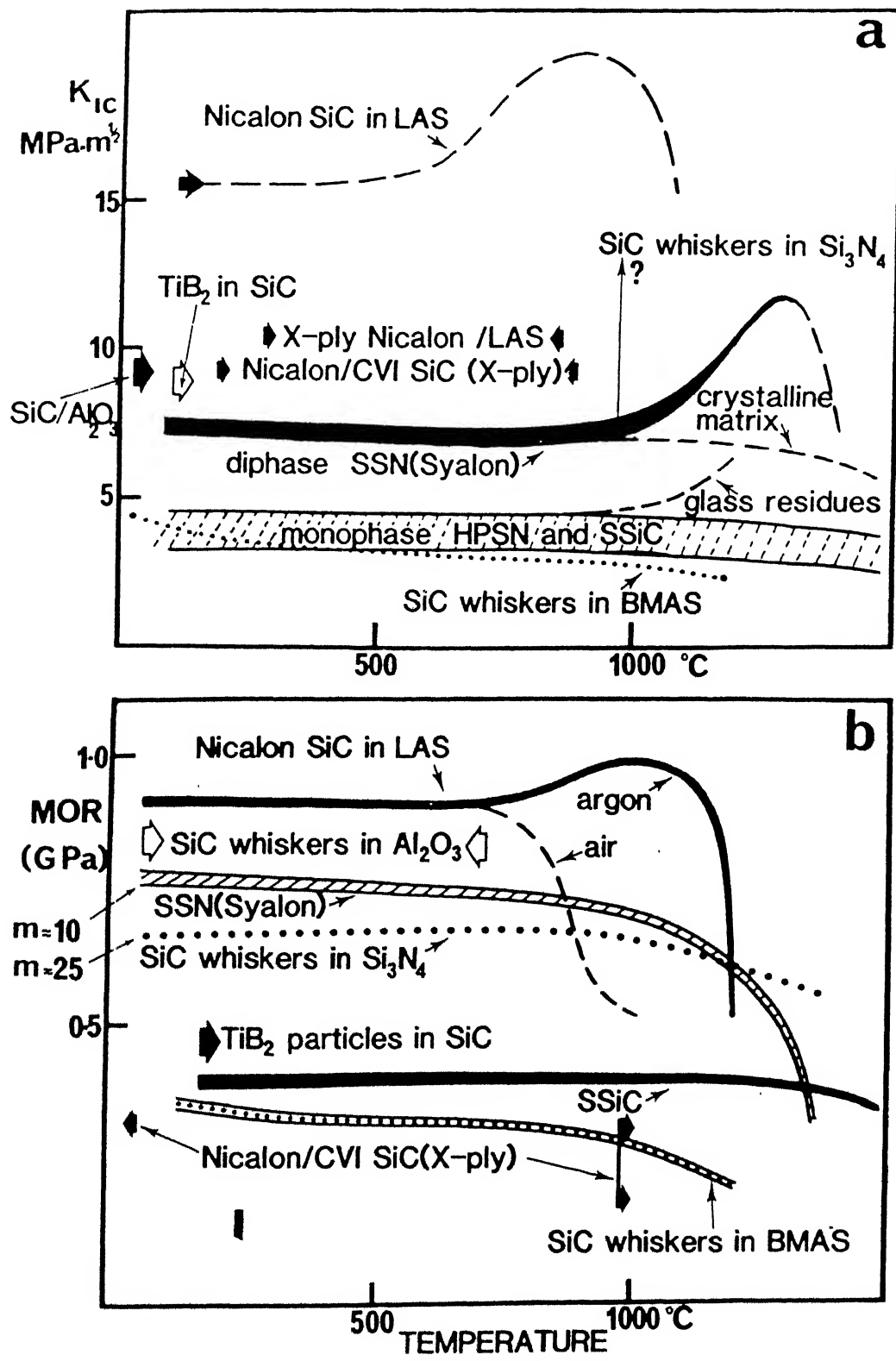


Fig. 2.4) Comparison of the MOR and K_{IC} vaalues for various composite systems and their temperature dependence.

2.2) Whisker Reinforced Ceramic Composites

Composites reinforced with continuous fibres generally display higher levels of strength and toughness than similar composites reinforced with whiskers or short fibres. However, the processing temperatures necessary to fully densify or infiltrate the particular matrix are often above the range of thermodynamic stability for most continuous fibres presently available(33-36). Furthermore, the fabrication of near-net-shape components is generally more difficult(if not impossible) for composites reinforced with continuous fibres as opposed to the other reinforcement types.

Because of recognised limitations of continuous fibre composites, much attention has been focussed on whisker-reinforced composites with matrices such as alumina, mullite, glass and glass-ceramic and to a lesser extent zirconia and silicon nitride and whiskers primarily of silicon carbide and to a lesser extent silicon nitride(37-59). Most of the work has been carried out on Al_2O_3 -SiC(w) system(41).

These studies revealed that the relative improvements in strength and fracture toughness compared to the unreinforced matrix differ substantially in ostensibly similar materials. Among the possible causes of these phenomena were the different interactions between the matrix and whisker properties, such as elastic modulus mismatch, thermal expansivity mismatch(causing thermally induced residual stresses) and chemical interactions, all of which varied with the particular matrix.

In order that a particular whisker and matrix will combine to form a successful composite, the following points must be

considered.

- 1) the difference between the co-efficient of thermal expansion of the whisker(α_w) and that of the matrix(α_m)
- 2) elastic moduli of the matrix(E_m) and the whisker(E_w)
- 3) chemical compatibility between the whisker and matrix at processing temperatures.

If $\alpha_w > \alpha_m$, the matrix is under radial tension and tangential compression and the whiskers under tension. Precompression of the matrix by the whiskers(such as SiC whiskers in codierite, mullite and Si_3N_4 , glass and glass-ceramics) would result in strengthening. If $\alpha_w < \alpha_m$, the matrix is under tangential tension and the fibre under compression. This applies to SiC whiskers in Al_2O_3 , ZrO_2 and B_4C matrices. In these cases, radial tensile stresses are introduced across the whisker-matrix bond which can influence the whisker-matrix interfacial shear strength. If sufficient tensile stresses develop in the matrix, microcracking may occur to further absorb cracking energy and enhance K_{Ic} (28,60).

2.2.1) Whiskers

Recent advances in whisker reinforced ceramic-matrix composites have been made possible, in part by the availability of ceramic whiskers in large quantities at a relatively moderate cost. The whiskers, primarily SiC, are commonly made by either the carbothermal reduction process, that is the rice hull process, or by the recently developed vapour-liquid-solid process. In the former rice hulls are calcined at approximately $900^{\circ}C$, prior to pyrolysis at $1700^{\circ}C$ to form SiC whiskers(61). For this process, the production cost is modest and there are no intrinsic

difficulties in scaling production to large quantities. The SiC whiskers produced from the rice hull process are typically less than $1\mu\text{m}$ in diameter and range from 10 to $50\mu\text{m}$ in length. They are characterised by a structure that is heavily faulted, consisting of planar defects in the closed-packed planes perpendicular to the growth direction, that is the long axis of the whiskers(62-64). The planar defects are a result of the arrangement of regions of the α and β polytypes of SiC. Impurities, for example Al, Mn, Mg, Fe and Ca and internal voids can also be present in the SiC whiskers. Furthermore, the surface chemistry tends to differ from that of the bulk in that the surfaces tend to be oxygen rich(51). Surface species commonly identified resemble either crystalline SiO_2 or amorphous Si-O-C(65).

In the vapour-liquid-solid process, hydrocarbons(e.g. CH_4) and SiO feed vapours are reacted to approximately 1400°C via a molten metal catalyst, to precipitate SiC whiskers(66). For this process, although production quantities are currently small and prices are quite high, the prognosis for modest cost whiskers is also good. The vapour-liquid-solid process is capable of producing whiskers in a variety of microstructures, but the typical dimensions are $5\text{-}6\mu\text{m}$ in diameter and upto $100\mu\text{m}$ in length. They are usually in the β form of SiC and exhibit a lesser degree of internal defects than rice hull whiskers(67).

Intrinsic thermal and chemical stability of ceramic whiskers is of great importance especially at elevated temperatures. They are single crystals of stoichiometric compounds with no tendency for oxidation, recrystallisation, internal chemical reactions, or other detrimental process. SiC whiskers are the most promising

reinforcements to date, as they retain their mechanical properties up to at least 1600°C.(67)

The only problem with whisker reinforcements is that they are difficult to handle and cause health hazard to the workers. Hence careful handling is needed. Secondly beyond 50 vol% whiskers in the composite, they have a tendency to agglomerate giving rise to defects during the processing.

2.2.2) Mixing and Compact Formation.

Two important objectives during whisker composite processing are:

- a) attainment of uniform distribution of whiskers
 - b) minimisation of mechanical and/or chemical damage to whiskers.
- These objectives must be borne in mind during preform fabrication, and also at the densification stage. Preform fabrication is commonly performed at room temperature while densification occurs at high temperatures(1000°C-2000°C).

Processing methods for whisker reinforced ceramics have developed from established methods used to process monolithic ceramics. An important advantage of whisker reinforced ceramics over continuous fibre reinforcement is that these well known processing techniques can be applied. However there is a major problem associated with the processing of whisker composites. Since whiskers are harvested and handled as dry ceramic powders, a high degree of whisker agglomeration is common. This leads to difficulties in dispersing whiskers and mixing them uniformly with matrix powders. Typical processing flaws observed in composites are primarily clusters of whiskers devoid of matrix. Additional

residual contamination in whiskers, particulates and foreign particles can also provide potential failure origins in composites.

However these potential flaw types can be eliminated by flotation and sedimentation techniques. Blends of whiskers and matrix powders can usually be processed by conventional means. A typical processing procedure consists of the following (fig. 2.5):

- 1) whisker purification by sedimentation to remove whisker agglomerates and particulates.
- 2) mixing of matrix powders and appropriate sintering aids by milling
- 3) mixing of matrix powders and whiskers by high speed blending and/or ultrasonic dispersion in a liquid medium by controlling the p^H of the medium.
- 4) drying to remove the liquid medium
- 5) shape forming by cold pressing, injection moulding or slip casting
- 6) densification by hot-pressing or sintering and/or hot isostatic pressing.

2.2.3) Densification Techniques

2.2.3.1) Hot Pressing

Hot pressing is the most popularly used process for producing dense composites. Whisker/matrix powder mixtures are typically pressed at temperatures from $1000\text{--}2000^\circ\text{C}$ in carbon or graphite dies. Hot pressing times and pressures for the commonly used systems are typically of the order of 30–3000 minutes and 30–70 MPa respectively. The use of a vacuum or inert atmospheres (e.g. argon)

WHISKER REINFORCED CERAMICS

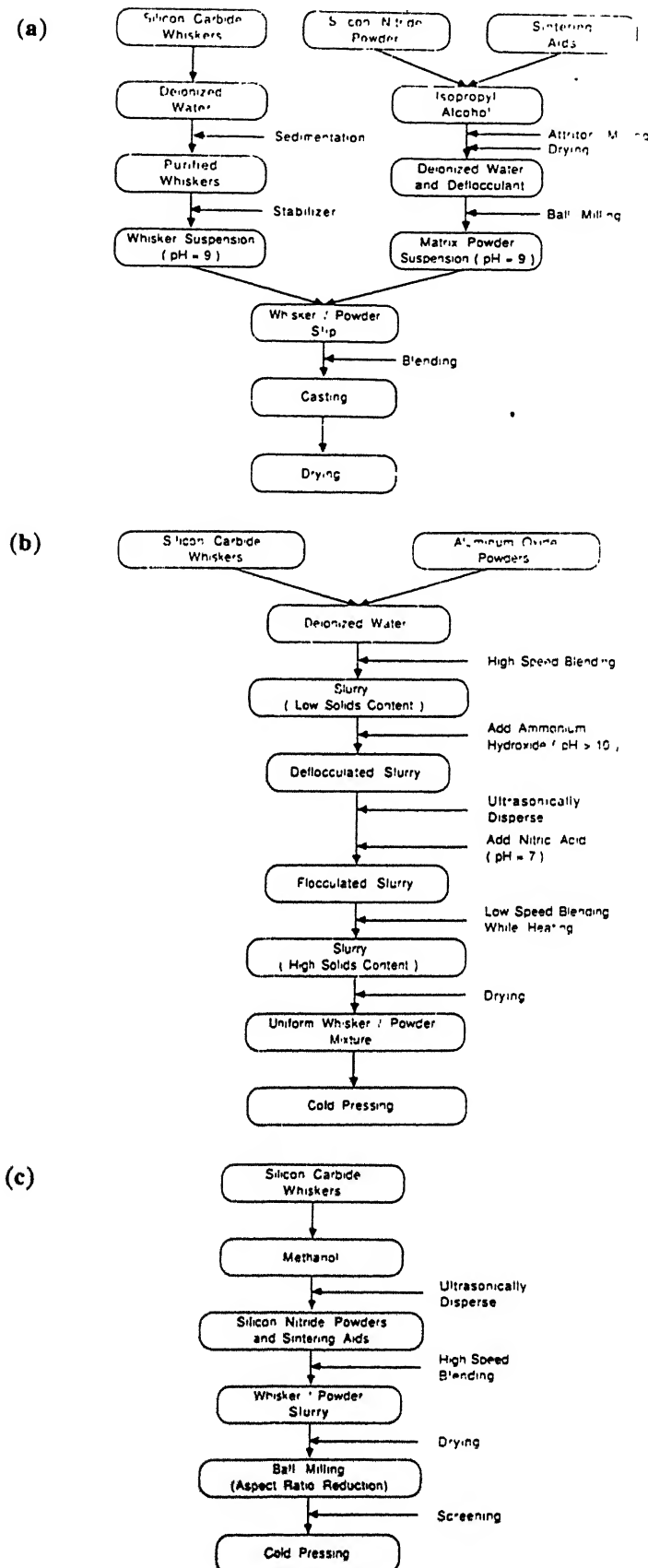


Fig. 2.5) Flow chart for the fabrication of whisker reinforced ceramics.

during hot pressing are necessary to prevent oxidation of the carbon or graphite dies and non-oxide components of the composites.

Numerous researchers have examined the effect of hot pressing parameters on the densification of whisker reinforced ceramics. Wei and Becher(41) performed extensive densification studies on SiC whisker/ Al_2O_3 matrix composites. They found that the densification rate was a function of hot pressing temperature and time. Homeney et.al.(49) examined the effect of hot pressing temperature and time on the densification of the same composite system. They found that the percent theoretical density increased with increasing time at a constant temperature or with increasing temperature at a constant time. However, it was noted that at the highest temperatures employed slight decreases in densities were observed, possible due to loss of material through the vapour phase. Buljian et.al.(50) examined the densification rate as a function of whisker content for SiCwhisker/ Si_3N_4 matrix composites. They found that the densification rate decreased with increasing whisker content and concluded that the whiskers substantially inhibited grain rearrangement.

2.2.3.2) Pressureless Sintering/Hot Isostatic Pressing(HIP)

Though hot pressing results in dense composites, it cannot be used to form very complex shapes. For achieving complex shapes pressureless sintering/hot isostatic pressing route has to be adopted. If composites of complex shapes can be sintered to the state where only closed porosity exists, then final densification can be achieved by hot isostatic pressing(HIP). Typical sintering and HIPing temperatures range from 1000-2000°C. Pressures upto

200MPa are employed during HIPing.

Several investigators have fabricated composites by sintering and/or HIPing. Tiegs and Becher(42) have demonstrated that SiC whisker/ Al_2O_3 matrix composites with less than 10vol% whiskers can be sintered to greater than 95% of theoretical density and subsequently HIPed without encapsulation to greater than 98% of the theoretical density. For whisker loadings greater than 10vol%, densification was severely inhibited since composites with open porosity were obtained. SiC whisker/ Si_3N_4 matrix composites were slip cast and sintered by Hoffman et.al.(68). They found that with increasing whisker content, from 0 to 20vol% sintered densities decreased from 98% to 88% of the theoretical density. Pezzotti et.al.(69) and Bjork and Hermansson(70) used HIPing successfully to densify SiC whisker/ Si_3N_4 matrix and SiC whisker/ Al_2O_3 matrix composites respectively. Composite preforms were presintered at a relatively low temperature to remove organic binders during cold pressing and encapsulated in glass prior to HIPing.

2.2.4) Mechanical Behaviour

2.2.4.1) Strength

The general theory of fibre reinforcement suggests that significant strengthening will occur if the elastic modulus of the fibre is greater than that of the matrix and if tensile stresses can be transferred to fibres(71,72). When the fibres are discontinuous as for whiskers, the difference of the strains in the whisker and matrix near a whisker end induces shear stress along the whisker axes. The shear forces acting near both ends of a whisker stress the whisker in tension. Through this transferring

of stress, the applied load can be dispersed among the whiskers.

The load transfer can be discussed using the concept of critical whisker length defined as the minimum length of whisker required for the stress to build upto the fracture strength of the whisker(σ_w). Assuming a simple relation which gives a linear build-up of stress from the whisker ends(73) the critical whisker length l_c is given by(74)

$$l_c = d\sigma_w / 2\tau \quad (2.9)$$

where τ denotes the interfacial shear stress and d the fibre diameter. It follows from the equation that l_c is dependent on τ and hence the strength of the composite material will depend on the strength of the interface.

Equation(2.9) is based on the assumption that the matrix is elastic-perfectly plastic, which results in a constant shear stress equal to the matrix yield stress at the interface. This assumption is not applicable to glass or glass-ceramics. Equation(2.8) however is applicable to a purely frictional bond. It has been indicated in(75) that a poor interface bond does not favour load transfer.

For long uniaxial fibre the composite strength is given by a simple law of mixtures(76) as

$$\sigma_c = v_f \sigma_{fu} + (1-v_f) \sigma_m \quad (2.10)$$

where σ_c is the composite strength, σ_{fu} and σ_m the fibre and matrix strengths respectively and v_f the volume fraction of the fibres in the composite.

For whisker reinforcements whose actual length is l and the critical length(refering to equation(2.9)) l_c this equation(2.10) cannot be applied in the above form. Here the load transfer is

restricted to the length l of the whisker and the efficiency of the load transfer is incorporated in the critical length term l_c . So the equation(2.10) for continuous fibres has to be modified for whisker composites.

$$\sigma_a = v_f \sigma_{fu} (1 - l_c / 2l) + (1 - v_f) \sigma_m \quad (2.11)$$

This equation is applicable when the whiskers are aligned in the direction of the applied stress. When the whiskers are not aligned in the direction of the applied stress a orientation term $\cos\phi$ has to be introduced(where ϕ is the mean angle of the whiskers to the direction of the applied stress).

$$\sigma_a = v_f \sigma_{fu} (1 - l_c / 2l) (\cos\phi)^4 + (1 - v_f) \sigma_m \quad (2.12)$$

Clearly angles much greater than 15° produce a rapid decline in the apparent strength for 60° the whiskers are apparently only $1/16$ as effective. Hence to get the maximum benefit from the whiskers reinforcements they should be aligned in the direction of the applied stress.

2.2.4.2) Toughening Mechanisms

Numerous investigators(77-79) have reviewed the toughening mechanisms relevant to whisker reinforced ceramic composites. The important toughening mechanisms relevant to whisker reinforcements are:

- I) Crack Deflection: It can contribute significantly to the fracture toughness, but calculations of toughening increments by

this mechanism indicate a maximum potential increase of 50-100%. This mechanism forces the crack out of the plane rather than through the whisker, that is the crack plane is no longer normal to the applied stress (fig 2.6b). Deflection results from residual stresses generated from either thermal expansion mismatches between the matrix and whiskers or from thermal expansion anisotropy in the whiskers, elastic mismatches between the matrix and whiskers which perturb local stress fields, or weak whisker/matrix interfacial bonding which offers the crack a low resistance path. This mechanism also requires a high whisker volume fraction. Crack deflection has the beneficial effects of increasing fracture surface area, increasing the energy absorbed during fracture and forcing mixed mode fracture. The shift from mode I to mode II and III greatly increases the difficulty in crack propagation, since K_{Ic} and K_{IIIc} are typically much higher than K_{Ic} in brittle materials.

The toughness predictions are invariant with particle size. The increase in toughness only depends on particle shape and the volume fraction of the second phase. The most effective morphology for deflecting propagating cracks is the rod of high aspect ratio. (fig. 2.6). which can account for four fold increases in fracture toughness. The toughening arises primarily from twist of the crack front between particles, as indicated from figure(2.6). Less effective in toughnening are disc-shaped particles and spheres, respectively.

II) Microcracking: microcracking can contribute significantly to the fracture toughness. This mechanism requires microcracks, either pre-existing or created during fracture, that decrease the stress

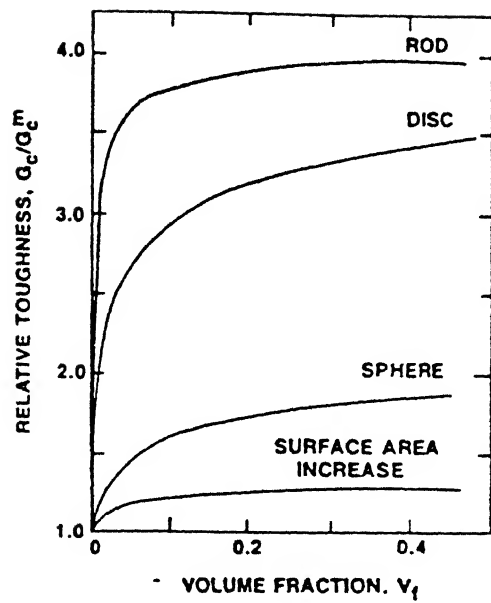


Fig. 2.6a) Shape effect on the strengthening of composite systems.

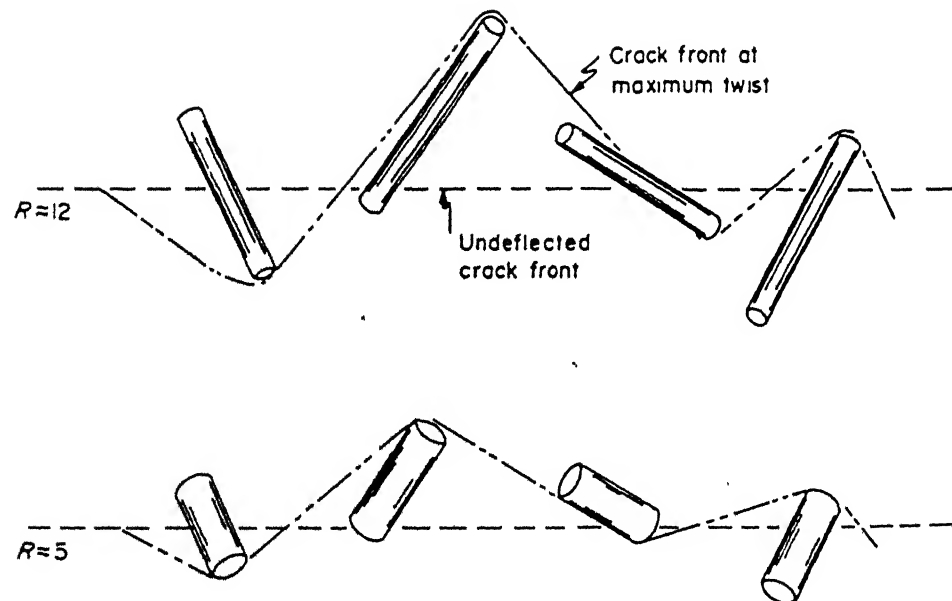


Fig. 2.6b) Effect of L/D ratio on the toughness of composite systems.

intensity at the main crack tip. Microcrack generation requires either dispersed second phases with large thermal expansion anisotropy or large expansion mismatches between the dispersoid second phases and the matrix. Large elastic mismatches between the dispersed second phases and the matrix may also interact with the stress field of the approaching crack and generate large stresses in the vicinity of the dispersed second phases. The main drawback to microcracking toughening is that it is limited to a narrow range of materials exhibiting significant anisotropy or mismatch.

III) Crack Bridging: crack bridging is a highly significant toughening mechanism. It requires that unfractured whiskers bridge the crack behind the crack tip. The closure forces exerted by the bridging whiskers reduce the crack opening displacement and the stress intensity at the crack tip. The operation of this mechanism generally requires strong whisker/matrix interfacial bonding, with a substantially higher strain to failure of the whiskers compared to the matrix. Whisker orientation is critical, as whiskers at a substantial angle to the normal to the crack plane will be subjected to shear and bending stresses and may not provide much bridging.

IV) Whisker Pull-out: whisker pull-out is also potentially a significant toughening mechanism. The mechanism requires relatively weak whisker/matrix interfacial bonding. As the whiskers pullout, the energy absorbed during crack propagation increases by the amount required to overcome the frictional forces at the whisker/matrix interface. The whisker orientation is an important factor, highly oriented whiskers normal to the crack plane being the most effective.

2.2.5) Strength and Toughness Increases in Glass and Glass-Ceramic Composites

Reinforcement of glasses and glass-ceramics by silicon carbide whiskers result in upto fourfold improvement in strength and fracture toughness. For an aluminoborosilicate glass strength increased from 100 to 340MPa and fracture toughness from 1 to $5\text{ MPa}\cdot\text{m}^{1/2}$ (37). The increase in fracture toughness appears to result mainly from a crack deflection mechanism. The presence of alkali-metal oxides in the matrix and the large thermal expansion mismatch between the whiskers and the matrix degrade the mechanical properties of the composite. The retention of a large fraction of room-temperature strength and toughness to elevated temperatures was found to be controlled by the presence of a residual glass phase in the matrix. A Ba-stuffed cordierite matrix with 25vol% whiskers had a strength of 215MPa at 1200°C a 60% retention of room-temperature strength(37). For M-A-S glass-ceramics with addition of 20% SiC whiskers the strength increased to 316MPa(which is twice the MOR value for the monolithic M-A-S glass-ceramic). Toughness values peaked at $4\text{ MPa}\cdot\text{m}^{1/2}$ (80). The dominant toughening mechanism was crack deflection with little evidence for whisker pull-out. For the PYREX-SiC composite, there is more than a two fold increment in MOR and K_{Ic} values over those for PYREX glass(80). Crack deflection depressions are clear on fracture surface. Whisker pull-out is limited by the irregular whisker shape and the good whisker/PYREX interface cohesion. Microcracks related to the presence of the α -cristobalite have a rather large size and may lead to the

composite failure.

For Si_3N_4 and SiC whiskers in aluminosilicate glass(code 1723) and borosilicate glass(code 7740) PYREX the composites exhibited room temperature flexural strengths of 140MPa with linear load-deflection curves to the point of fracture and very brittle surfaces with essentially no whisker pullout(12). The strength of a 7740(PYREX) glass bar tested in flexure under similar conditions was 60MPa. Thus the whiskers strengthened the glass, but did not change its fracture characteristics appreciably. Further VLS grown SiC whiskers were incorporated in both 1723 aluminosilicate glass and L-A-S glass-ceramic matrices. While some of the composites attained flexural strengths of 276 MPa, the basic brittle nature of the fracture surface and linear load-deflection curves were still in evidence.

In the work of Wei and Becher(41) on Al_2O_3 /SiC whisker composites, the composites were hot pressed at 1850°C and 41 MPa. They have done extensive mechanical property evaluation of this system. The room-temperature flexural strength of the 20vol% SiC whisker composite with the CR-10 alumina matrix was 805MPa as compared to a value of 600 MPa for the LindeA alumina-matrix material. Depending on the type of Al_2O_3 matrix, the strength decreased to 520 MPa or 450 MPa at 1200°C . The fracture mode appears brittle, no serrations in the load vs. deflection curves(at room temperature or at 1200°C) were observed. The fracture toughness values of the 20 vol% SiC whisker/ Al_2O_3 matrix composites were substantially greater than those of single-phase monolithic ceramics. The K_{Ic} values for the CR-10 Al_2O_3 composites was around $9 \text{ MPa m}^{1/2}$ and LindeA Al_2O_3 composite was $8.6 \text{ MPa m}^{1/2}$.

Observation of the fractured surfaces indicated whisker pullout in both the types of composites. Deflection of cracks by the whiskers also appears to be operative, especially in the case of crack propagation in the direction perpendicular to the hot pressing axis. The mechanical properties of the various whisker composite systems is listed in table (2.5)

2.3) Platelet Composites

Many materials grow naturally in platelet form and though platelets are not normally as strong as whiskers they can still have strength comparable to the whiskers. Some of the materials found in platelet form are Al_2O_3 , TiB_2 , mica and SiC. Of these single crystal SiC platelets are the most potential reinforcements. SiC platelets have edges which are parallel to the important directions of crystal. Thus they have hexagonal or eqilateral triangular shape. Mica(which is also found to have platelet form) on the other hand is produced in irregular shapes, due to the grinding it has been subjected to after mining. The imperfections of edges cause the strength of mica platelets to be much less than the potential strength of the material. In composites mica appears to break at 0.85 GPa compared to the potential strength of 2.7 GPa for mica not weakened by edge effect. Platelets have the advantage over fibres and whiskers in the fact, that when suitably, oriented they can stiffen a material in two dimensions rather than only one. However they cannot impart as much strength to composite as one might expect owing to interactions between nearest neighbour platelets(81).

Table I. Properties of LAS and CAS Matrix/SiC Whisker Composites (30 vol% Whiskers)

Comp. No.	Matrix	Whisker	Flex Strength (MPa)			RT K_Ic (MPa·m ^{1/2})
			RT	800°C	1000°C	
289-88 290-88 718-88 645-89 96-89 359-88	Corning 9608 LAS LAS LAS CAS LAS LAS	AC-1	103		<69	0.85
		TK-1	393	400	290	4.44
		TK-2	338	496	248	4.20
		TK-2	372	358	310	4.06
		AMI	363	348	276	4.98
		LANL	193	207	110	2.83
			110	131	69	2.24

Whisker content (vol%) (β_i)	Matrix material	Fracture strength (MPa)	Fracture toughness (MPa m ^{1/2})	Test temperature (°C)	References
0	Mullite	201	2.45	25	[33]
30 ^a	Mullite	386	3.52	25	[33]
30 ^c	Mullite	329	3.60	25	[33]
0	Mullite	-	2.2	25	[11]
20 ^a	Mullite	440	4.6	25	[11]
0	ZrO ₂	1150	6.0	25	[34]
20 ^c	ZrO ₂	600	10.5	25	[34]
30 ^c	ZrO ₂	600	11.0	25	[34]
0	MoSi ₂	150	5.3	25	[35]
20 ^b	MoSi ₂	310	8.2	25	[35]
0	Alumino-borosilicate glass	103	1.0	25	[36]
35 ^a	Alumino-borosilicate glass	327	5.1	25	[36]

Table 2.5) Mechanical Properties of the various whisker composite systems.

CENTRAL LIBRARY
I.I.T., KANPUR

Acc. No. A. 116271

2.3.2) Fabrication of Platelet Composites

Platelet-reinforced composites are processed using the simple powder processing routes used for monolithic ceramics. The platelets grown in the natural form do not agglomerate like whiskers. This is the main advantage that platelet reinforced composites have over whisker composites. Their manufacture via the powder processing route(analogous to the manufacture of monolithics) is much less problematic than that of fiber and whisker reinforced composites i.e. it involves no health hazard, yields better homogeneity requires less sophisticated technology and is therefore less expensive.

2.3.3) Mechanical Behaviour

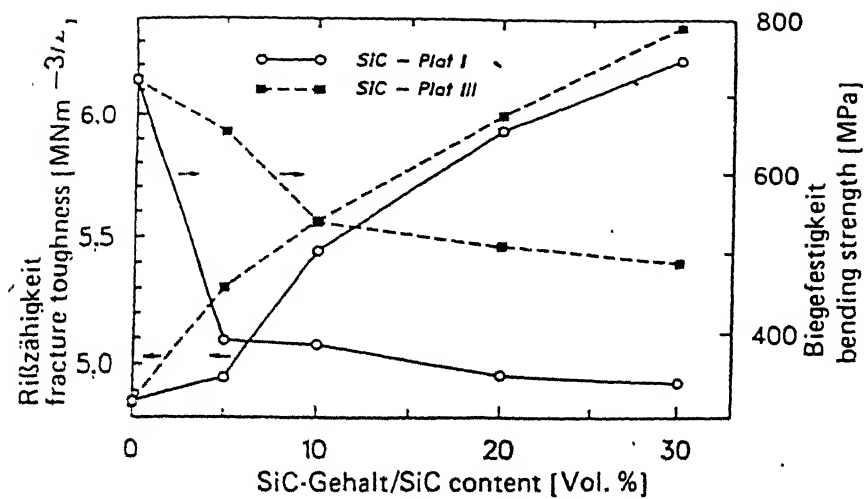
Very less work has been done on the platelet reinforced composites. Some of the work carried out on platelet reinforced composites relates to the use of Al_2O_3 , TiB_2 and SiC platelets in composite systems(82-83).

The strengthening mechanisms for the platelet reinforced composites follows on the same lines of whisker composites i.e. load transfer from the matrix to the platelets.

Results of platelet reinforcement experiments show promising toughness values. The reinforcing mechanisms apparently consist mainly of crack deflection and for an optimal interfacial structure, crack bridging and pullout. One of the main problems encountered is that the size of the presently available platelets(10 to 100 μm) can cause a loss of strength because the critical size of the flaws appears to be controlled by the largest

platelets. Major gains in strength levels are anticipated for smaller platelets and/or orientation of the platelets in parallel with the effective tensile stress.

In one work carried out on SiC-platelet reinforced reaction bonded silicon nitride(HIPed) by Claussen(84) they have used SiC platelets from two sources(fig 2.7). The mean particle size of the two kinds of platelets was $70\mu\text{m}$ and $12\mu\text{m}$. The results are shown in the figure(2.6). They observed that the K_{ic} values were around $8\text{MPa.m}^{1/2}$ and the MOR values were around 600MPa . Major gains in strength and toughness were achieved for the smaller size platelets where the mean particle size was $12\mu\text{m}$.



SiC-plat I:
 (American Matrix, USA)
 mean particle size 70 µm
 variation 5–200 µm
 SiC-plat II:
 (C-Axis Techn., Canada)
 mean particle size 12 µm
 variation 5–20 µm
 Additive 1.75 wt.% $\text{Y}_2\text{O}_3 + \text{Al}_2\text{O}_3$
 HIP 1 850 °C/180 MPa

Fig. 2.7) Fracture toughness and bending strength of SiC-platelet reinforced silicon nitride.

2.4) Superplasticity in Glass-Ceramic Composites

The term superplasticity is used for those materials where tensile elongations of several hundred percent can be achieved, provided that the experiments are carried out within a certain range of strain rates and temperatures. The large elongations are a result of high strain-rate-sensitivity(m) of the material and fracture resistance. The strain-rate-sensitivity is defined as m in the constitutive equation for flow:

$$\dot{\epsilon}_e = k \sigma_e^n \quad (2.13)$$

or

$$\dot{\sigma}_e = k' \dot{\epsilon}_e^m \quad (2.14)$$

where $m = 1/n$, $\dot{\epsilon}_e$ is the effective strain rate, σ_e the effective stress, and k and k' are constants which depend on microstructure and temperature. The strain-rate-sensitivity in general is between 0 and 1. When $m = 1$, equation(2.14) reduces to the equation for newtonian viscous flow. Glass, which obeys this equation, owes its high formability to m being equal to 1. The physical reason as to why a high strain-rate-sensitivity leads to large tensile elongations is that it slows the rate of growth of a defect along the gauge length of the specimen. However only high strain rate sensitivity is not a sufficient condition for superplasticity. In addition to high strain sensitivity the material should have high fracture strength at forming temperatures.

Among various studies on the superplasticity of structural ceramics, the zirconia based ceramics have received more attention so far (85-87). The microstructural features of interest for

achieving superplasticity in ceramics are grain size and shape while the grains should be equiaxed, the grain size requirement for ceramics is of the order of submicron which is much finer than that of metals ($\leq 10\mu\text{m}$) (88). The requirement of submicron grain size is to promote the grain boundary diffusion and prevent the cavity nucleation at the grain boundaries. Although enhanced plasticity in compression gives an indication of superplasticity in these materials, obtaining a high elongation to failure in tension is essential because samples which exhibit superplasticity in compression, may fail prematurely in tension by grain boundary separation or cavitation. Hence most of the recent studies in ceramics have been mainly on tensile samples. For example, alumina, the main high temperature structural material, exhibits superplasticity at 1460°C with a tensile elongation of 50-65% under an applied stress of 30 MPa (89).

3 Vol% yttria stabilised tetragonal Zirconia (3YT2P) was the first polycrystalline ceramic which has been drawn strated to be truly superplastic (90,91). Wakai et. al (90) obtained 200% elongation with a grain size of $0.3\mu\text{m}$. Later Nien et. al (91) reported an elongation of 800% in a similar material tested at 1550°C and a strain rate of $8.3 \times 10^{-5} \text{ s}^{-1}$; now elongation of grater than 200% are obtained in zirconia.

Further Wakai et. al (92) systematically studied the superplastic properties of $\text{ZrO}_2\text{-Al}_2\text{O}_3$ composites with various additions of Al_2O_3 i.e. ranging from 20-80 wt%. Elongation to failure decreases with increasing alumina content, the higher than 120% elongation was obtained in the $\text{ZrO}_2\text{-80 wt% Al}_2\text{O}_3$ tested at 1550°C and a strain rate of $2.8 \times 10^{-4} \text{ s}^{-1}$. A maximum elongation of

500% (with $m = 0.5$) has been reported in Y-T2P composite containing 20wt% Al_2O_3 (93). Beyond this elongation, the ductility is restricted due to nucleation of cavities at $\text{ZrO}_2/\text{Al}_2\text{O}_3$ and $\text{ZrO}_2/\text{ZrO}_2$ influences. A similar study has also been carried out on ZrO_2 - mullite composites (94).

A good example of a non-oxide composite material exhibiting superplasticity is a fine grained Si_3N_4 -20wt% SiC, which is prepared from amorphous Si-C-N powder (produced by vapour phase reaction) with sintering aids of $\text{Y}_2\text{O}_3+\text{Al}_2\text{O}_3$. This composite exhibited an elongation of over 150% at 1600°C and a strain rate of $4 \times 10^{-5} \text{ s}^{-1}$ (85). The sintering aids formed a substantial amount of intergranular liquid at 1600°C and could resist cavitation during elongation. However problems such as composite grain growth of β grain and deterioration of surface quality due to evaporation of grain boundary liquid, need to be solved.

The situation in most of the glass-ceramics having an in-situ crystalline phase is similar to a polycrystalline ceramics with grain boundary phase. Wang and Raj(97) performed experiments on two β -spodumene glass-ceramic materials. They found that, within their range of deformation variables, large tensile elongations could be obtained. The ductility was found to be limited, however, not by strain-rate-sensitivity, but by the onset of intergranular failure.

The two most important creep deformation mechanisms are the diffusional creep and power-law creep. Diffusional creep leads to a strain-rate-sensitivity of unity. This mechanism is independent

of flow caused by dislocations in the crystal matrix. The latter usually has a power-law stress dependence where $n = 5$ (or $m = 0.2$) when the bonding is metallic or ionic. Since diffusional creep and power-law creep are additive mechanisms of deformation the following type of flow equation results:

$$\dot{\epsilon}_e = k_d \sigma_e + k_p \sigma_e^5 \quad (2.15)$$

where k_d and k_p are related to diffusional creep and power law creep respectively. To obtain superplastic flow, the first term in the equation(2.15) must be dominant. In ceramic materials crystal bonds are strong, so that dislocations are difficult to move. This means that the second term in the equation is likely to be weaker than the diffusional creep term, increasing the chances of obtaining superplastic flow. The probability is even higher if the rate of diffusion along the grain boundary can be enhanced by a fluid phase. From this point of view, the fine-grained glass-ceramic materials, including those materials which are processed using a liquid phase, are excellent candidates for superplastic flow.

The flow equations for ceramic poly-crystals which contain some fluid phase have been considered by several authors most recently by Raj(95) and Pharr and Ashby(96). The difference between the latter two models is that in one(95) all deformation accrues by the transport of atoms through the liquid phase and in the other(96) the fluid is assumed to corrode the neck region when the nearly spherical crystal grains press against each other. As a result, the contact stresses are assumed to corrode the neck region when the nearly spherical crystal grains press against each other. As a result, the contact stresses are assumed to increase

to a point where plastic deformation by crystal dislocations occurs. The flattened regions are resharpened by liquid corrosion. However this mechanism has limited applicability to ceramic systems because of the absence of dislocation motion in ceramic systems.

The first model depends on the postulate that the atomic structure of the two-grain junctions consists of islands where adjacent crystals meet and an interpenetration liquid phase. The islands support normal stress and normal stress gradients, whereas the liquid expedites the transport of matter. If x is the area fraction of the islands then the model leads to the following equations.

$$\sigma_s = (\sigma_s \Omega / kT) (k_4^4 c / L) [1/(1-x)] \quad (2.16)$$

or

$$\sigma_s = (2.3 \sigma_s \Omega L \alpha / \eta L^3) [1/(1-x)] \quad (2.17)$$

where Ω is the atomic volume, L the grain size, $k_4^4 c$ the linear growth velocity of the interface for a driving force of 1 $kT/\text{molecule}$, η the fluid viscosity, c the equilibrium solubility of the crystal in the fluid, and α a constant of the order unity.

Equation(2.6) is valid when the strain rate is controlled by the interface reaction between the crystal and the fluid and equation(2.7) is valid when the diffusion of matter through the fluid is rate-limiting. The slower of the two equations will limit the rate of deformation.

2.5) OBJECTIVES OF THE WORK

From the literature survey it has emerged that most of the work on discontinuous reinforcements has concentrated on whisker reinforced composites. Much less work has been carried out on platelet reinforced composites. Some of the work carried out on platelet reinforced composites relates to the use of Al_2O_3 , TiB_2 & SiC platelets in composite systems (82,83). No work has been reported for platelet reinforced glass & glass ceramics. Glass and glass - ceramic composites have emerged as leading contenders for composite system because of their ease of fabrication. From the fig. (2.6a). (shape effect on the strengthening of composite systems) platelets have excellent potential for use in composite systems. Other discontinuous reinforcements like whiskers have the inherent problems of agglomeration and are hazardous. The main objective of this work is to study the relatively unexplored field of platelet reinforced glass - ceramic composites.

In this investigation, the matrix material used is Pyrex glass whereas the reinforcement is SiC platelets. The pyrex glass has some special characteristics which make it an ideal choice for use in composite systems. It has a very low thermal expansion coefficient ($\alpha=3.3 \times 10^{-6}/^\circ\text{C}$), which imparts a very good thermal shocks resistance to the system. It also has low viscosity at elevated temperatures and hence infiltration and densification can be done easily via hot pressing at fairly low temperature. However, the major limitation of Pyrex glass is the crystallisation of silica to cristobalite which deteriorates the mechanical

properties. SiC platelets were chosen to the base Pyrex matrix because of the good chemical compatibility between the pyrex glass and SiC platelets. Besides the Youngs modulus for SiC platelets is 500 GPa which is substantially more then that of Pyrex glass (65 GPa). Hence, the SiC platelets have the potential to reinforce the Pyrex galss.

In the present work the following three aspects of the pyrex glass - SiC platelets composites have been studied:

1. To evolve a processing route where the crystallisation of silica from the glassy matrix face is minimized.
2. To study the effect of volume fraction of SiC platelets on the processing and mechanical behaviour of Pyrex - SiC platelets composites.
3. To study the elevated temperature deformation behaviour of the Pyrex - SiC platelet composites from the view point of the strain rate sensitivitiy of the flow behaviour in particular.

References: Chapter 2

- 1) Rice R.W. "Mechanisms of Toughening in Ceramic Matrix Composites" Ceram. Engg. Sci. Proc., 2 [7-8] 661-701 (1981)
- 2) Marshall D. B., Evans A. G., "Failure Mechanisms in Ceramic-Fiber/Ceramic-Matrix Composites" J. Am. Ceram. Soc., 68 [5] 225-31 (1985)
- 3) Hayami R., Keno K., Kondo I., Toibana Y., "Si₃N₄-SiC Composite Ceramics" presented at conference on tailoring multiphase and composite ceramics, Penn. State Univ., July 1985
- 4) Rice R. W., "Ceramic Composites-Processing Challenges" Ceram. Engg. Sci. Proc., 2 [7-8] 493-508 (1981)
- 5) Schioler L. J., Stiglich J. J., "Ceramic Matrix Composites: A Literature Review" Am. Ceram. Soc. Bull., 65 2 289-303 (1986)
- 6) Sambell R. A. J., Bowen D. H., Phillips D. C., "Carbon Fibre Composites with Ceramic and Glass Matrices Part1-Discontinuous Fibres" J. Mat. Sci., 7 [6] 663-75 (1972)
- 7) Sambell R. A. J., Bowen D. H., Phillips D. C., "Carbon Fibre Composites with Ceramic and Glass Matrices Part2-Continuous Fibres" J. Mat. Sci., 7 [6] 676-81 (1972)
- 8) Phillips D. C., "Interfacial Bonding and the Toughness of Carbon Fiber Reinforced Glass and Glass-Ceramics" J. Mat. Sci., 9 [11] 1847-54 (1974)
- 9) Brennan J.J., Prewo K. M., "Silicon Carbide Fiber Reinforced Glass-Ceramic Matrix Composites Exhibiting High Strength and Toughness" J. Mat. Sci., 17 [8] 2371-83 (1982)
- 10) Prewo K. M., Brennan J. J., "High Strength Silicon Carbide Fiber Reinforced Glass Matrix Composites" J. Mat. Sci., 15 [2] 463-68 (1980)
- 11) Prewo K. M., Brennan J. J., "Silicon Carbide Yarn Reinforced Glass Matrix Composites" J. Mat. Sci., 17 [4] 1201-1206 (1982)
- 12) Prewo K. M., Brennan J. J., Layden G. K., "Fiber Reinforced Glasses and Glass-Ceramics for High Performance Applications" Am. Ceram. Soc. Bull., 65 [2] 305-313 (1986)
- 13) Hasegawa Y., Iimara M., Yajima S., "Synthesis of Continuous Silicon Carbide Fiber-Part 2, Conversion of Polycarbosilane Fiber into Silicon Carbide Fibers;" J. Mat. Sci., 15 720-28 (1980)
- 14) West R., David L.D. et.al., "Polysilastystrene, Phenylmethylsilane Dimethylsilane Copolymers as Precursors to Silicon Carbide" Am. Ceram. Soc. Bull., 62 [8] 899-903 (1983)

- 15) Seyforth D., Wiseman G. H., "High Yield Synthesis of Si₃N₄/SiC Ceramic Materials by Pyrolysis of a Novel Polyorganosilazane" J. Am. Ceram. Soc., 67 [7] C 132-133 (1984)
- 16) Seyforth D., Wiseman G. H., Prudhomme C., "A Liquid Silazane Precursor to Silicon Nitride" J. Am. Ceram. Soc., 66[1] C13-14 (1983)
- 17) Warren J. W., "Fiber and Grain-Reinforced Chemical Vapour Infiltration (CVI) Silicon Carbide Matrix Composites" Ceram. Engg. Sci. Proc., 5 [7-8] 648-93 (1985)
- 18) Caputo A.J., Lackey W. J., "Fabrication of Fiber-Reinforced Ceramic Composites by Chemical Vapour Infiltration" Ceram. Engg. Sci.-Proc., 5 [7-8] 654-67 (1984)
- 19) Caputo A. J., Lackey W. J., Stinton D. P., "Development of a New, Faster Process for the Fabrication of Ceramic Fiber-Reinforced Ceramic Composites by CVI" Ceram. Engg. Sci. Proc., 6 [7-8] 694-706 (1985)
- 20) Corbin M. D., Rossetti G. A., Hartime S. D., "Microstructure, Property Relationship for SiC Filament Reinforced RBSN" Am. Ceram. Soc. Bull., 55 [9] 781-84 (1986)
- 21) Rice R. W., Spann J. R., Lewis D., Cobling W., "The Effect of Ceramic Fiber Coatings on the Room-Temperature Mechanical Behaviour of Ceramic Fiber Composites" Ceram. Engg. Sci. Proc., 5[7-8] 614-24 (1984)
- 22) Bender B. A., Lewis D., Coblenz W. S., Rice R. W., "Electron Microscopy of Ceramic Fiber-Ceramic Matrix Composites-Comparison with Processing and Behaviour" Ceram. Engg. Sci. Proc., 5[7-8] 513-59 (1984)
- 23) RuhleM., Evans A. G., "High Toughness Ceramics and Ceramic Composites" Progress in Materials Science, 33 85-167 1989
- 24) Budiansky B., Hutchinson J. W., Evans A. G., Journal Mech. Phys. Solids 34 167 (1986)
- 25) Cao H. C., et.al., "A Test Procedure for Characterising the Toughening of Brittle Composites" Acta Metall., 37[11] 2969-77 (1989)
- 26) Thouless M. D., Evans A. G., "Effect of Pullout on the Mechanical Properties of Brittle Matrix Composites" Acta. Metall., 36[3] 517-22 (1980)
- 27) Thouless M. D., et.al., "Effect of Interface Mechanical properties on pullout in SiC fiber-reinforced L-A-S glass-ceramics" J. Am. Ceram. Soc., 72 525-32 (1989)
- 28) Campbell G. H., Evans A. G., "Whisker Toughening: A Comparison Between Al₂O₃ and Si₃N₄ toughened by SiC" J. Am. Ceram. Soc., (1989)

- 29) Prewo K. M., Bacon J. F., "Glass Matrix Composites I) Graphite Fiber Reinforced Glass" Proc. Second International Conference on Composites, Edited by Noton B., AIME 1978, pp. 64-74
- 30) Prewo K. M., Bacon J. F., Dicus D. L., "Graphite Fiber Reinforced Glass Matrix Composites" SAMPE Quarterly, 10 [4] 42 (1979)
- 31) Prewo K. M., "A Compliant, High Failure Strain Fibre Reinforced Glass Matrix Composite" J. Mat. Sci., 17 3549-3563 (1982)
- 32) Brennan J. J., Prewo K. M., "Silicon Carbide Fibre Reinforced Glass-Ceramic Matrix Composites Exhibiting High Strength and Toughness" J. Mat. Sci., 17 2371 (1982)
- 33) Mah T., Hecht N. L. et.al., "Thermal Stability of SiC Fibers (NICALON)" J. Mat. Sci., 19 1191-201 (1984)
- 34) Johnson S. M., Brittain R. D. et.al., "Degradation Mechanisms of Silicon Carbide Fibers" J. Am. Ceram. Soc., 71 [3] C132-35 (1988)
- 35) Luthra K. L., "Thermchemical Analysis of the Stability of Continuous SiC Fibers" J. Am. Ceram. Soc., 69 [10] C231-33 (1986)
- 36) Pysher D. J., Goretta K. C., Hodder R. S., Tresslar R. E., "Strength of Ceramic Fibers at Elevated Temperatures" J. Am. Ceram. Soc., 72 [2] 284-88 (1989)
- 37) Gadkarre K. P., Chyung K., "Silicon-Carbide Whisker-Reinforced Glass and Glass-Ceramic Composites" Am. Ceram. Soc. Bull., 65 [2] 370-76 (1986)
- 38) Gac F. D., Petrovic J. J., Milewski J. V., Shalek P. D., "Performance of Commercial and Research Grade SiC Whiskers in a Borosilicate Glass Matrix" Ceram. Engg. Sci. Proc., 7 [7-8] 978-82 (1986)
- 39) Chokshi A. H., Porter J. R., "Creep Deformation of an Alumina Matrix Composite Reinforced with Silicon Carbide Whiskers" J. Am. Ceram. Soc., 68 [6] C144-145 (1985)
- 40) Becher P. F., Wei G. C., "Toughening Behaviour in SiC-Whisker-Reinforced Alumina" Am. Ceram. Soc. Bull., 64 289-304 (1985)
- 41) Wei G. C., Becher P. F., "Development of SiC Whisker Reinforced Ceramics" Am. Ceram. Soc. Bull., 64, 289-304 (1985)
- 42) Tiegs T. N., Becher P. F., "Whisker Reinforced Ceramic Composites" Materials Science Research Vol.20, Plenum Press, New York, 1986 pp. 634-47
- 43) Samanta S. C., Musikant S., "SiC Whisker Reinforced Ceramic Matrix Composites" Ceram. Engg. Sci. Proc., 6 [7-8] 663-72 (1985)

- 44) Claussen N., Petzow G., "Whisker reinforced Zirconia toughened Ceramics" Materials Science Research Vol. 20 Plenum Press, New York 1986 pp. 649-62
- 45) Shalek P. D., Petrovic J. J., Huxley G. F., "Hot-Pressed SiC Whisker/Si₃N₄ Matrix Composites" Am. Ceram. Soc. Bull., 65 [2] 351-56 (1986)
- 46) Lundberg R., Kalman L. et.al., "SiC Whisker-Reinforced Si₃N₄ Composites" Am. Ceram. Soc. Bull., 66 [2] 330-33 (1987)
- 47) Tiegs T. N., Becher P. F., "Sintered Al₂O₃-SiC Whisker Composites" Am. Ceram. Soc. Bull., 66 [2] 339-43 (1987)
- 48) Porter J. R., Lange F. F., Chokshi A. H., "Processing and Creep Performance of SiC Whisker Reinforced Al₂O₃" Am. Ceram. Soc. Bull., 66 [2] 343-47 (1987)
- 49) Homeny J., Vaughn W. C., Ferber M. K., "Processing and Mechanical Properties of SiC Whisker-Al₂O₃ Matrix Composites" Am. Ceram. Soc. Bull., 66 [2] 333-39 (1987)
- 50) Buljan S. T., Baldoni J. G., Huckabee M. L., "Si₃N₄-SiC Composites" Am. Ceram. Soc. Bull., 66 [2] 347-53 (1987)
- 51) Homeny J., Vaughn W. L., "Whisker Reinforced Ceramic Matrix Composites" Mater. Res. Bull., 72 66-71 (1987)
- 52) Kandori T., Kobayashi S. et.al., "SiC Whisker Reinforced Si₃N₄ Composites" J. Mat. Sci. Lett., 6 1356-58 (1987)
- 53) Becher P. F., Tiegs T. N., "Toughening Behaviour Involving Multiple Mechanisms: Whisker Reinforcement and Zirconia Toughening" J. Am. Ceram. Soc., 70 [9] 651-54 (1987)
- 54) Akinnine Y., Katano Y., Shichi Y., "Mechanical Properties of Silicon Carbide Whisker/Aluminium Oxide Matrix Composites" Ceram. Engg. Sci. Proc., 8 [7-8] 848-59 (1987)
- 55) Becher P. F., Hsueh C. H., Angelini P., Tiegs T. N., "Toughening Behaviour in Whisker-Reinforced Ceramic Matrix Composites" J. Am. Ceram. Soc., 71 [12] 1050-61 (1988)
- 56) Evans A. G., "On Prevalent Whisker Whisker Toughening Mechanisms in Ceramics" Mater. Res. Soc. Symp. Proc., 78, 295-302 (1987)
- 57) Chain R., Baum L., Brandon D. G., "Mechanical Properties and Microstructure of Whisker-Reinforced Alumina-30vol.% Glass Matrix Composites" J. Am. Ceram. Soc., 72 [9] 1636-42 (1989)
- 58) Gibbs W. S., Petrovic J. J., Honnel R. E., "SiC Whisker-MoSi₂ Matrix Composites" Ceram. Engg. Sci. Proc., 8 [7-8] 645-48 (1987)

- 59) Iio S., Watanabe M., Matsubara M., Matsuo Y., "Mechanical Properties of Alumina/Silicon Carbide Whisker Composites" J. Am. Ceram. Soc., 72 [10] 1880-84 (1989)
- 60) Claussen N., Steeb J., Pabst R. O., "Effect of Induced Microcracking on the Fracture Toughness of Ceramics" Bull. Am. Ceram. Soc., 56 [6] 559-62 (1972)
- 61) Karpman M. Clark J., "Economics of Whisker-Reinforced Ceramics" Composites 18 121-124 (1981)
- 62) Sarin V. K., Ruhle M., "Microstructural Studies of Ceramic Matrix Composites" Composites 18 129-134 (1987)
- 63) Nutt S. R., "Defects in Silicon Carbide Whiskers" J. Am. Ceram. Soc., 71 149-156 (1988)
- 64) Nutt S. R., "Microstructure and Growth Model for Rice Hull Derived SiC Whiskers" J. Am. Ceram. Soc., 71 149-56 (1988)
- 65) Karasek K. R., Bradley S. A., Donner J. T., "Characterisation of Silicon Carbide Whiskers" J. Am. Ceram. Soc., 72 1907-1913 (1989)
- 66) Milewski J. V., Gac F. D., Petrovic J. J., Skaggs S. R., "Growth of Beta-Silicon Carbide Whiskers by the VLS Process" J. Mat. Sci., 20 1160-1166 (1985)
- 67) Petrovic J. J., Milewski J. V., Rohr D. L., Gac F. D., "Tensile Mechanical Properties of SiC Whiskers" J. Mat. Sci., 20 1167-77 (1985)
- 68) Hoffman et.al., "Slip Casting of SiC Whisker Reinforced Si₃N₄ Composites" J. Am. Ceram. Soc., 72 765-769 (1985)
- 69) Pezzotti G., Tanak I., Okamoto T., Miyamoto Y., "Processing and Mechanical Properties of Dense Si₃N₄-SiC Whisker composites Without Sintering aids" J. Am. Ceram. Soc., 72 1461-64 (1989)
- 70) Bjork L., Hermansson A. G., "Hot Isostatically Pressed Alumina-Silicon Carbide Whisker Composites" J. Am. Ceram. Soc., 72 1436-38 (1989)
- 71) Donald I. W., McMillan P. W., J. Mat. Sci., 11 949 1976
- 72) Krock R. H., Broutman L. J., "Modern Composite Materials" Addison-Wesley 1967
- 73) Forsyth D. J. E. "Composite Materials" (ILIFE London) 1966
- 74) Hull D., "An Introduction to Composite Materials" (Cambridge Press) 1981
- 75) Chou T. W., Kelly A., Ann. Rev. Mat. Sci., 10 229 (1980)

- 76) McColm I. J., Clark N. J., "High Performance Ceramics" Chapman and Hall, New York, U. S. A., 1988
- 77) Warren R., Sarin V. K., "Fracture of Whisker-Reinforced Ceramics in Composite Materials" series 6 edited by Friedrich K., Elsevier, Oxford pp. 571-614
- 78) Rice R. W., "Ceramic Matrix Composite TougheningMechanisms: an update" Ceram. Engg. Sci. Proc., 6 589-607 (1985)
- 79) Homeny J., "Whisker Reinforced Ceramics" Ceramic-Matrix Composites. edited by Richard Warren, Chapman and Hall, New York, (1992)
- 80) Li Jie, "SiC Whisker Reinforced Glass-Ceramics" M. S. Thesis, Univ. of Warwick June 1988
- 81) Piggott M. R., "Load Bearing Compsoites" Pergaman Press 1980)
- 82) Marple B. R., Green D. J., conf. Proc., 91st Annual meeting of American Ceramic Society (1989)
- 83) Warren R., Sarin V. K., "Particulate Ceramic-Matrix Composites" Cerammic Matrix Composites edited by Richard Warren Chapman and Hall, New York 1992
- 84) Ziegler G. "Advanced Ceramic Development Trends" cfi/Berlin DKG No. 9 68 399-404
- 85) K.R. Venkatachari and R.Raj, J. Am. Ceram. Soc. 69 (1986) 135.
- 86) T.G. Nieh and J. Wadsworth, Jpn Jl Appl. Phys. 28 (1989) 69.
- 87)S.L. Hwang and I.W. Chen, J. Am. Ceram. Soc. 73 (1990) 1626.
- 88) O.D. Sherby and J. Wadsworth, Prog. Mater. Sci. 33 (1989) 169.
- 89)P. Gruffel, P. Carry and A. Mocellin, 'Science of Ceramics' Vol. 14 ed: D. Taylor, The Institute of Ceramics, Shelton, UK 1988 p. 587.
- 90)F. Wakai, S. Sakaguchi and Y. Matsumo, Adv. Ceram, Mater. 1 (1986) 259.
- 91)T.G.Nieh and J. Wadsworth and O.D. Sherby, Proc. Mater. Res. Soc. 7 (1989) 251.
- 92)F. Waki and H. Kato, Adv. Ceram. Mater. 3 (1988) 71.
- 93)T.G. Nieh, C.M. McNally and J. Wadsworth, Script Metall 23 (1989) 457.
- 94)C.K. Yoon and I.W. Chen, J. Am. Ceram. Soc. 73 (1990) 1555.

- 95) Raj R. "Creep in polycrystalline aggregates by matter transpo through a liquid phase" J. Geophys. Res., 87 [B6] 4731 (1982)
- 96) Pharr and Ashby "On Creep Enhanced by a liquid Phase" Ac Metall., 31, 129-38 (1983)
- 97) Wang J. G., Raj R., "Mechanism of Superplastic Flow i; Fine-Grained Ceramic Containing Some Liquid Phases" J. Am. Cera Soc., 67 [6] 399-409 (1984)

III EXPERIMENTAL DETAILS

3.1) Matrix and Reinforcement

A commercial (Corning Glass Works, USA) PYREX glass (code 7740) was selected as the matrix material. It greatly facilitated the fabrication process of the composite due to its low viscosity at the hot pressing temperature of 900°C. The other attractive properties which make it an ideal material for composites is its excellent resistance to thermal shock (low thermal expansion co-efficient $\alpha_p = 3.3 \times 10^{-6}/^\circ\text{C}$) and thermal expansion match with reinforcing SiC platelets ($\alpha_{\text{SiC}} = 4.5-5.5 \times 10^{-6}/^\circ\text{C}$).

The composition of this particular glass is 81% SiO_2 , 13% B_2O_3 , 4% Na_2O , 2% Al_2O_3 . As follows from the metastable immiscibility diagram of the sodium borosilicate system, this glass falls in the range of the compositions prone to phase separation(1). The small additions of aluminium oxide (2% Al_2O_3) reduces the tendency towards phase separation, while the addition of 4% Na_2O results in the opposite effect.

The reinforcement used was SiC platelets supplied by Third Millennium Technologies Inc., Tennessee, USA. The shape of these platelets is hexagonal. Typical dimensions of length and thickness of these platelets are 25-50 μm and 1-2 μm respectively.

3.2) Matrix Preparation

Pyrex (code 7740) glass used in the composite fabrication was obtained from the glass blowing laboratory. The glass was crushed into small pieces and ground in a mortar and pestle to coarse powder. Two different routes have been made for the fabrication of

base matrix: a) cold compaction and sintering b) hot pressing.

The coarse glass powder was wet(methanol) ball milled for 24 hours with alumina balls. The slurry was then filtered, dried and sieved through a 270 mesh sieve(sieve opening 53 μ m). The ball milled pyrex powder was stored in air tight plastic containers.

3.3) Fabrication of Composites

3.3.1) Dry Mixing

Initially appropriate amount of pyrex powder and SiC platelets were weighed using an electronic balance. The matrix and SiC Platelets(varying from 10-50 vol%) were mixed for 24 hours. using a dry mixing technique with small HIPed Si_3N_4 cylindrical pellets.

3.3.2) Hot Pressing of the composites

A small Hot Press(Sintering Press DSP6 Dr. Fritsch KG, West Germany) was used to hot press the composite mixture(fig.3.1). The Hot Press is based on the principle of heating by short circuit current similar to an electric welding apparatus. The special feature of this Hot Press was that we could use a very high rate of heating and cooling during hot pressing. This was made possible by using a very high current (500 to 1000 A) in the Hot Press system.

The graphite die and punch system was fabricated keeping in mind the size and capacity of the small Hot Press and extremely high heating and cooling rates that we required during hot pressing. A tight fit was used for the die and punch system. This

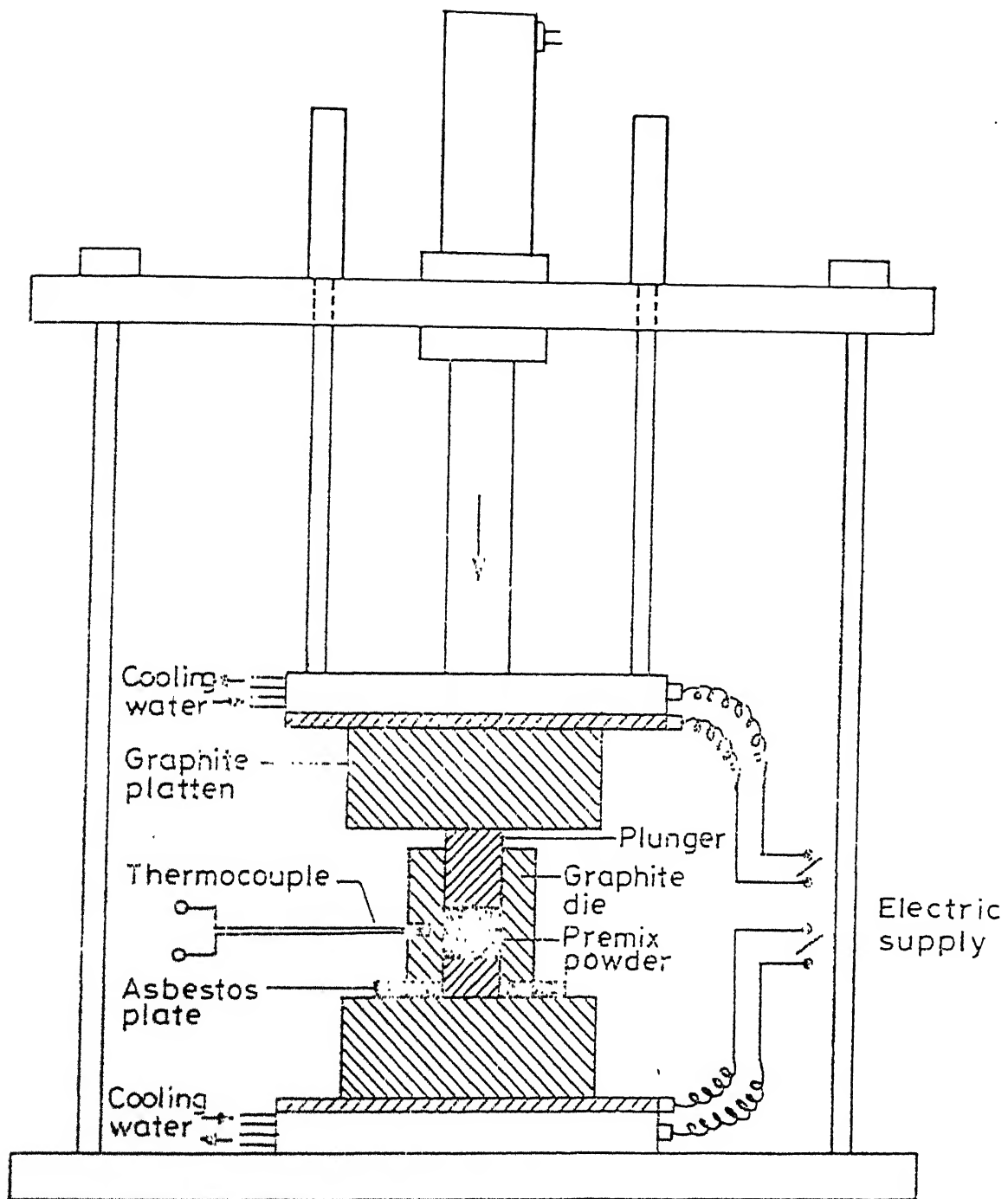


Fig. 3.1 .Schematic of the Hot Pressing Setup

was done to ensure proper electrical contact between the die and the punch and to prevent leakage of the low viscosity pyrex matrix at elevated temperatures.

The punches were made in two different diameters(12.54mm and 9.5mm). The height of the punches was selected in such a manner that in the final configuration(during hot pressing) the exposed length of the punches on either side of the die is around 6mm. Prior to hot pressing graphite dies were dip coated with a thin layer of BN. A circular asbestos ring($\phi_{outer} = 50\text{mm}$, $\phi_{inner} = 15\text{mm}$, height = 6mm) was used as insulating material, between the graphite die and the base graphite block of the Hot Press. Hot pressing was done using a pressure of 10 MPa at 900°C .

3.4) Characterisation of Composites

3.4.1) Optical Microscopy

To examine the surface morphology specimens were polished respectively by $0/0.1/0.2/0.3/0.4/0$ SiC emery papers followed by $0.1\mu\text{m}$ diamond paste. Typical dimensions of the hot pressed pellets were(diameter = 12.56, 9.56 mm, and height = 9.56, 12.56 mm)Platelet distribution in composites were examined by optical microscopy at magnifications of 100, 200 and 500X using a Leitz "METALLOBART" optical microscope. As polished and HF etched specimens were used.

3.4.2) X-ray Diffraction (XRD)

Crystallisation of the matrix in composites as well as in sintered and HP pyrex matrix was explored by X-ray diffraction technique from polished surfaces at a scanning speed of $3^{\circ}/\text{min}$ and

2θ angle of $10^\circ - 140^\circ$. The lattice parameter d was calculated using Bragg's equation $\lambda = 2ds\sin\theta$ where $\lambda = 0.154\text{nm}$ is the $\text{K}\alpha$ wavelength for Cu target X-rays. Phases were identified using a JCPDS file.

3.4.3) Scanning Electron Microscopy (SEM)

All the composite and the monolithic base matrix (both hot pressed and sintered) samples were characterised using SEM (Jeol JSM-840A). Various sections were cut from the composites and polished to $0.1\mu\text{m}$ finish. A thin silver coating was given on all the specimens before introducing into the SEM to prevent charging. Both polished and fractured samples were observed in secondary as well as back scattered modes. Back scattered mode was used to examine the finer details of crystallisation, crack deflection etc.

3.5) Density Measurements

The density of the hot pressed pellets was measured using an Archimedian method. The surface layer of the hot pressed pellets was first polished to remove the graphitic coating before measurement. The weight of the pellets was measured in air and distilled water using an electronic balance. The density(D) is obtained from the relation.

$$D = \frac{\text{weight in air}}{(\text{weight in air} - \text{weight in water})} \quad (3.1)$$

3.6) Mechanical Testing

The strength of base matrix material and the various composites was evaluated in compression mode. Appropriate

cylindrical specimens of the size were used and minimum of 6 samples were tested for each category. The l/d ratio for all the specimens was one. No lubricant was used for room temperature testing.

To obtain perfect parallel surfaces on each tested sample a mild steel jig was fabricated. These parallel surfaces were polished to $0.1\mu\text{m}$ finish to avoid crack initiation from the surface notches.

Compression testing of the pellets was done on a 10 ton Instron machine(Instron 1105). Initially hot pressed pellets of pure pyrex powder were tested in compression. A minimum of 6 specimens for each volume fraction were next tested in compression. Care was taken to see that the surfaces of the pellets were aligned with the platens of the compression jig.

Each of the specimen was tested till failure. The fractured pieces were used for fractography.

3.7) Elevated Temperature Testing of the Composites.

To study the elevated temperature behaviour of the composites strain rate change tests were carried out in compression. These tests were carried out on a Materials Testing System(MTS 810.12) machine fitted with a furnace capable of operating upto 1000°C . The special characteristic of this machine which makes it ideal for changing strain rate testing is that it can be programmed for multiple crosshead velocities, one after the other in the same test.

The sample preparation for elevated temperature testing followed the same pattern as for the compression testing, except

that the 1/6 ratio for elevated temperature testing was kept equal to 1.5 .

Initially the surfaces of the polished specimens were coated with a thin layer of BN which acted as the lubricant. The specimens were next placed between two stainless steel platens which were specially built for testing upto 800°C . Care was taken to maintain perfect alignment between the platens and the test specimen. A special furnace with three different temperature zones has been used for testing at elevated temperatures. Temperature was recorded at three locations viz. top platen, specimen and bottom platen. The output of these thermocouples was fed to an automatic temperature controller. Further the temperature was also checked using a multimeter whose probes were constantly connected to the three different thermocouples. Room Temperature correction was also applied.

The strain rate change tests were carried out at 625°C , 650°C , 675°C and 700°C . Starting at the lowest strain rate the specimens were tested at each strain rate till the flow stress reached a steady value. The strain rate was then changed to the next one(strain rates were changed in jumps of two) and the procedure repeated. The strain rate range of 10^{-8} to $10^{-5}/\text{s}$ was explored for each specimen. The tests were repeated for confirmation.

The above tests were conducted for the matrix and 10 - 50vol% composites using the same temperature range.

IV RESULTS AND DISCUSSION

4.1) Borosilicate(Pyrex)-SiC Composites

4.1.1) Borosilicate(Pyrex) Glass

Pyrex glass was chosen as the matrix material for the composite. The properties of pyrex glass(corning code 7740) are given in the table(4.1). This glass has many special characteristics which make it an ideal choice for use in composite systems. These are mentioned below:

- 1) It has a very low thermal expansion co-efficient($\alpha_p = 3.3 \times 10^{-6}/^{\circ}\text{C}$). This imparts a very good thermal shock resistance to the system.
- 2) It has low viscosity at elevated temperatures and hence infiltration and densification can be done easily via hot pressing at fairly low temperatures(in this work a hot pressing temperature of 900°C was used). In addition to the ease of fabrication, most of the reinforcing materials available are stable at these relatively low forming temperatures.

The powder used in this study is $< 50 \mu\text{m}$ size. The glass transition temperature of this glass was determined to be 718°C from DTA analysis.(fig. 4.1)

4.1.2) SiC Platelets

As discussed in section 2.2.4, improvement in mechanical properties depends on the shape factor. Whiskers having fairly large aspect ratios are ideal for composites. However, processing SiC whiskers(1,2) is difficult and handling is hazardous. Thus SiC platelets were chosen as reinforcing material. Some of the

THERMAL ANALYSIS DATA

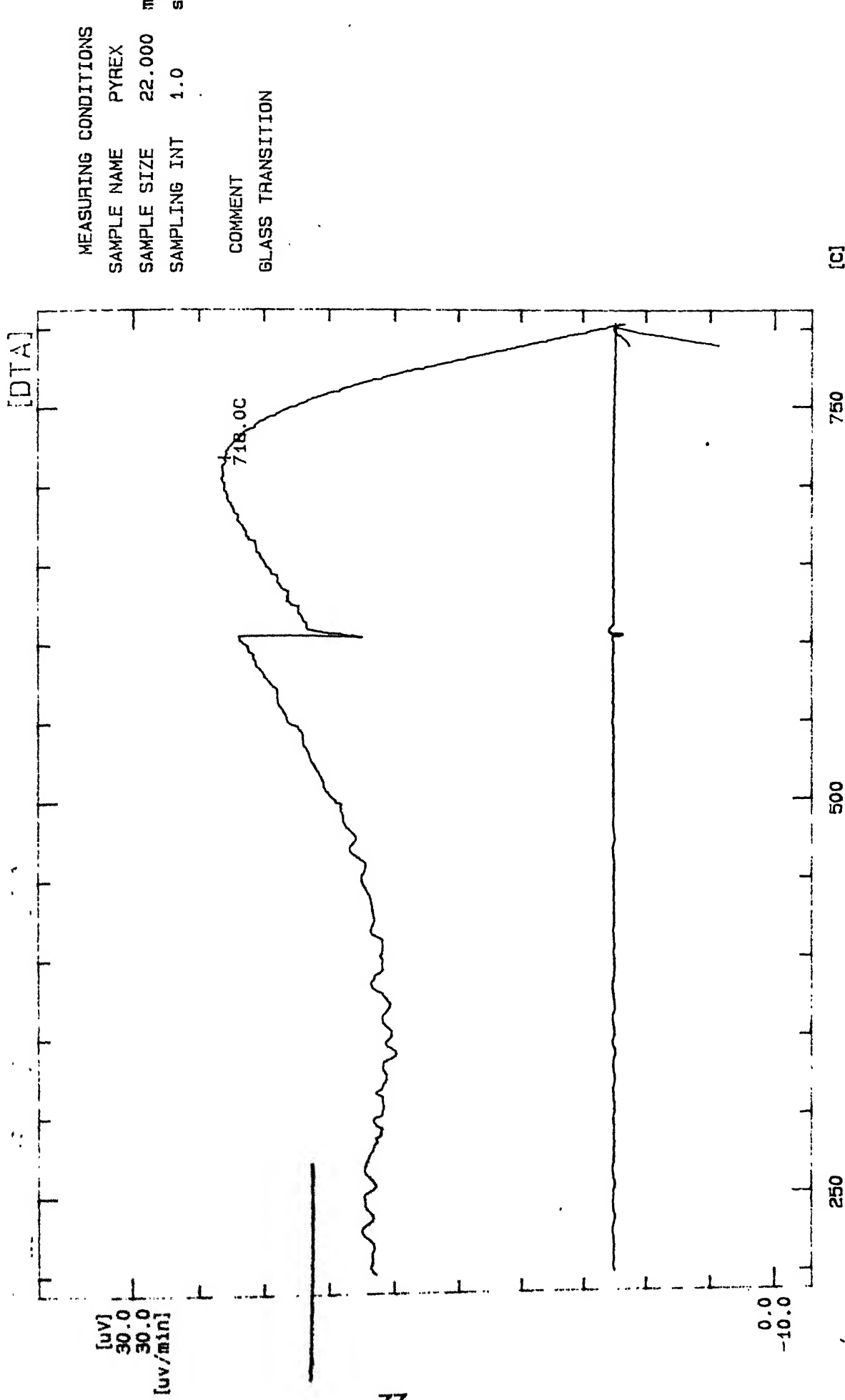


Fig. 4.1 DTA Plot for Determining Glass Transition Temperature
of Pyrex Glass

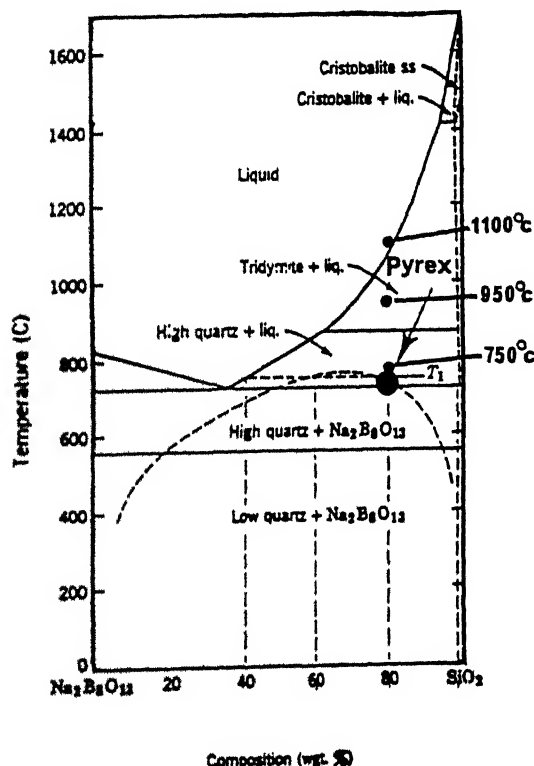
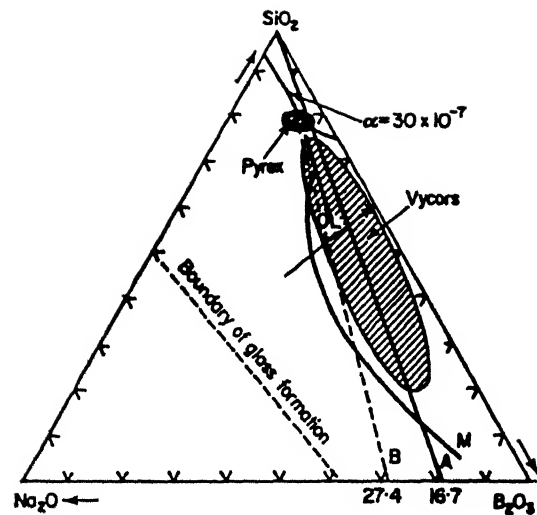


Fig. 4.2 Phase Diagram for Borosilicate Glass System

Table 4.1 : Properties of Composite Components

Material	MOR (MPa)	Modulus (GPa)	Density (g/cm ³)	Thermal Expansion Coefficient (x10 ⁻⁶ /°C)
Pyrex Glass	95	65	2.23	5.3
SiC Platelets	2x10 ³	400-500	3.2	4.5-55

additional characteristics of SiC platelets which are of interest for this composite system are:

- 1) The Young's modulus for SiC platelets is 500 GPa, which is substantially more than that of pyrex glass(65 GPa).
- 2) Unlike SiC whiskers and fibres SiC platelets are stoichiometric. Hence they are stable upto fairly high temperatures(1800°C).
- 3) Thermal expansion co-efficient of SiC platelets($\alpha_{\text{SiC}} = 4.5 - 5.5 \times 10^{-6}/^{\circ}\text{C}$) is very close to pyrex glass($\alpha_p = 3.3 \times 10^{-6}/^{\circ}\text{C}$). This prevents excessive residual stresses in the system on cooling from hot pressing temperatures.
- 4) Unlike whiskers, platelets do not agglomerate and conventional powder processing routes can be used for fabrication of platelet reinforced composites

SiC platelets as shown in figure(4.Ph1) have a faceted morphology and are found to be hexagonal in shape. SiC is of stoichiometric composition and is a mixture of various polytypes(mainly 3C, 2H, 4H, 6H, 21R, 33R)(fig.4.3)

4.2) Sintering of Pyrex Glass

To study the densification of the matrix material, pyrex glass compact was sintered using various time and temperature schedules. The temperature variation from $825 - 900^{\circ}\text{C}$ with a holding time of 12 to 24 hours was used. The microstructure of sintered pyrex material is shown in figure(4.Ph2). It has been observed that the matrix has been crystallised into α -cristabolite, a polymorph of silica with a high thermal expansion co-efficient. Cracking is observed in the microstructure(fig 4.Ph2) and it can be attributed to the thermal stresses arising from thermal mismatch between

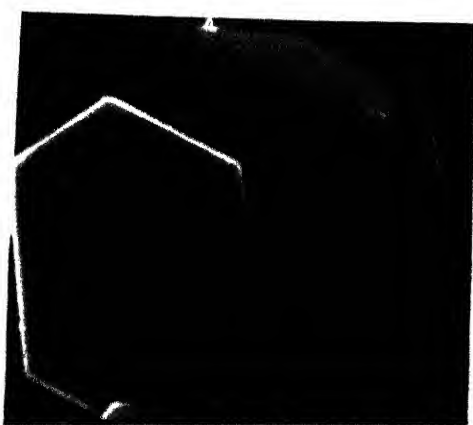


Fig. 4. Phi1) SiC Platelets

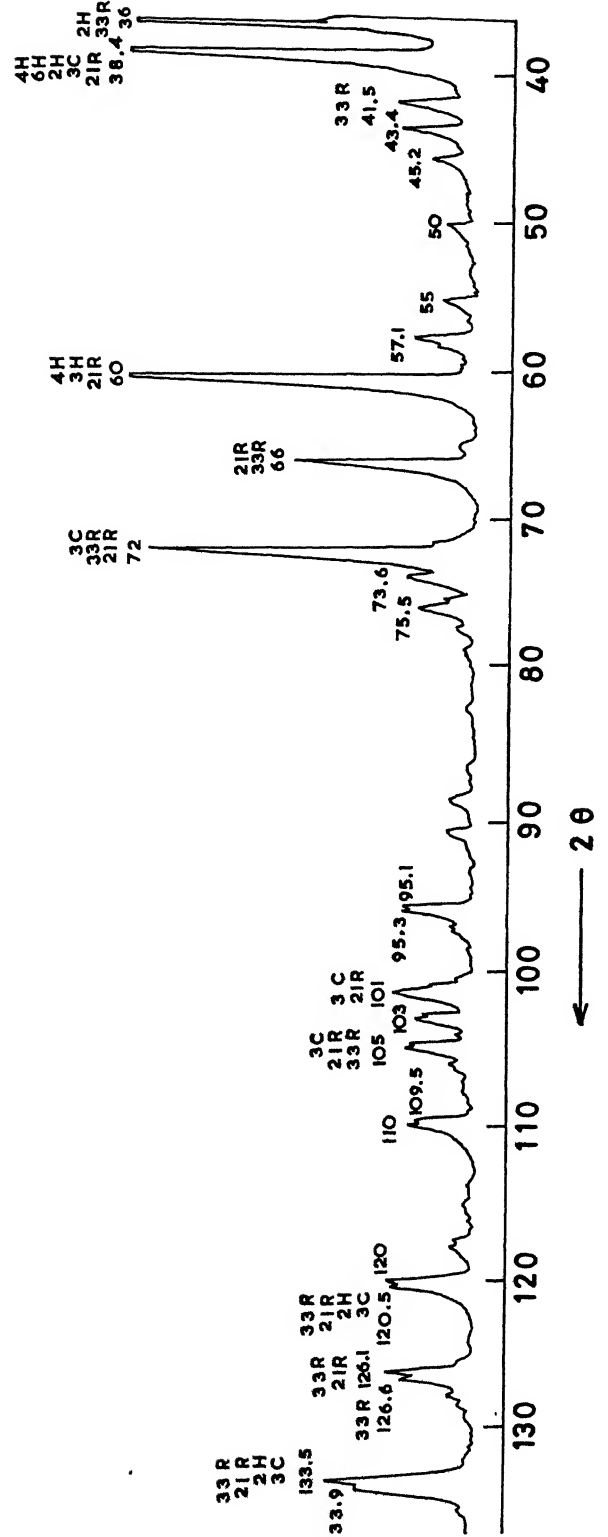


FIG.4.3 XRD OF SiC PLATELETS SHOWING VARIOUS POLYTYPES.

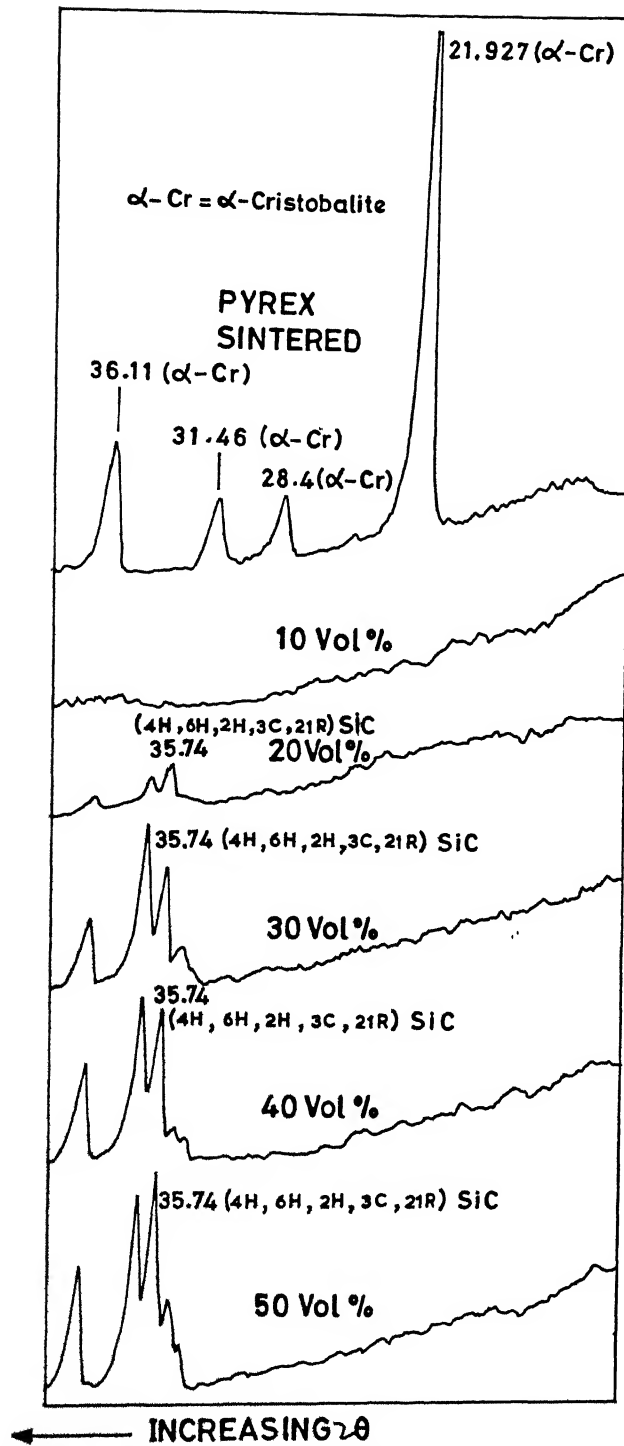


FIG.4.4 COMPARISON OF THE XRD PATTERNS OF PYREX (SINTERED) WITH H.P. SAMPLES CONTAINING VARIOUS VOL% SiC PLATELETS FOR α -CRISTOBALITE FORMATION.

α -cristobalite ($\alpha_{cr} = 12.5 - 50 \times 10^{-6}/^{\circ}\text{C}$) and the residual glass ($\alpha_p = 3.3 \times 10^{-6}$).

This glass (composition $\text{SiO}_2 = 81\%$, $\text{B}_2\text{O}_3 = 13\%$, $\text{Na}_2\text{O} = 4\%$, $\text{Al}_2\text{O}_3 = 2\%$) falls in the range of the composition prone to phase separation (3) (fig. 4.2). Phase separation and crystallisation are independent phase transformation processes. However, phase separation can significantly affect the glass crystallisation which normally occurs later than phase separation. This is affected in two ways, first due to phase separation the compositions of glass-forming phases can approach those of crystalline phases and second there is a clearly defined development of interfaces. Both significantly increase the rate of crystal phase nucleation.

In the pyrex glass, boron atoms are triangularly co-ordinated (boron-oxygen triangles) and the addition of oxides of sodium oxide (Na_2O) leads to the formation of boron-oxygen tetrahedra. From the data of Zhdanov (3) boron-oxygen triangles and boron-oxygen tetrahedra form different structures than the rest of the glass. The immiscibility in pyrex glass results from the incompatibility of the silicon-oxygen tetrahedra with the boron-oxygen triangles and tetrahedra. Thus in pyrex glass phase separation produces regions rich in silica and regions rich in Na_2O and B_2O_3 . These silica rich regions and the interface developed increase the rate of crystal phase nucleation and α -cristobalite crystals are formed.

Cristobalite (α form) formation in the matrix has been confirmed using various techniques such as X-ray diffraction back scattered SEM (fig 4. Ph2). The cristobalite crystals formed are of

the order of $10\text{-}20\mu\text{m}$, as revealed by SEM observations on HF etched samples (fig 4.Ph2). It is also anticipated that reinforcement such as SiC will further promote the cristobalite formation.

Because of extensive cracking in sintered samples, another densification method viz., hot-pressing has been tried.

4.3) Hot Pressing of Pyrex Glass

Pyrex powder was hot pressed using various heating and cooling rates at 900°C for a holding time of 10 minutes. Using the fastest heating and cooling rates possible on the equipment crystallisation of cristobalite was suppressed to fairly low levels (fig. 4.Ph3). The suppression of α -cristobalite formation in the hot pressed samples can be explained as follows.

The initial phase separation in pyrex producing silica rich regions occurs by a spinodal decomposition and that remains the same for both sintered as well as hot pressed specimens. It is the second part of the process of crystallisation which is different for the sintering route and the hot pressing route. In the sintering route the holding time (12 to 24 hours) as well as the slow heating and cooling rates (furnace heating and cooling) are sufficiently large for the α -cristobalite to nucleate and grow which is evident from the sintered specimens (almost all silica has been crystallised to α -cristobalite). However, for the hot pressing route the holding time (10 minutes) and the heating and cooling rates (heating from room temperature to 900°C in 6 minutes and cooling to room temperature after holding in 8-10 minutes) are relatively small compared to the sintering route. These short



Fig. 4.Ph2) Sintered Pyrex($T\ 900^{\circ}\text{C}$)
(HF etched)



Fig. 4.Ph3) Hot Pressed Pyrex($T\ 900^{\circ}\text{C}$)
(HF etched)

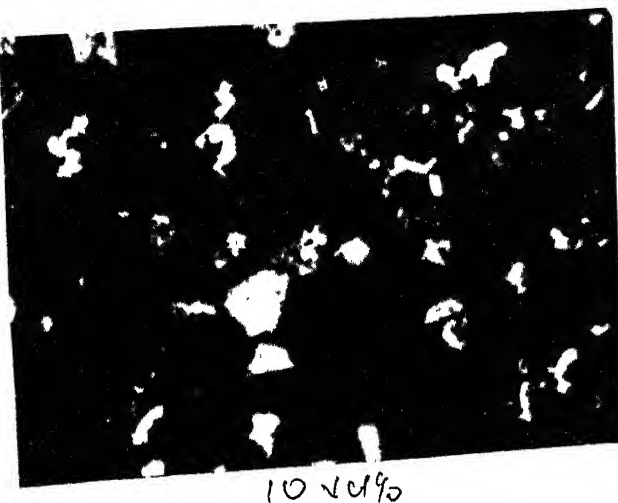
times do not allow the nucleation and growth of α -cristobalite to the same extent as for the sintered specimens. The suppression of cristobalite is evident from the XRD results. Although the smaller degree of the cristobalite could not be detected using X-Ray technique some crystals have been detected (corresponding to approximately 5-6% SiO_2) in HF etched samples. (fig 4. Ph.3)

In view of the above, the same hot pressing cycle has been adopted for the densification of various volume fraction composites.

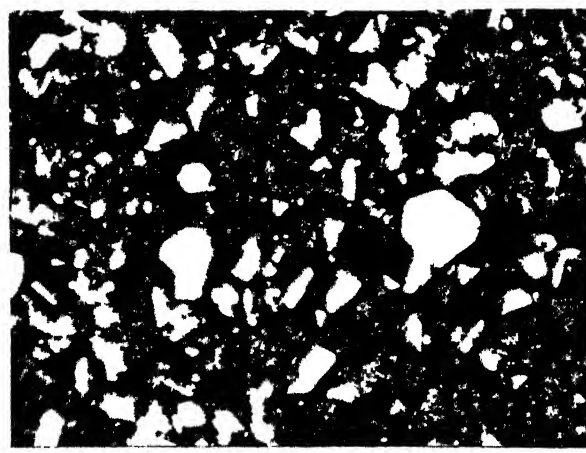
4.4) Hot Pressed Pyrex-SiC Platelet Composites

Optical micrographs for different pyrex-SiC platelet composites, with platelets varying from 10-50 vol% are shown in figure(4. Ph4). Platelets are uniformly distributed within the matrix and to some extent aligned preferentially in a plane perpendicular to the hot pressing direction. The same kind of preferred orientation is commonly reported in hot-pressed samples(4,5). However, for the 50 vol% platelet loading, agglomeration of platelets at some regions is evident. The high volume fraction of platelets(i.e. 50 vol%) form an interlocking network which is rigid and does not collapse throughout the process of hot pressing. These networks have a void volume as high as 50%, which is sometimes higher than the matrix. Additionally, infiltration of the highly viscous silicate matrices through torturous paths becomes extremely difficult. Therefore matrix cannot fully infiltrate the platelet network.

The platelets are fairly stable in the pyrex matrix at the hot pressing temperatures used in this investigation and no



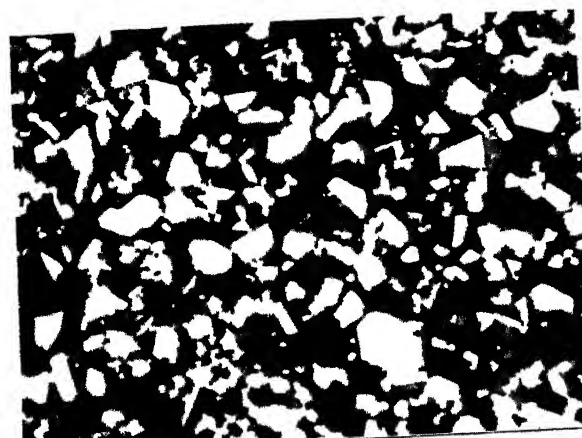
10 Vol%



20 Vol%



30 Vol%



40 Vol%

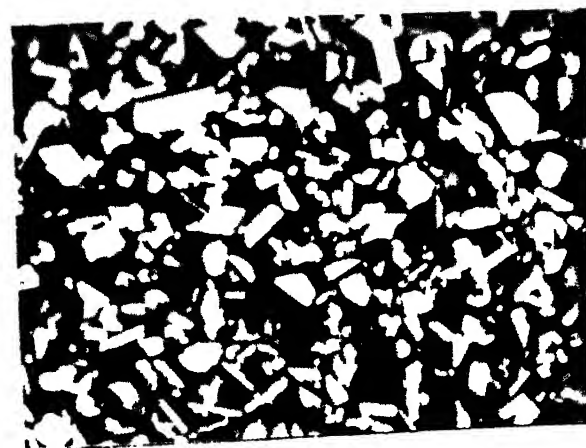


Fig. 4.Th4) Pyrex-SiC Composite Microstructures
(10vol% to 50vol% top to bottom)
(225X) 50 Vol%

interfacial reaction between the matrix and the platelets could be detected using SEM(fig. 4.Ph5). Further, the presence of platelets is expected to provide sites for heterogeneous nucleation thereby encouraging crystallisation of silica. However, using X-Ray diffraction technique, no cristobalite has been detected(fig. 4.4). HF deep etching technique has revealed that cristobalite growth is still in early stages, in all samples(for example 10, 50 volt SiC composites are shown in the figure(fig 4.Ph6a-b)), like in the case of hot pressed pyrex glass(fig 4.Ph3).

4.5) Density Measurements for Pyrex-SiC Composites

The retained porosity in various composites is depicted in figure(4.5). Values of density approaching the theoretical density have been achieved for composites containing platelets less than 40 volt. However, for the 50 volt platelet loading the density has registered a sharp drop.

The basic nature of the density curve is similar to that reported in the literature for whisker composites. It has been reported that it is not possible to fully densify whisker reinforced composites beyond 25-30 volt whisker loading even with the application of very large pressures(6-7). This is mainly attributed to the rigid network formed by the reinforcements during hot pressing.

4.6) Mechanical Behaviour of Pyrex-SiC Composites

4.6.1) Compressive Strength

The stress strain curves for all the volt loading of SiC platelets are linear till failure with no evidence of any plastic



Fig. 4.Ph5) Hot Pressed Pyrex-SiC(10vol%)
(BE)



Fig. 4.Ph6a) Hot Pressed Pyrex-SiC(10vol%)
(HF etched)

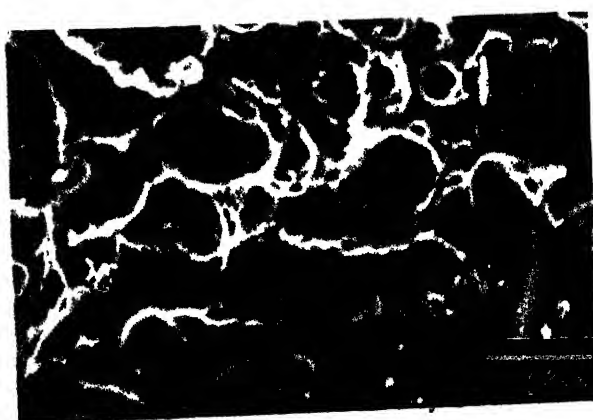


Fig. 4.Ph6b) Hot Pressed Pyrex-SiC(50vol%)
(HF etched)

Table 4.2 : Compressive Strength of Pyrex-SiC Composites

Composite System	Sample 1 (MPa)	Sample 2 (MPa)	Sample 3 (MPa)	Mean (MPa)
Pyrex	159.3	175.3	164.6	166.4
Pyrex-SiC 10 Volt	346.1	288.7	317.4	317.4
Pyrex-SiC 20 Volt	407.3	331.6	459.4	399.4
Pyrex-SiC 30 Volt	481.1	461.1	504.7	482.3
Pyrex-SiC 40 Volt	501.3	512.9	520.6	514.6
Pyrex-SiC 50 Volt	203.6	158.4	225.7	195.9

TABLE FOR THEORETICAL DENSITY
OF PYREX-SiC COMPOSITES

SR NO	SYSTEM	THEORETICAL DENSITY gm/cc
1)	PYREX - SiC 10V0%	2.327
2)	PYREX - SiC 20V0%	2.424
3)	PYREX - SiC 30V0%	2.521
4)	PYREX - SiC 40V0%	2.618
5)	PYREX - SiC 50V0%	2.715

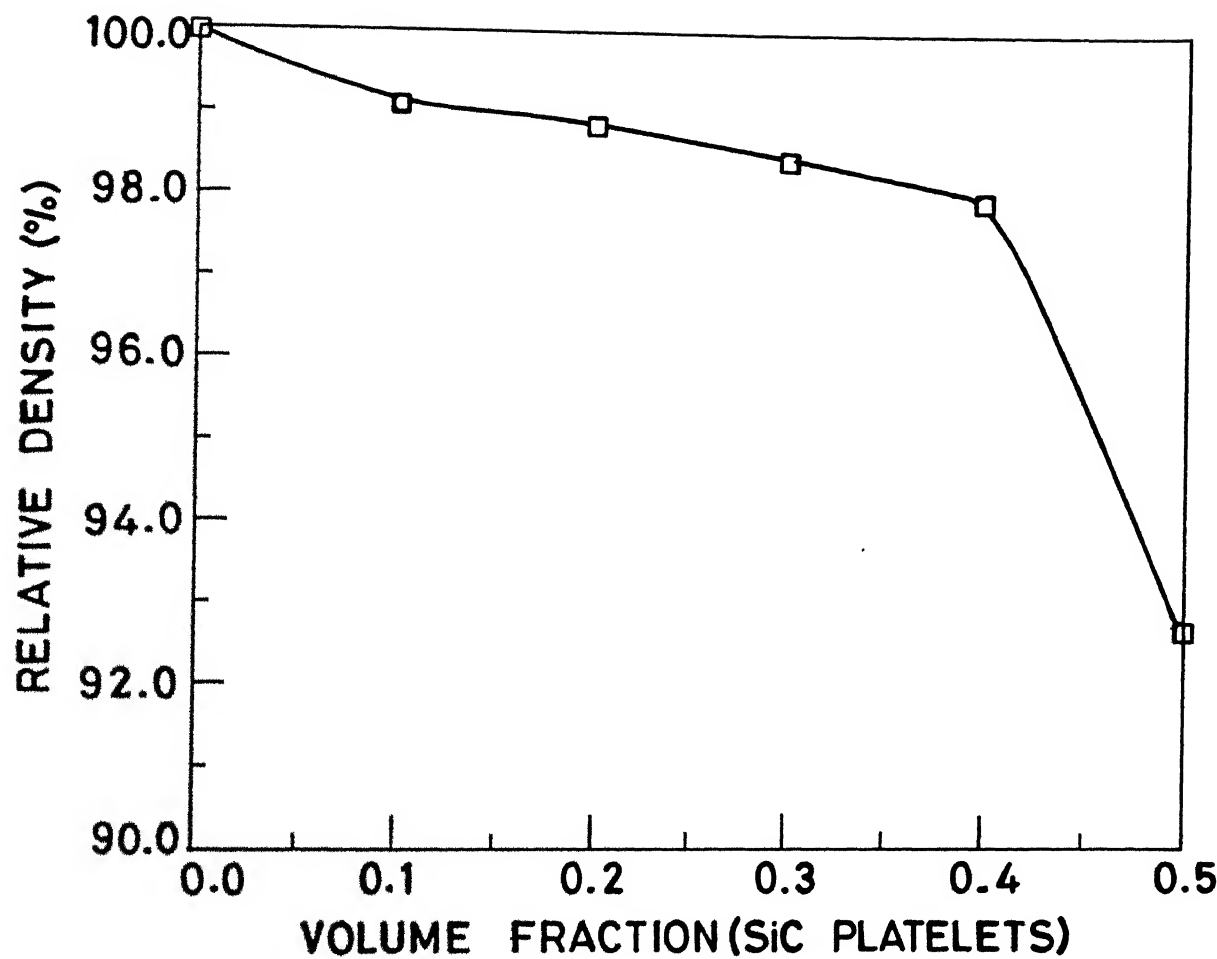


FIG.4.5 DENSITY MEASUREMENTS FOR PYREX-SiC COMPOSITES (HP).

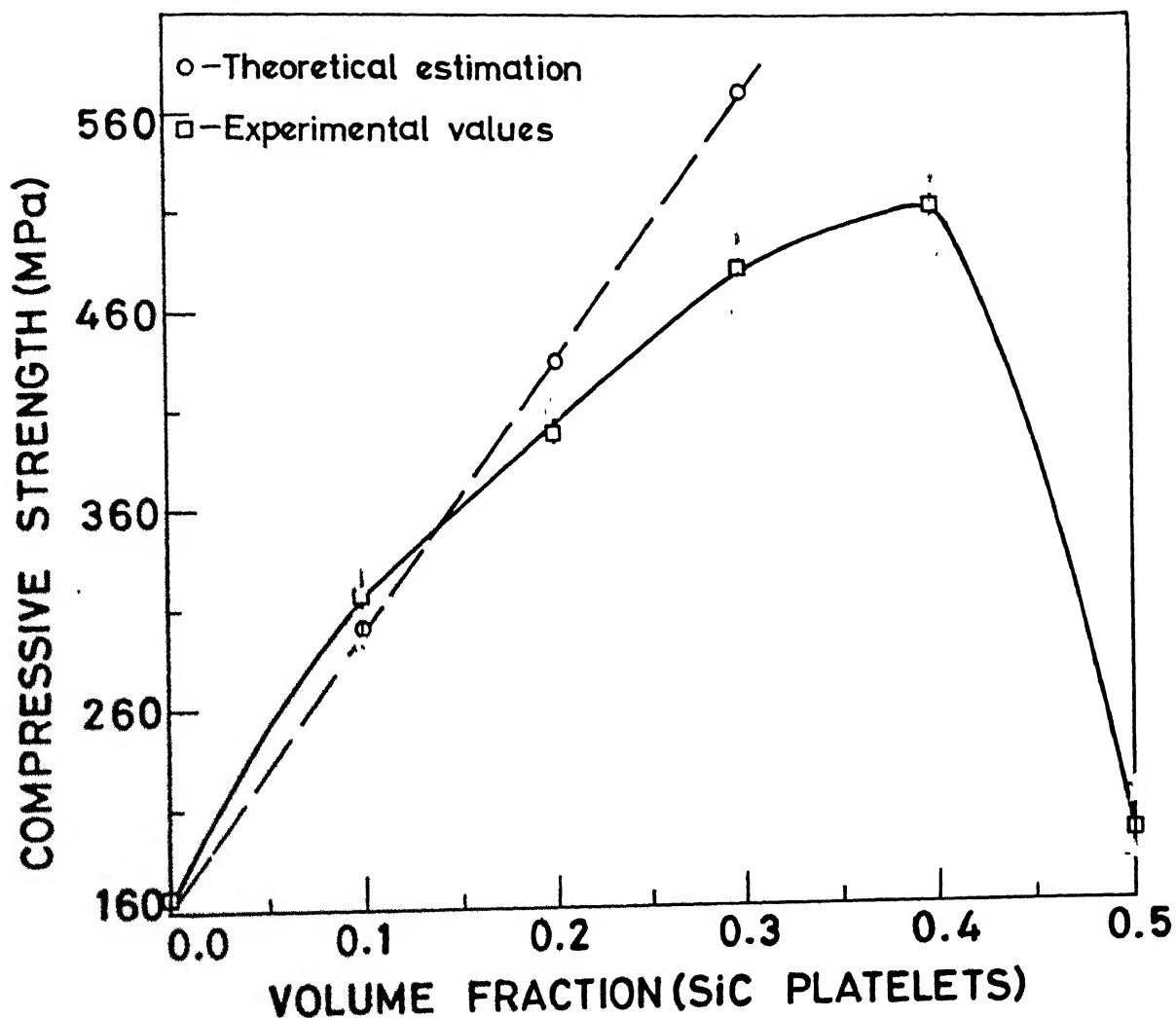


FIG.4.6 COMPRESSIVE STRENGTH OF PYREX-SiC COMPOSITES.

deformation(fig 4.7). The basic nature of the stress strain curve has remained the same as that of the pure pyrex glass, only the level of stress has increased with increasing vol% platelet loading upto 40 vol% composites. The strain at failure for all the composites is in the range of 1%.

As shown from the stress strain curves(fig. 4.7) (for all vol% composites) at higher stress levels some form of steps are observed in the load vs. displacement curves. This could be due to repeated crack propagation and crack arrest due to crack interaction with SiC platelets.

With increasing vol% platelet loading the slope of the stress strain curve has increased, thereby indicating that the effective Youngs modulus of the composite is increasing with increasing vol% composites. Applying the rule of mixtures for calculating the effective Youngs modulus for platelet composites.

$$E_{\text{eff}} = v_p E_p (1 - l_c/l) + v_m E_m \quad (4.1)$$

where E_p and E_m are the elastic modulii of the fibre and the matrix respectively and v_p and v_m are the volume fraction of the platelet and the matrix respectively and l and l_c are the length and the critical length of the platelets respectively.

Using $l_c = 1.6 \times 10^{-5} \text{ m}$ and $l = 5 \times 10^{-5} \text{ m}$ the theoretical values for the effective Youngs modulus was calculated.(table 4.3). It was found that the order by which the modulus increases(by incorporating various volume fraction of the platelets)agrees with the theoretical predictions.

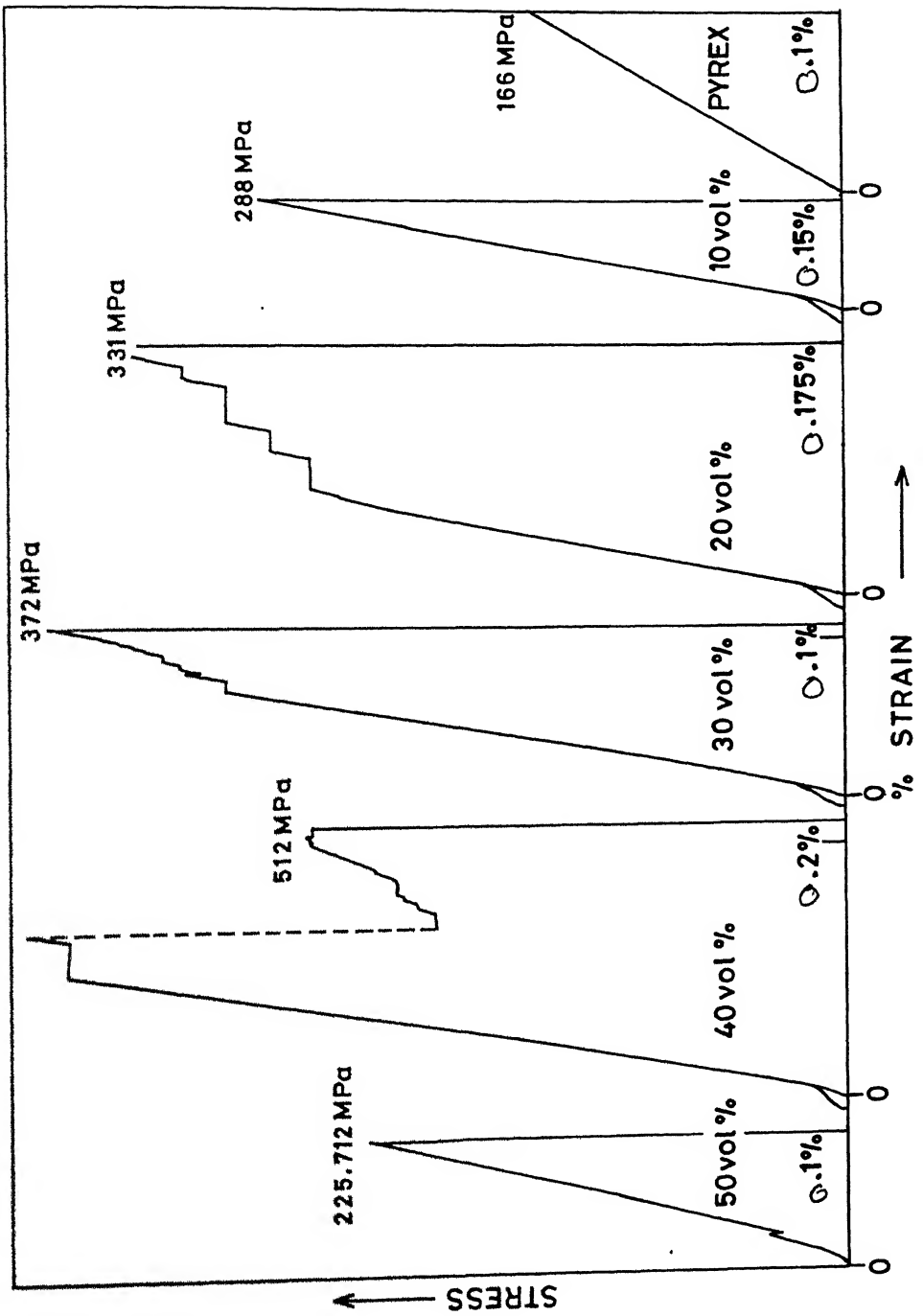


FIG.4.7 VARIATION IN THE COMPRESSIVE STRENGTH OF PYREX-SiC COMPOSITE WITH INCREASING VOL% OF SiC PLATELETS.

The compressive strength of the pyrex-SiC composites versus the vol% of SiC is plotted in figure(4.6). The compressive strength of pyrex glass is around 160 MPa. For the composites the strength steadily increased upto 40 vol% platelet loading, and after which it dropped sharply for the 50 vol% composites. The peak strength was achieved for the 40 vol% platelet composites which was around 510 MPa, more than three times the strength of pure pyrex glass(160MPa). This shows that substantial increment in strength can be achieved by reinforcing with SiC platelets. This increase in the strength of pyrex glass by the addition of SiC platelets takes place by load transfer from the matrix to the platelets.(refer 2.2.4) The simple rule of mixtures used for fibre and whisker composites is applicable for aligned platelets. To calculate the upper bound for increase in strength the following modified equation of the rule of mixtures is used

$$\sigma_c = v_f \sigma_{fu} (1 - l_c / 2l) + (1 - v_f) \sigma_m \quad (4.2)$$

where l is the average length of the platelets, l_c the critical length, σ_{fu} and σ_m the strength of platelets and pyrex glass respectively(refer table 4.1) and v_f the volume fraction of SiC platelets. Using $l_c = 1.6 \times 10^{-5}$ m the theoretical values of strength for the composites was calculated(table 4.3). It was found that the experimentally obtained values agree fairly well with the theoretical estimates at lower volume fraction of SiC platelets. However, there is some deviation at higher volume fractions(fig 4.6). This is because of the fact that at higher volume fractions the strength is limited by flaws in the form of agglomerates of SiC platelets, porosity.

For a given composite system, the only variable in the above equation is the volume fraction of the platelets. Also in the above equation the term associated with platelets (the first term represents the load carried by the platelets and the second term represents the load carried by the matrix) is dominant. Therefore it is evident from the equation that the strength of the composite has increased with increasing platelet loading (fig 4.6). This is what has been observed upto 40 vol% composites, where increasing the vol% of SiC platelets, has resulted in a steady increase in the strength values.

Actually, for the 50 vol% composites SiC platelets agglomerate at various locations. These regions are devoid of any matrix material. These aggregates have no interfaces with the matrix, so instead of load sharing, these platelets act as flaws which weaken the composites. In addition, other inherent process-related flaws are present for the 50 vol% composites. The relative density of the 50 vol% composites is around 90%. Thus the sharp fall in the strength of the 50 vol% composite is the combined effect of agglomeration of the platelets coupled with the other process-related griffith flaws.

In this study, the compressive strength of pyrex is around 160 MPa and the peak strength for the 40 vol% composite is 510 MPa, while MOR values for base pyrex and pyrex-SiC whisker (30 vol%) composites are 90 MPa and 250 MPa respectively as reported in the literature (8-9).

The basic nature of the stress strain curve for the platelet reinforced composite is similar to that for all whisker reinforced

composites reported including pyrex-SiC whisker composite. The stress strain curve is linear till failure with no evidence of any plastic flow, finally leading to catastrophic failure. This means that incorporating the SiC platelets in the pyrex matrix does not change the nature of the stress strain curve, but only strengthens the glass.

A comparison between whisker/fibre reinforced borosilicate composites currently developed has been made in table(4.4). The pyrex-SiC fibre composite shows far higher strength and toughness values compared to the pyrex-SiC platelet composites. The increase in the level of strength is attributed to the superior load sharing capability of the fibres compared to the platelets. The major toughness increment is attributed to pullout of fibres in fibre composites which is absent in the platelet reinforced composite.

4.6.2) Fracture Behaviour

From the fracture surface examination, crack deflection and crack twisting were observed to be the dominant toughening mechanisms with little evidence for pull-out. Crack deflection(fig. 4.Ph7a) is related to the presence of a relatively weak interface and to the thermal expansion mismatch between the platelets and the pyrex matrix. The thermal expansion co-efficient for SiC platelets is $\alpha_{SiC} = 4.5-5.5 \times 10^{-6}/^{\circ}C$, which is more than that of pyrex glass($\alpha_p = 3.3 \times 10^{-6}/^{\circ}C$). This builds up a hoop compression and radial tension in the matrix during cooling from the hot-pressing temperature because $\alpha_{SiC} > \alpha_p$. In addition, crack



Fig. 4.Ph7a) Fractured Surface(Pyrex-SiC composite)
showing crack deflection process



Fig. 4.Ph7b) Fractured Surface(Pyrex-SiC composite)
showing crack twisting processes



Fig. 4.Ph7c) Fractured Surface(Pyrex-SiC composite)
showing pullout processes

Table 4.4 : Strength of Pyrex-SiC Platelet Composites From the Literature

Composite System	Strength (MPa)	Source
Pyrex-SiC Platelet Composite (40 Vol%)	Compressive Strength 514.6	Present Study
Pyrex-SiC Whisker Composite (30 Vol%)	MOR 220	Ref. 80
L.A.S. SiC Whisker Composite (30 Vol%)	MOR 370-400	Ref. 12
Si_3N_4 Matrix-SiC Whisker Composite (30 Vol%)	MOR 800	Ref. 46
SiC Fiber-Reinforced Borosilicate Glass (Pyrex)	MOR 830	Ref. 10
SiC Fiber-Reinforced L.A.S. Glass-Ceramic	MOR 950-1400	Ref. 12

twisting(fig 4.Ph7b) was also observed particularly for the higher vol% composites. For this mechanism to operate in addition to a relatively weak interface and thermal expansion mismatch, presence of a large no. of platelets distributed uniformly through the matrix is required. Hence, some platelets are always oriented favourably for this mechanism to operate.

Platelet pullout has only been observed for the 30 and 40 vol% composites(fig 4.Ph7c). Even in these cases the pullout has been negligible. Platelet pull-out is limited by the relatively good platelet/pyrex interface cohesion and the random distribution and orientation of the platelets.

The basic fracture mechanisms for the platelet composites are similar to those of whisker reinforced composites(10,11).The main mechanism for toughness in pyrex-SiC(w) composites is crack deflection with little or no evidence for pullout.

4.6.3) Temperature Dependence of Strength

The temperature dependence of strength for the matrix as well as the composites for all the vol% platelet loading is shown in the figure(4.8). As expected the strength decreases with increase in temperature for all the vol% platelet loading as well as the matrix.

Increasing vol% loading of the composite, the reinforcement dominates the mechanical properties. This is because of load transfer from the weak matrix to the strong platelets which support most of the load, that is applied to the composite. This load transfer takes place through the interface. At room temperature the interface is fairly strong. Besides residual

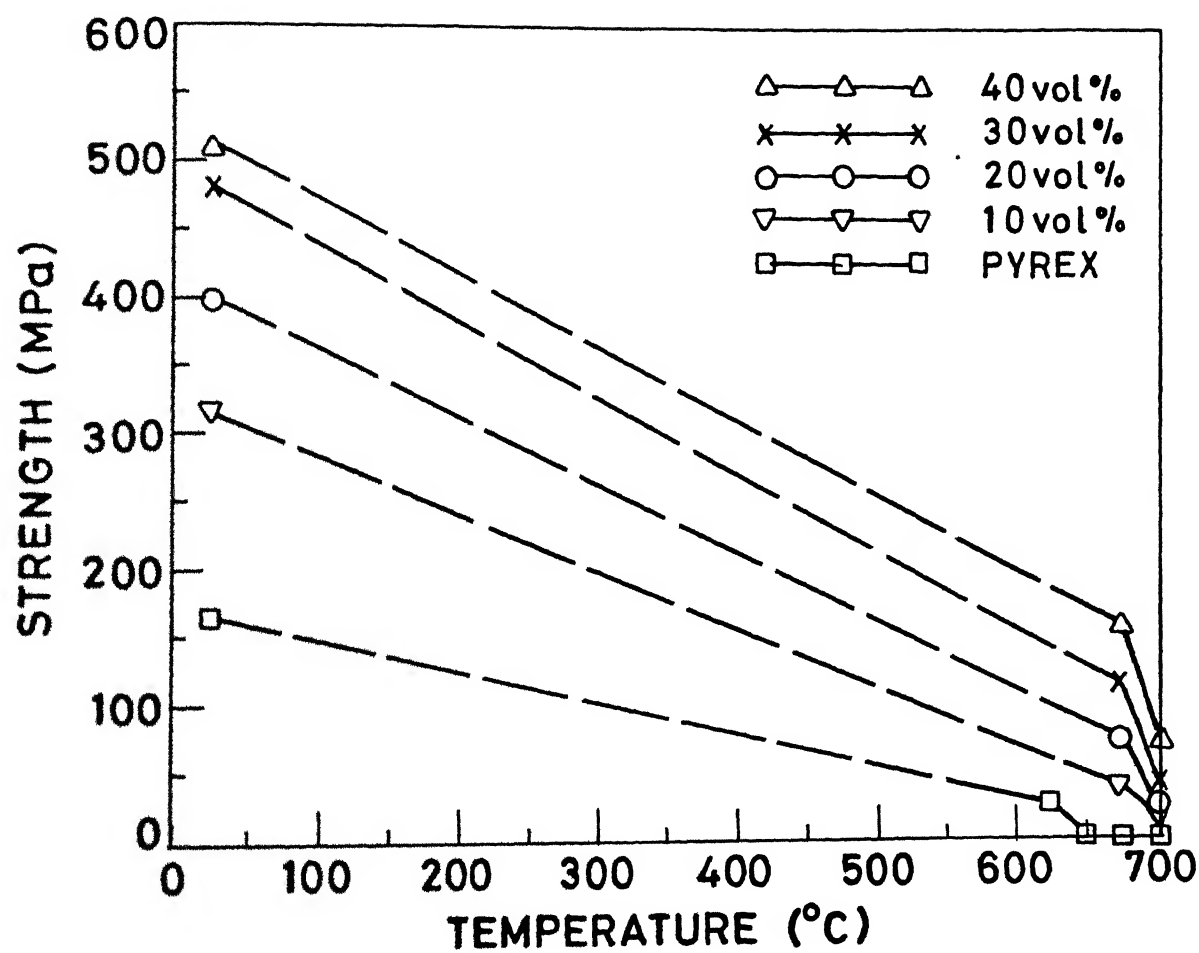


FIG.4.8 TEMPERATURE DEPENDENCE OF STRENGTH FOR PYREX-SiC COMPOSITES.

stresses(clamping stresses) are also present at room temperature. So the interface is strong enough to be able to transfer most of the load to the platelets at room temperature. However, as the temperature increases the residual stresses(i.e. clamping stresses) are no longer present. Also the interface becomes weak and very less load can be transferred to the platelets. This becomes more prominent as temperatures increases. Moreover as the temperature increases , diffusion in the base matrix, pyrex also increases and the relaxation effects also become prominent. Thus the matrix strength also goes down with increasing temperature.

In all the volt composites the fall in strength with increasing temperature is the combined effect of these two phenomena viz. decrement of load transfer and matrix strength loss.

4.6.4) Effect of Volt Loading on Strength.

The strength of the composite at various temperatures is plotted as a function of the volt platelet loading(4.9). It is observed that, at any given temperature the strength of the composite increases with increasing volt platelet loading.This is because of the fact that with increasing volume fraction the reinforcement dominates the mechanical properties. However at higher temperatures the effect of the reinforcement is reduced and the behaviour is dominated by the matrix properties. So the difference in strength is bridged at higher temperatures.

4.6.5) Elevated Temperature Behaviour of Pyrex-SiC Composites

The flow stress at the various strain rates for the base Pyrex matrix is plotted for the temperature regime from 625 to 700°C in the Fig.(4.10). A typical plot of the strain rate change test conducted for Pyrex Glass is also shown in the Fig.(4.13). The strain rate sensitivity (m) for all the cases were found to be one. This behaviour is expected of a glass system (Refer 2.5)

The flow stress at the various strain rates is plotted for the 10-40 Volt at the temperatures of 675°C and 700°C (Fig. 4.11 and 4.12). A typical plot of the strain rate change test conducted for Pyrex-SiC composite is also shown in the Fig. (4.14). The strain rate sensitivity (m) for all the cases was found to be the same as that for the Pyrex Matrix (i.e. the strain rate sensitivity was one).

The flow stress vs. strain rate plots (Fig 4.11 and 4.12) are linear with the line passing through the origin confirming to the flow equation for Newtonian flow.

$$\sigma = K^1 \dot{\epsilon} \quad (\text{Refer 2.5})$$

Thus the introduction of the platelets has not effected the flow behaviour of the pyrex glass, only the level of flow stress has increased (Fig. 4.15 and 4.16).

The necessary and sufficient conditions for superplastic behaviour are :

- a) The strain rate sensitivity should be close to one.
- b) The material should have good fracture resistance.

It has been established that Pyrex-SiC composites have strain rate sensitivity equal to one. Thus they can be expected to show superplastic behaviour. However, the superplastic behaviour of

these composites can be limited by cavity formation and matrix-platelet interface separation. Similar behaviour has been reported by Wang and Raj (12) (refer. 2.5) This phenomenon could not be established as the testing of these composites was conducted in compression.

The activation energy for Pyrex glass was determined to be 495 KJ mol⁻¹ from the Arrhenius Plot (Fig. 2.17). It has been reported that activation energy (370 to 640 KJ mol⁻¹) values is associated with the viscous (diffusion) mechanisms in Pyrex(13). Thus the values are in agreement with the reported literature

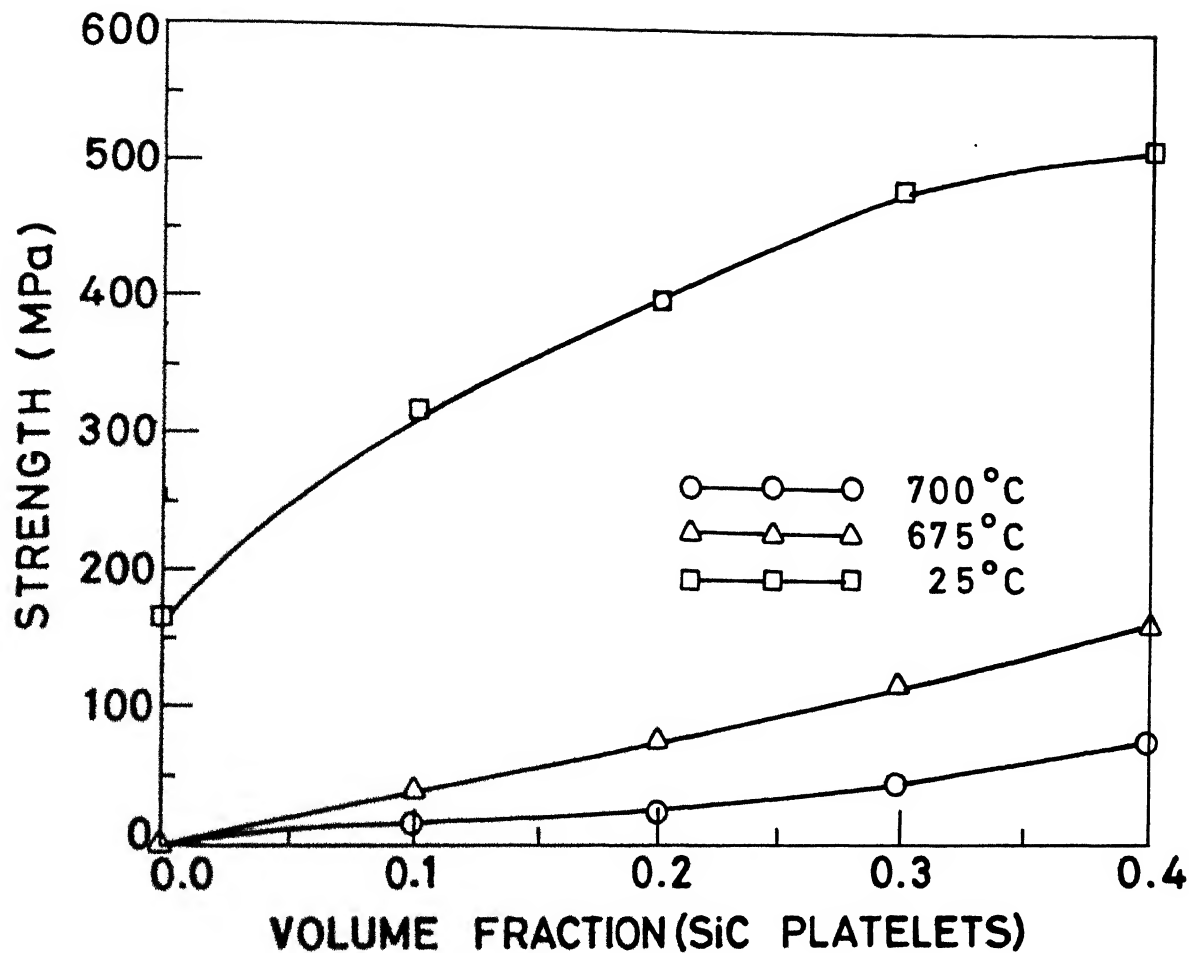


FIG.4.9 STRENGTH OF PYREX-SiC(COMP.) WITH VARYING VOL% AT DIFFERENT TEMPERATURES.

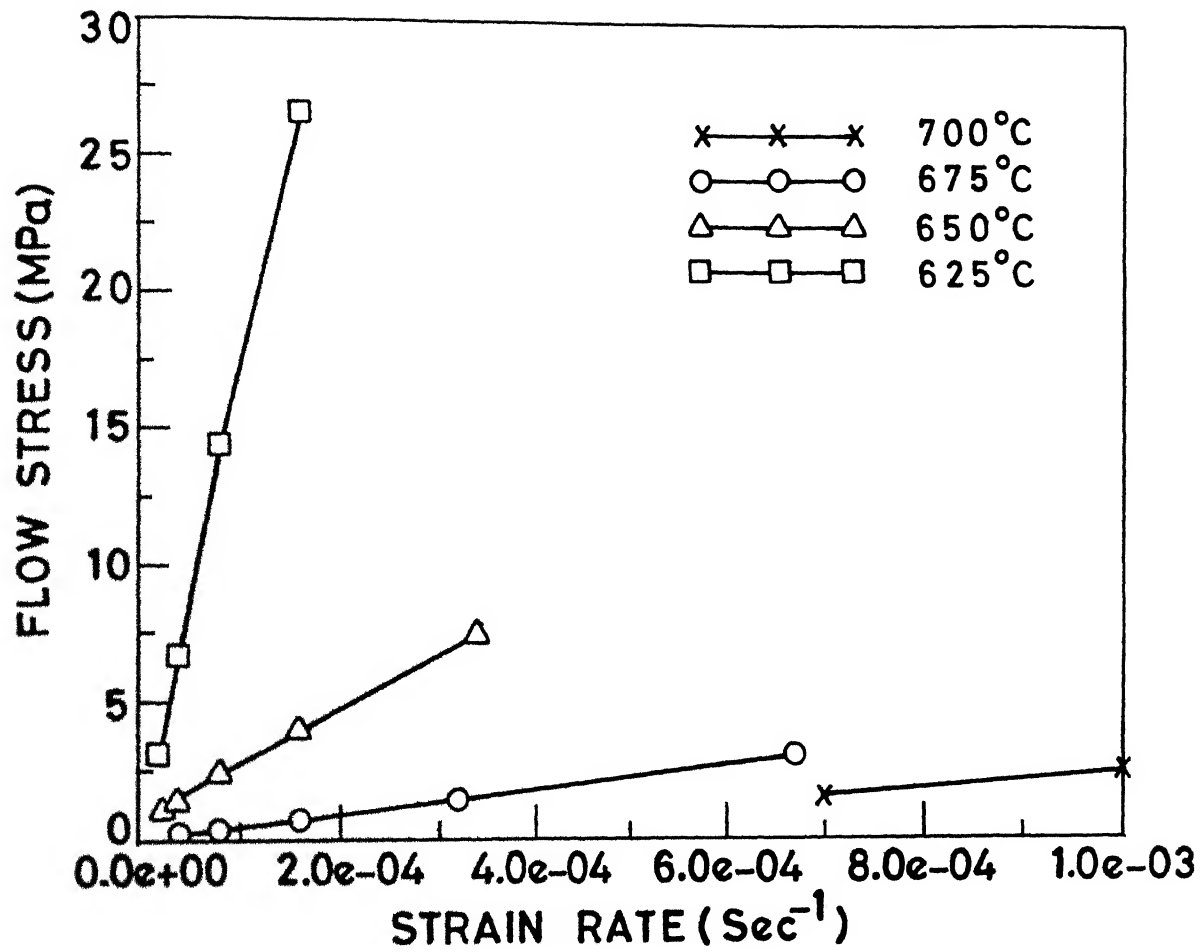


FIG.4.10 CONFIRMATION OF NEWTONIAN BEHAVIOUR OF PYREX GLASS.
 $e = \text{exponential}$

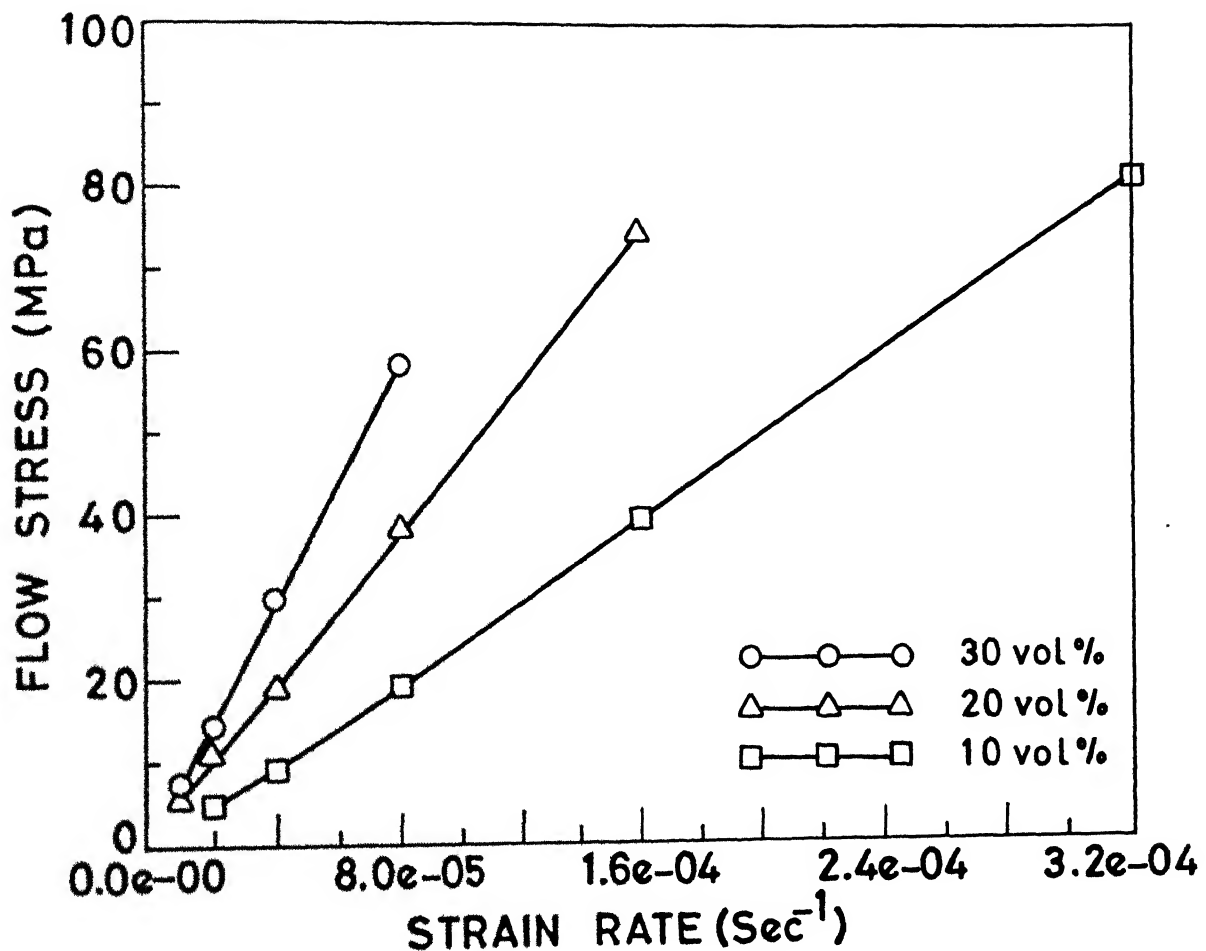
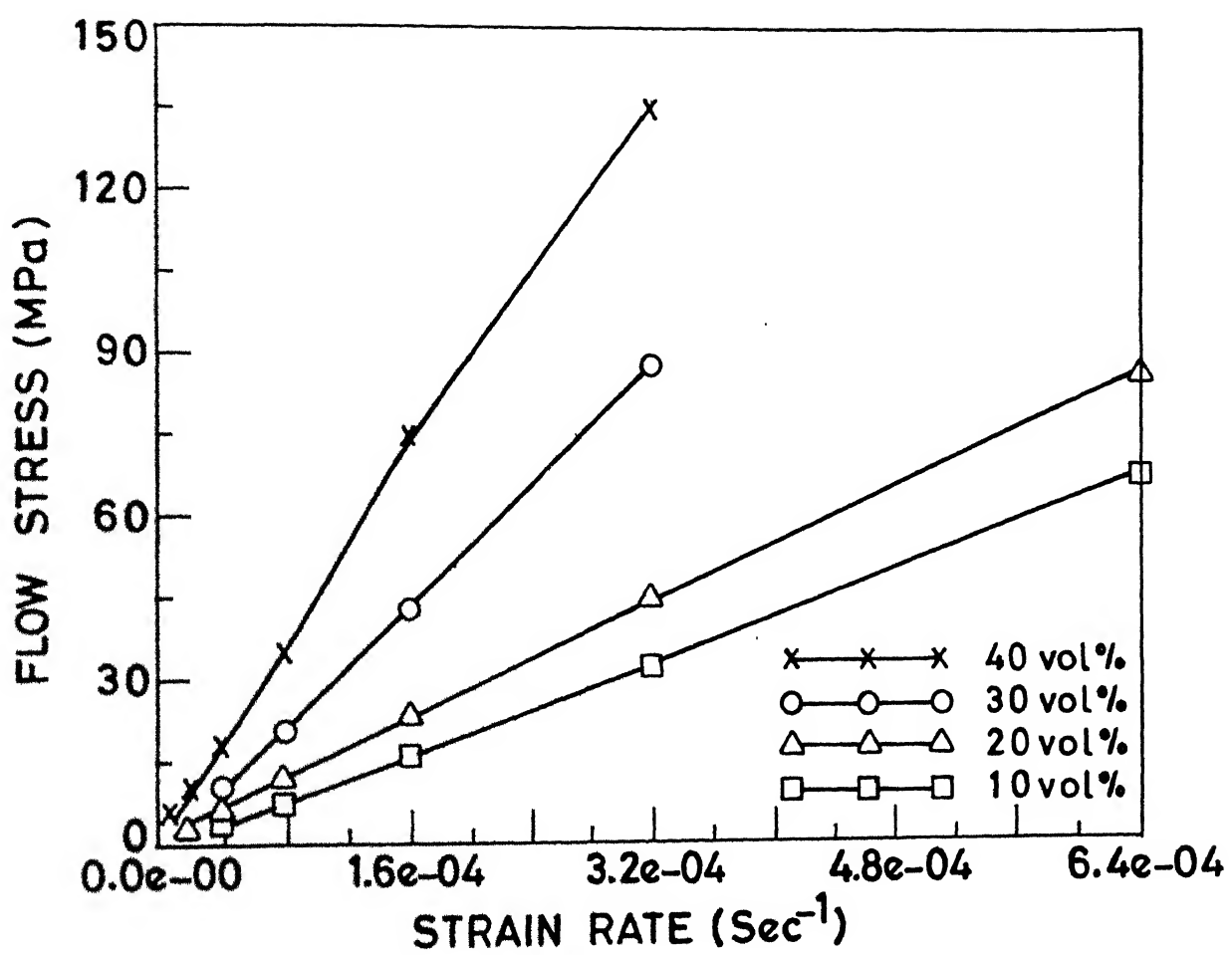


FIG.4.11 COMPARISON OF FLOW STRESS AT 675°C (PYREX-SiC).
 $e = \text{exponential}$



**FIG.4.12 COMPARISON OF FLOW STRESS
AT 700°C (PYREX-SiC)**

$e = \text{exponential}$

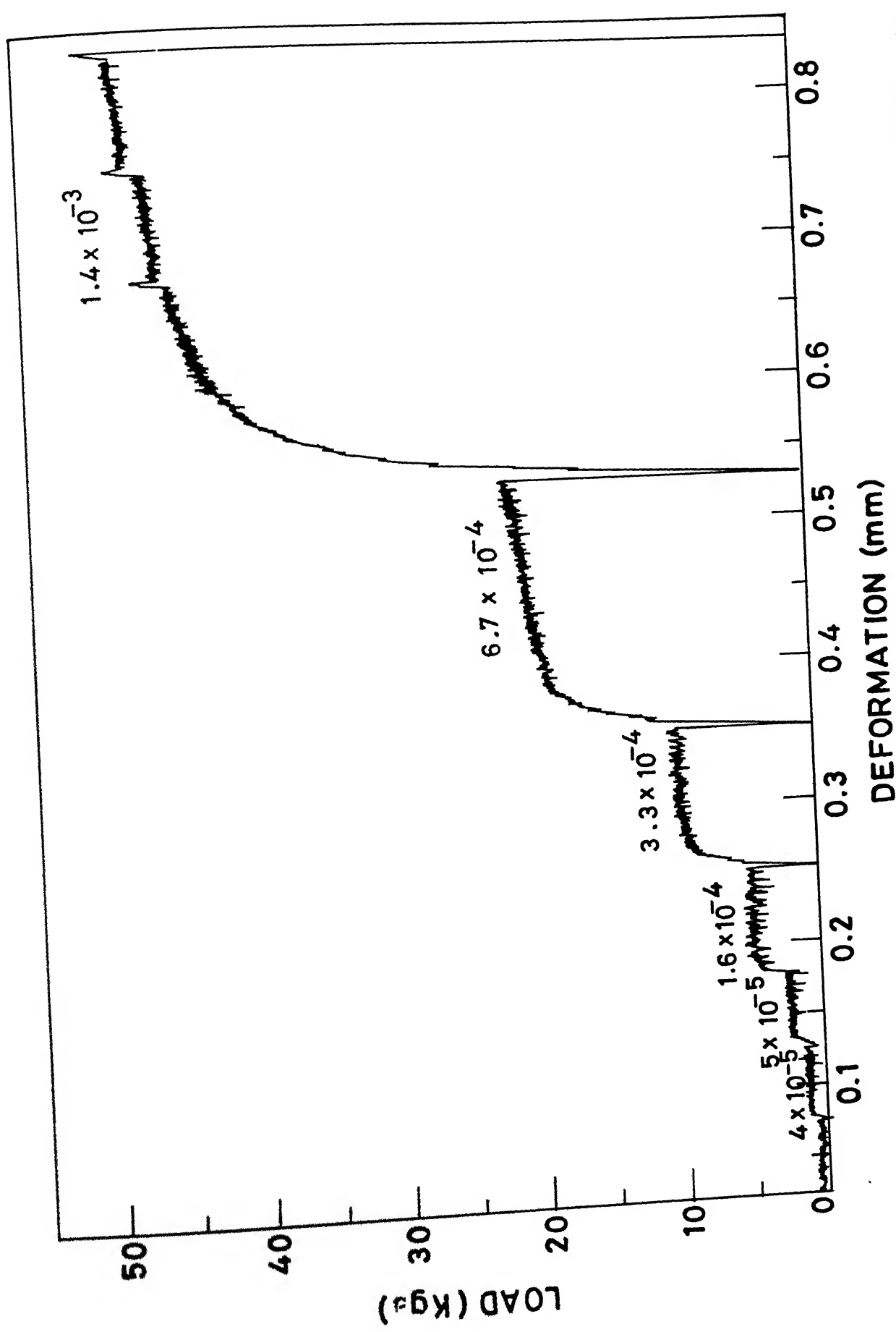


FIG. 4.13 CHANGING STRAIN RATE TEST IN COMPRESSION AT
675°C FOR PYREX.

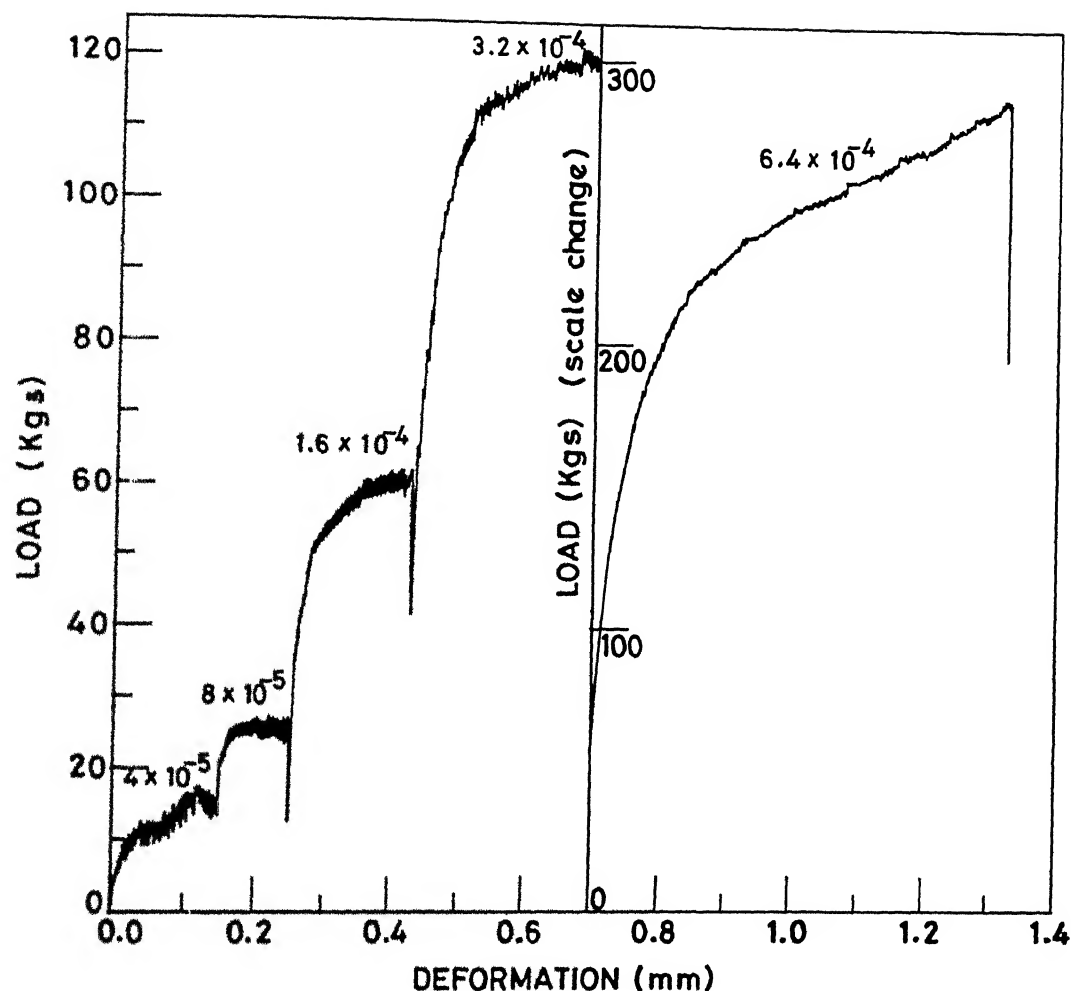


FIG.4.14 CHANGING STRAIN RATE TEST IN COMPRESSION AT 700°C FOR PYREX-SiC 10 VOL%.

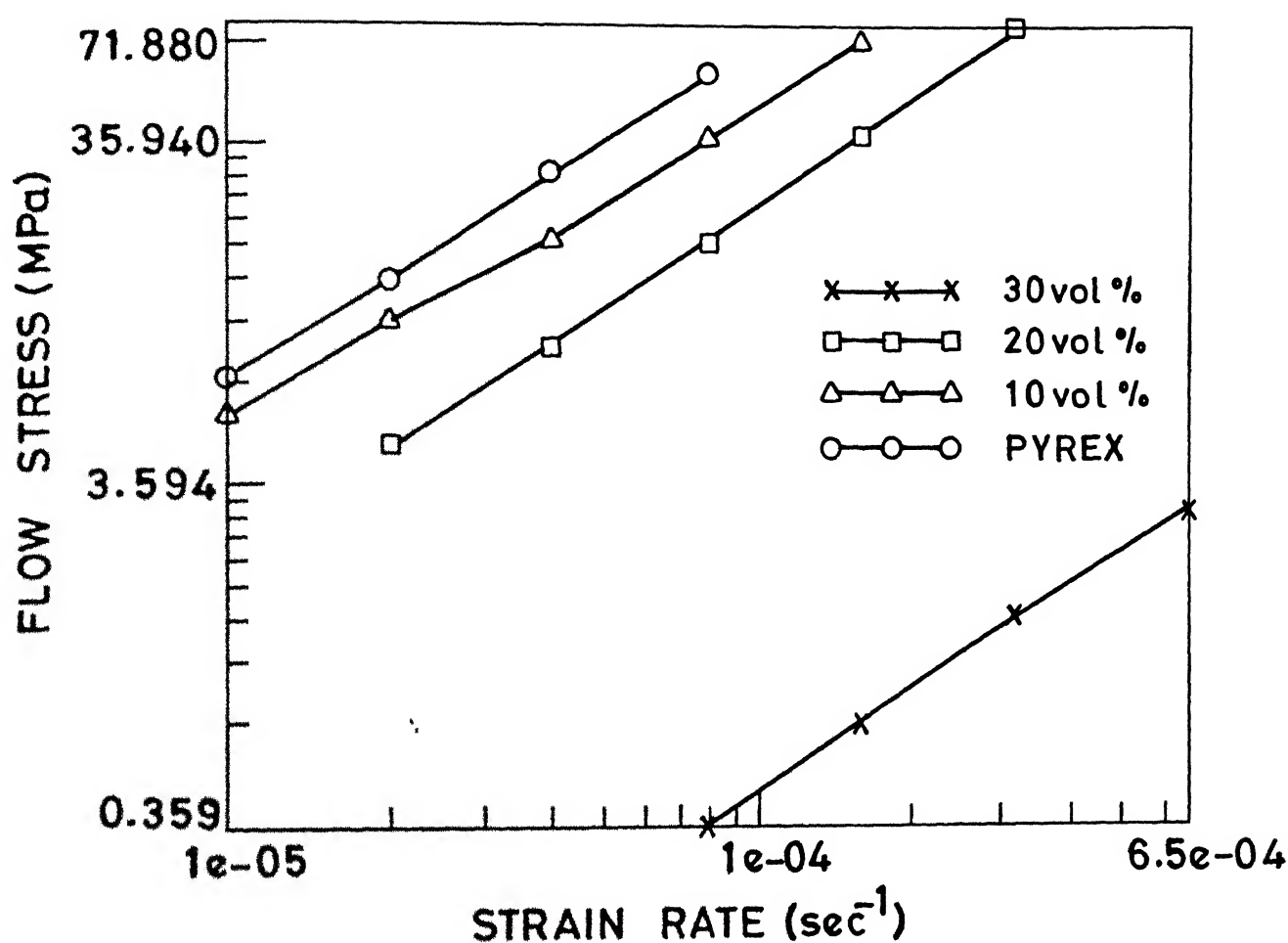


FIG.4.15 INCREASE IN THE LEVEL OF FLOW STRESS OF PYREX GLASS (675°C) BY INCORPORATING VARIOUS VOL% SiC PLATELETS.

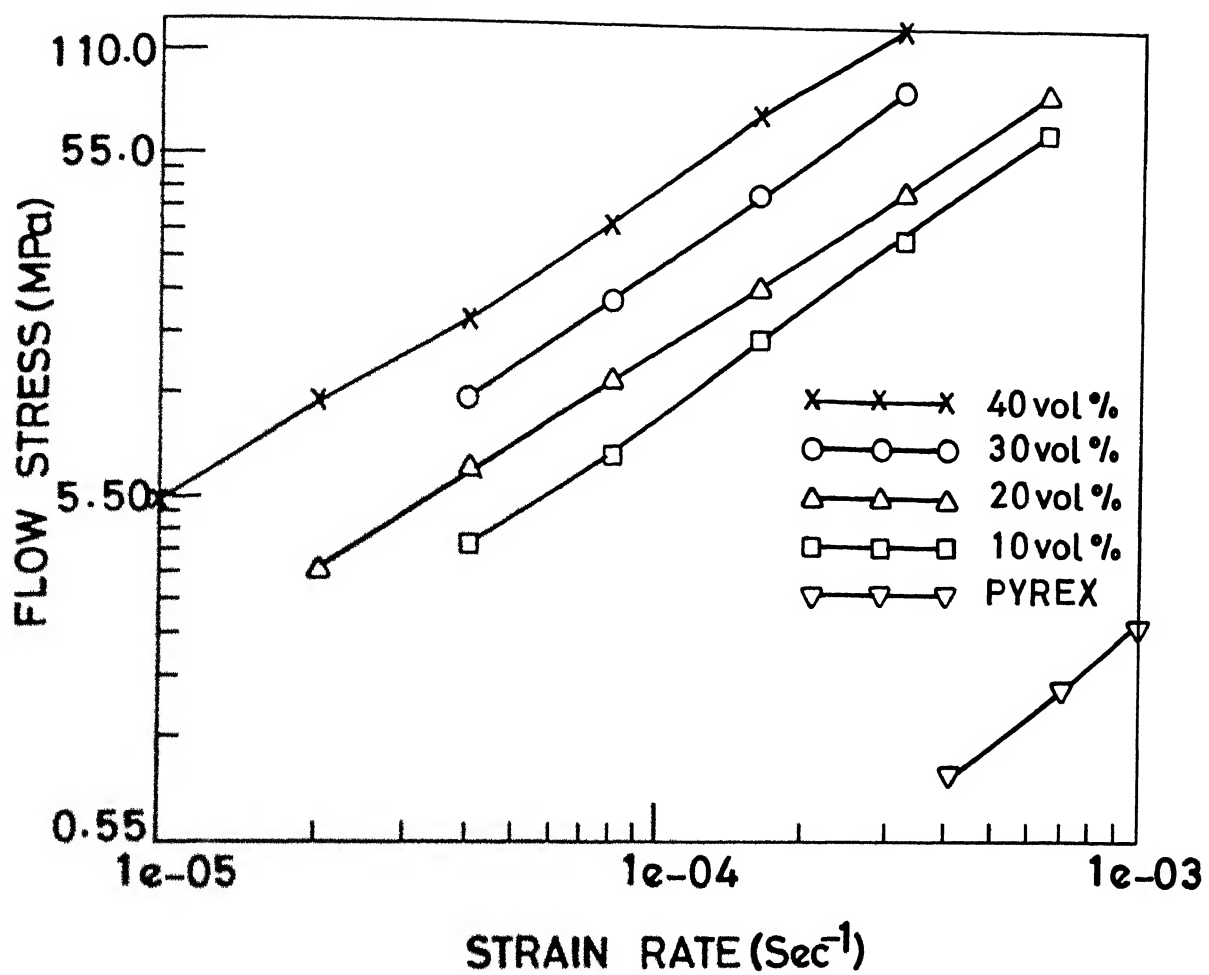


FIG.4.16 INCREASE IN THE LEVEL OF FLOW STRESS OF PYREX GLASS (700°C) BY INCORPORATING VARIOUS VOL% SiC PLATELETS.
 $e = \text{exponential}$

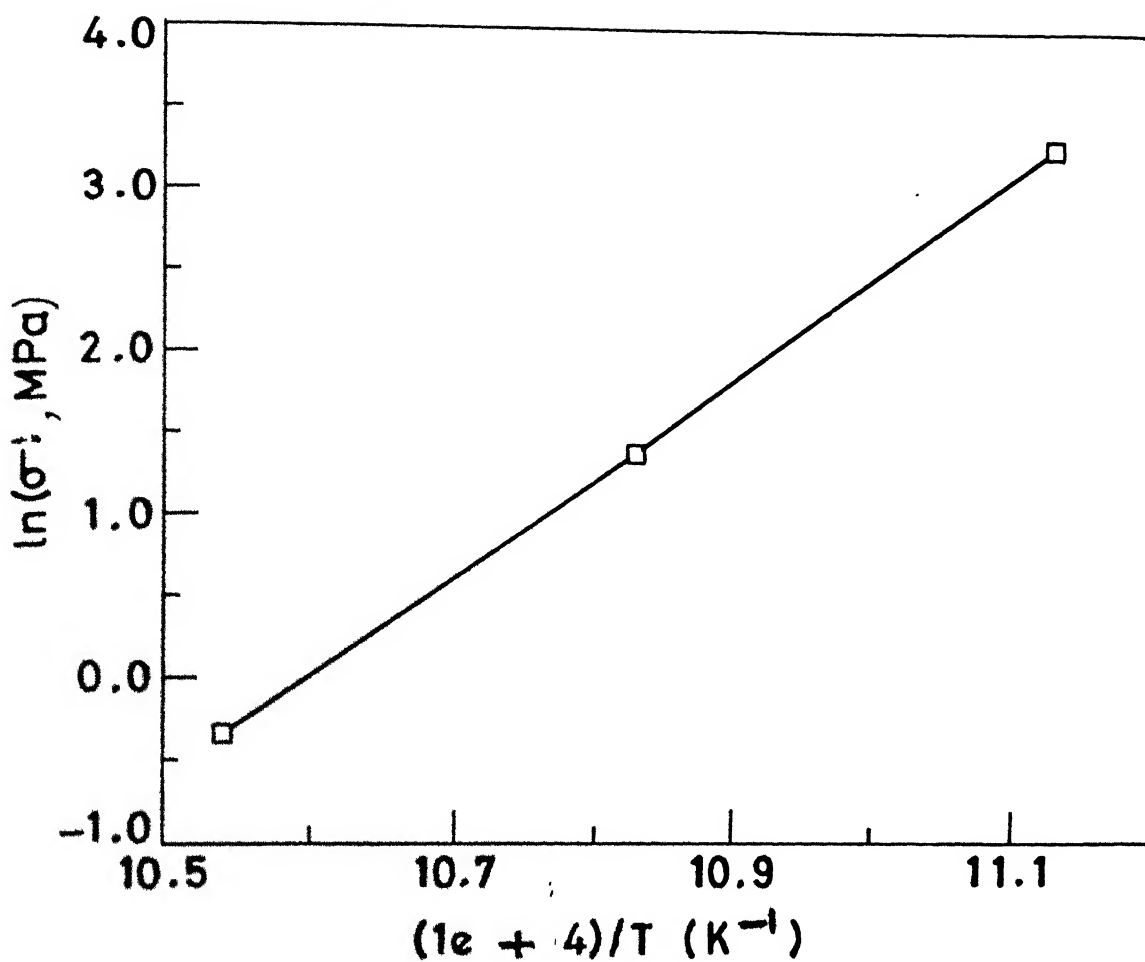


FIG.4.17 ARRHENIUS PLOT FOR PYREX GLASS.

References (Chapter 4)

1. Lundberg R., Nyberg B., Williamdes K., Persson M., and Carlsson R., "Processing of Whisker-Reinforced Ceramics", Composites, [18] 125-27(1987).
2. Lee K. W., Sheargold S.W., "Particulate Matters in Silicon Carbide Whiskers", Ceram Engg. Sci. Proc. [8] 702-11, (1987).
3. Mazurin O.V., Porai-Koshits E.A., "Phase Separation in Glass", North Holland Publishers (1984).
4. Homeny J., Vaughn W.L., Fuller M.K., "Processing and Mechanical Properties of SiC Whiskers Al_2O_3 Matrix Composites", Bull. Am. Ceram. Soc. 66-333-38 (1987).
5. Wei G.C., Becher P.F., "Development of SiC Whisker Reinforced Ceramics: Bull. Am. Ceram. Soc. 64, 298-304 (1985).
6. Homuy J., Vaughn W.L. "Whisker-Reinforced Ceramic Matrix Composites", Mater. Res. Bull., 22 66-71(1987).
7. Porter J.R., Lange F.F. and Chokshi A.H., "Processing and Creep Performance of SiC Whisker Reinforced Al_2O_3 " Am. Ceram. Soc. Bull., 66 [2] 343-47 91987).
8. Li Jie, "SiC Whisker Reinforced Glass-Ceramics", M.S. Thesis, University of Warwick, June 1988.
9. Prewo K.M., Brennan J.J., Layden G.K., "Fiber Reinforced Glass and Glass-Ceramics for High Performance Applications", Bull. Am. Ceram. Soc., 65[2] 305-313 (1986).
10. Gadkaree K.P., Chyunq K., "Silicon-Carbide-Whisker-Reinforced Glass and Glass-Ceramic Composites", Am. Ceram. Soc. Bul. 65[2] 370-76 (1986).
11. Gac F.B., Petrovic J.J., Milewski J.V., Shaula D.D., "Performance of Commercial and Research Grade SiC Whiskers in a Borosilicate Glass Matrix", Ceram. Engg. Sci. Proc., 7[7-8] 978-82 (1986).
12. Wang J.G., Raj R. "Mechanism of Superplastic Flow in a Fine Grained Ceramic Containing Some Liquid Phases", J. Am. Ceram. Soc., 67[6]399-499 (1984).
13. Kassowsky R., Miller D.G., Diaz E.S., J. Mat. Sci., 10, 983 (1975).

V CONCLUSIONS

1. The processing of the pellets of borosilicate matrix through cold compaction and sintering resulted in appreciable crystallization to cristobalite phase. Consequently, there was appreciable microcracking because of the thermal expansion between borosilicate glass and cristobalite. Subsequently all the composites were processed through hot pressing under optimal conditions to minimise the crystallization of glass matrix.
2. The resulting composites are observed to be fully dense with nearly homogeneous distribution of SiC platelets upto 40 Vol.% of the reinforcement. But above 40 Vol.% SiC platelets significant porosity was observed in the composites. The rigid network formed by SiC platelets at these Vol.%, results in poor infiltration of the viscous Pyrex glass matrix, leading to porosity and agglomeration of SiC platelets.
3. The compressive strength tests show that the strength increases with increasing Vol.% loading of SiC platelets, upto 40 Vol.% loading and then decreases. This decrease is primarily because of agglomeration at higher Vol.% loading. Thus it is possible to get maximum strength increase using an optimum Vol.% loading. Fractured samples show that crack deflection is mainly responsible for toughness while pullout is minimal.
4. Increasing the temperature of the compressive strength test leads to deterioration in the compressive strength. This was because matrix properties begin to dominate at the elevated temperatures where diffusion mechanisms in the matrix begin

to operate more vigorously.

5. The strain rate change tests show that the strain rate sensitivity for all the composites remains equal to one. Moreover, the flow behaviour of Pyrex glass was not affected by the introduction of platelets. Thus the composites were found to possess the necessary condition for superplasticity. However, the superplastic behaviour of the composite may be limited by cavity and matrix/platelet separation.

i) Model Calculation for Theoretical density (Pyrex-Sic 40Vd8)

$$\begin{aligned}
 D_{th} &= V_f D_f + V_m D_m \\
 &= .4 \times 3.2 + .6 \times 2.23 \\
 &= \boxed{2.618 \text{ gms/cm}^3}
 \end{aligned}$$

ii) Model Calculation for Strength (Theoretical) of Pyrex-Sic 40Vd8 Composite.

(formulae used)

$$\sigma_c = V_f \sigma_{fu} (1 - l_c/z_l) + V_m \sigma_{mu}(1)$$

$$\text{where } l_c = d \sigma_f / 2z$$

$$\text{where } z = \lambda c p'$$

$$p' = \frac{E_m}{2\lambda} \frac{1 - \frac{1}{4}}{1 - V_m} \Omega$$

$$\begin{aligned}
 \Omega &= (\alpha_m - \alpha_w) \Delta T \\
 &= (3.3 \times 10^{-6} - 5 \times 10^{-6}) \times 600 \\
 &= -1.2 \times 10^{-3}
 \end{aligned}$$

$$\lambda = 0.5$$

$$\begin{aligned}
 \therefore p' &= - \frac{6.5 \times 10^9 \times 0.6}{2 \times 1/2 \times 3/4} \times 1.2 \times 10^{-3} \\
 &= -6.24 \times 10^7 \text{ N/mm}^2
 \end{aligned}$$

$$\begin{aligned}
 z &= 0.1 \times 6.24 \times 10^7 \text{ N/mm}^2 \\
 &= 6.24 \times 10^6 \text{ N/mm}^2
 \end{aligned}$$

$$\Rightarrow l_c = \frac{1 \times 10^{-6} \times 2 \times 10^6}{2 \times 6.24 \times 10^6} = 1.6 \times 10^{-5} \text{ mm}$$

$$\begin{aligned}
 \sigma_c &= V_f \sigma_{fu} (1 - l_c/z_l) + V_m \sigma_{mu} \\
 &= (.4 \times 1.8 \times 10^3 \left(1 - \frac{1.6 \times 10^{-5}}{2 \times 50 \times 10^{-6}}\right) + .6 \times 165) \\
 &= \boxed{643.8 \text{ MPa}}
 \end{aligned}$$

σ_c = composite strength

V_f = Vol. fraction of platelets

V_m = Vol. fraction of matrix

l_c = critical length of the platelet

l = length of the platelet

d = thickness of the platelet

Ω = interfacial shear stress

λ = const.

p' = clamping pressure
 E_m = elastic modulus of the matrix

α_m = C.T.E. for matrix

α_w = C.T.E. for platelets

Ω = thermal mismatch

ΔT = temperature diff.
 (between processing & room temperature)

A 100/1

ME-1993-M-VER-PRO